

UCSF

UC San Francisco Electronic Theses and Dissertations

Title

Transcriptional Control of Neural Crest Development by MEF2C

Permalink

<https://escholarship.org/uc/item/4923n790>

Author

Agarwal, Pooja

Publication Date

2009

Peer reviewed|Thesis/dissertation

Transcriptional Control of Neural Crest Development by MEF2C

by

Pooja Agarwal

DISSERTATION

Submitted in partial satisfaction of the requirements for the degree of

DOCTOR OF PHILOSOPHY

in

Biomedical Sciences

in the

GRADUATE DIVISION

of the

UNIVERSITY OF CALIFORNIA, SAN FRANCISCO

I dedicate this work to my parents for their unconditional love and support. I'll never forget the countless sacrifices you have made, and will always strive to make you proud of me.

ACKNOWLEDGEMENTS

I am a strong believer in luck, and I find the harder I work the more I have of it.

Benjamin Franklin (1706 - 1790)

It is a true privilege to be able to wrap up my graduate career at UCSF by acknowledging the people who made it such a wonderful and fulfilling experience. First and foremost, I would like to thank Brian Black, my graduate advisor, for his mentorship and support. Brian is a brilliant scientist and a great teacher. He devotes a lot of time and effort in training his graduate students to not only be strong independent scientists, but also effective writers and excellent presenters. One of the most important lessons he has taught me is that the best way to do good science is to be your own biggest critic. I am also grateful to him for instilling in me the confidence to face the competitive and aggressive world of science.

Of course life at UCSF would not be half as much fun for me if it wasn't for the members of the Black Lab. Over the past few years, we have all become really good friends, sharing tears over failed experiments, and smiles over little successes. I'll dearly miss our stimulating lab meetings and academic debates just as much as our yearly camping trips and social excursions. I especially want to thank Mike Verzi for being such a great collaborator. Mike is not only an amazing scientist, but also a wonderful human being, and I will cherish our friendship for years to come.

I also want to take this opportunity to thank my committee members, John Rubenstein and Holly Ingraham, for their sound advice and constructive criticism, and to express my gratitude to Lisa Magargal in the Biomedical Sciences program for taking such good care of us graduate students.

Completing this PhD would have been impossible without the unconditional love and support of my family and friends. My parents are, and always will be, my best friends. I will never forget the sacrifices they have made for me, and thank them for the good values they have instilled in me. My husband, Amit, is a true gem. Being married to a graduate student is no easy task, but Amit was beside me every step of the way, to cushion every fall, wipe every tear, and cheer every small victory. I also want to thank a very dear friend, Gopinath Ganji, for constantly reminding me of my strengths, helping me battle my weaknesses, and for pushing me to pursue my passion for science.

All of the data presented in Chapter 1, and part of the work presented in Chapter 2, was reprinted from *Developmental Cell*, volume 12(4), by Michael P. Verzi, Pooja Agarwal, Courtney Brown, David J. McCulley, John J. Schwarz and Brian L. Black, entitled: The Transcription Factor MEF2C Is Required for Craniofacial Development, April 2007, Pages 645-652.

ABSTRACT

MEF2 transcription factors are well-established regulators of cardiac and skeletal muscle development. We have identified a novel role for MEF2C in the neural crest where its function is required for craniofacial development. Conditional inactivation of *Mef2c* in the neural crest results in severe defects in multiple bones of the craniofacial skeleton, leading to neonatal lethality due to upper airway obstruction.

Here I have identified the molecular pathways involving MEF2C during craniofacial development. I show that MEF2C directly regulates *Dlx5* and *Dlx6* expression in the craniofacial mesenchyme through a novel branchial arch-specific enhancer in the *Dlx5/6* locus. In addition, MEF2C and *Dlx5* transcriptionally synergize on the *Dlx5/6* enhancer, suggesting that *Dlx5* is not only a downstream target but also a cofactor of MEF2C during craniofacial development. I present strong evidence to show that MEF2C and *Dlx5* can physically interact through their DNA binding domains. In addition to this transcriptional synergy and physical association, MEF2C and *Dlx5* genetically interact. Heterozygosity at either locus (*Dlx5/6*^{+/-} or *Mef2c*^{+/-}) results in viable mice with no obvious phenotype, but heterozygosity at both loci (*Dlx5/6*^{+/-};*Mef2c*^{+/-}) results in perinatal lethality. *Dlx5/6*^{+/-};*Mef2c*^{+/-} mice exhibit a significant cleft of the posterior palate, caused due to a delay in the elevation and closure of palatal shelves, suggesting that MEF2C and *Dlx5/6* may coregulate palatogenesis. Preliminary evidence suggests that this palate defect may be due to a delay or defect in osteogenic differentiation within the palatal shelves.

In addition to craniofacial defects, neural crest-specific knockouts of *Mef2c* also show reduced expression of several melanocyte genes during development, and a significant reduction in the number of melanocytes at birth. We have strong evidence to suggest that MEF2C is a direct transcriptional target and cofactor of Sox10 in the melanocyte lineage.

Taken together, the results presented in this thesis identify two neural crest lineages, the craniofacial skeleton and melanocytes, in which MEF2C cooperates with lineage-specific transcription factors to potentiate cell fate decisions. These data also lend significant insight into our understanding of the transcriptional complexes and signaling pathways facilitating the development of these lineages.

TABLE OF CONTENTS

Acknowledgements.....	iv
Abstract.....	vi
Table of Contents.....	viii
List of Tables.....	ix
List of Figures.....	x
Introduction.....	1
Chapter 1.....	17
Chapter 2.....	27
Chapter 3.....	62
Methods.....	81
References.....	101

LIST OF TABLES

Table 1: Genetic interaction between <i>Mef2c</i> and <i>Dlx5/6</i> results in neonatal lethality in compound heterozygous mice.....	61
--	----

LIST OF FIGURES

Fig. 1: The neural crest gives rise to multiple cell types.....	12
Fig. 2: <i>Mef2c</i> is expressed in the neural crest-derived craniofacial mesenchyme.....	13
Fig. 3: <i>Mef2c</i> was inactivated in the neural crest using a conditional gene inactivation Approach.....	14
Fig. 4: Gross and histological examination of neural crest conditional <i>Mef2c</i> knockout heads	15
Fig. 5: Skeletal analysis of <i>Mef2c</i> neural crest knockout heads.....	16
Fig. 6: Cranial neural crest precursors migrate along distinct pathways.....	25
Fig. 7: <i>Mef2c</i> is required for the branchial arch expression of <i>Dlx5</i> , <i>Dlx6</i> , and <i>Hand2</i> ...	26
Fig. 8: An evolutionarily conserved enhancer in the <i>Dlx5/6</i> locus contains several consensus MEF2 sites.....	50
Fig. 9: The <i>Dlx5/6</i> enhancer is bound and activated by MEF2C	51
Fig. 10: The <i>Dlx5/6</i> enhancer directs expression to the craniofacial mesenchyme during embryonic development.....	52
Fig. 11: The <i>Dlx5/6</i> branchial arch enhancer is synergistically activated by MEF2C and <i>Dlx5</i>	53
Fig. 12: MEF2C and <i>Dlx5</i> physically interact through their DNA binding domains.....	54
Fig. 13: Mice heterozygous for both <i>Mef2c</i> and <i>Dlx5/6</i> exhibit palate defects.....	55
Fig. 14: <i>Dlx5/6</i> ^{+/-} ; <i>Mef2c</i> ^{+/-} animals have hypoplastic palatal and pterygoid bones.....	56
Fig. 15: Palatal shelf elevation and closure is defective in <i>Dlx5/6</i> ^{+/-} ; <i>Mef2c</i> ^{+/-} animals...	57
Fig. 16: Skeletal analysis shows cleft palate in <i>Dlx5/6</i> ^{+/-} ; <i>Mef2c</i> ^{+/-} mice at E16.5.....	58
Fig. 17: Reduced osteogenic differentiation at the site of palate closure in <i>Dlx5/6</i> ^{+/-} ;	

<i>Mef2c</i> ^{+/-} embryos.....	59
Fig. 18: <i>Dlx5</i> functions as a transcriptional target and cofactor of MEF2C during craniofacial development	60
Fig. 19: Highly conserved enhancer within the <i>Mef2c</i> locus directs expression to neural crest lineages.....	76
Fig. 20: Reduced number of melanocytes in <i>Mef2c</i> neural crest knockout neonates.....	77
Fig. 21: Fewer melanosomes per melanocyte in <i>Mef2c</i> neural crest knockout neonates..	78
Fig. 22: <i>Mef2c</i> is required for the proper expression of several melanocyte genes during Development.....	79
Fig. 23: <i>Sox10</i> expression in the peripheral nervous system is not dependent on MEF2C.....	80

INTRODUCTION

The Neural Crest and its Derivatives

The neural crest is a transient, migratory, multipotent, progenitor population, that is induced at the border between the neural plate, which forms the central nervous system, and the non-neural ectoderm (Le Douarin, 1999). As the neural plate folds over itself to form the neural tube, neural crest progenitors are positioned within, and adjacent to, the dorsal neural tube. Upon neural tube closure, these progenitors undergo an epithelial to mesenchymal transition and migrate throughout the body to give rise to different types of tissues (Fig. 1) (Knecht and Bronner-Fraser, 2002; Le Douarin, 1999).

I. Discovery and Origin of the Neural Crest

The neural crest was first described in chicken embryos by His (His, 1868) as a band of cells sandwiched between the presumptive epidermis and the neural tube. He called this band *Zwischenstrang*, meaning the intermediate chord. Since this first evidence, neural crest cells have been found in selachians, teleosts, amphibians, and all forms of vertebrates, including the most primitive vertebrate, lamprey (Le Douarin, 1999).

Some of the most significant contributions to our understanding of the neural crest and its derivatives were made by Le Douarin in the 1970s, and stemmed from her observation that cells from Japanese quails and chicks differed in that the interphase

nuclei of all embryonic and adult cells in the quail contained a large amount of heterochromatin (Le Douarin 1969; Le Douarin, 1973). She exploited this difference by generating embryonic quail-chick chimeras, in which distinct segments of neural folds from chick embryos were replaced with corresponding segments of neural folds from developmentally matched quail embryos prior to neural crest migration (Le Douarin 1969; Le Douarin, 1973). Using this quail-chick chimeric model, Le Douarin and her colleagues successfully mapped the destination and developmental fate of neural crest cells originating from different regions of the anterioposterior neural axis, and showed that the axial level of origin determined the migratory pathways taken by neural crest cells (Le Douarin, 1980; Le Douarin, 1999). These seminal experiments also showed that the neural crest makes some contribution to virtually every tissue in the embryonic and adult body (Le Douarin, 1980; Le Douarin, 1999). Since then, advances in transgenic analysis have allowed us to use the promoters of neural crest-specific genes to label the neural crest population with fluorescent and *lacZ* reporters, and conditionally inactivate genes specifically in the neural crest using tissue-specific recombinases (Chai et al., 2000; Danielian et al., 1998). For instance, *Wnt1*, which is transiently expressed during embryogenesis in the dorsal neural primordium and in the early migrating neural crest, has been successfully used to inactivate numerous genes early in the neural crest (Danielian et al., 1998).

II. Derivatives and Segmentation of the Neural Crest

The neural crest is remarkably multipotent, giving rise to a variety of diverse cell types. These include dorsal root and sympathetic ganglia, the glial cells of the peripheral

and enteric nervous systems, melanocytes, endocrine cells, and most of the bones and cartilage elements of the craniofacial skeleton (Fig.1) (Le Douarin, 1999).

Based on their migration patterns and developmental potential, neural crest cells can be divided into two distinct segments (Dupin et al., 2006):

Cranial or cephalic neural crest cells arise from the forebrain, midbrain and hindbrain (up to rhombomere 8) region of the neural tube, and migrate along a dorsolateral pathway to give rise to cranial neurons and glia, as well as most of the cartilage, membranous bones, and connective tissues of the face (Fig.1) (Dupin et al., 2006; Le Douarin and Dupin, 2003). In addition, cephalic neural crest cells also contribute to the thymus and the outflow tract (Dupin et al., 2006). Cells destined to form thymic cells, odontoblasts of the tooth primordia, and the bones of middle ear and jaw, first migrate into the pharyngeal arches, and pouches, and subsequently differentiate into these cell types (Couly et al., 2002). Interestingly, in teleosts, mesenchymal cells fated to contribute to craniofacial mesenchyme originate from both the cranial as well as trunk region, but in higher vertebrates only cells from the cephalic domain of the neural axis contribute to the craniofacial skeleton (Dupin et al., 2006; Le Douarin and Dupin, 2003).

Trunk neural crest cells give rise to enteric neurons and ganglia, melanocytes, and sympatho-adrenal cells (Fig.1) (Dupin et al., 2006; Le Douarin, 1999). The neural crest cells that are destined to become dorsal root ganglia, sympathetic ganglia, and the adrenal medulla, exit from the neural tube and migrate ventrolaterally through the anterior half of each sclerotome. Those trunk neural crest cells that remain in the sclerotome form the dorsal root ganglia containing the sensory neurons, while the cells that continue more

ventrally form the sympathetic ganglia and adrenal medulla (Dupin et al., 2006). Neural crest cells destined to become the pigment-synthesizing melanocytes migrate dorsolaterally into the ectoderm and subsequently make their way toward the ventral midline of the belly (Dupin et al., 2006; Le Douarin, 1999).

III. Disorders of the Neural Crest

The proper development of neural crest derivatives requires timely specification, migration, proliferation and differentiation of the mesenchymal precursors. Even subtle perturbations in one or more of these processes results in neurocristopathies (Farlie et al., 2004; Trainor, 2005). Neurocristopathies can present as tumors of neural crest cells, such as neurofibroma, neuroblastoma, medullary thyroid cancer, pheochromocytoma, melanoma and several less common neoplasms, or as congenital anomalies, including craniofacial, conotruncal, pigmentation (piebaldism, albinism, Waardenburg), and innervation defects (Hirschsprung) (Farlie et al., 2004; Trainor, 2005). Craniofacial defects can present as isolated clefts of the lip or palate, or as more complex malformations in multiple cranial neural crest derivatives, as seen in patients of Treacher Collins Syndrome and DiGeorge Syndrome (Farlie et al., 2004; Trainor, 2005). Several transcription factors have been identified to play important roles in the neural crest, and mutations in the genes encoding these factors result in neurocristopathies. The work presented here highlights the function and cofactor interactions of one such transcription factor, MEF2C, in the development of two neural crest derivatives - the craniofacial skeleton and melanocytes.

The MADS-Domain Transcription Factor MEF2C

MEF2C belongs to the Myocyte enhancer factor 2 (MEF2) family of MADS (present in MCM-1, *Agamous*, *Deficiens*, and Serum Response Factor) domain transcription factors (Shore and Sharrocks, 1995). There are four vertebrate MEF2 genes (MEF2A, MEF2B, MEF2C, and MEF2D), and a single *Mef2* gene in *Drosophila*. In *Drosophila*, *Mef2c* is first expressed in early mesoderm and subsequently in different muscle cell lineages where it is required for myoblast differentiation (Bour et al., 1995; Lilly et al., 1995; Ranganayakulu et al., 1995). The four vertebrate MEF2 genes are expressed in multiple embryonic and adult lineages, including the heart, skeletal muscle, central nervous system, and immune cells (Black and Olson, 1998; Potthoff and Olson, 2007).

Mef2c is the first member of the MEF2 family to be expressed during development, and is widely appreciated for its role in the development of several lineages, including cardiac and skeletal muscle, immune cells, and the central nervous system (Edmondson et al., 1994; Potthoff and Olson, 2007). *Mef2c*-null mice die around E9.5 due to vascular and cardiac looping defects (Lin et al., 1997). *Mef2a*-null mice survive to birth, but exhibit perinatal lethality due to an array of cardiovascular defects (Naya et al., 2002). *Mef2d*-null mice appear phenotypically normal (Arnold et al., 2007).

Interestingly *Mef2c* expression in these diverse developmental lineages is transcriptionally regulated through distinct modular enhancers, and thus has served as an excellent model to define early transcriptional pathways controlling the development of

multiple lineages (De Val et al., 2004; Dodou et al., 2004; Dodou et al., 2003; Verzi et al., 2005; Wang et al., 2001). In addition, MEF2C activity as well as its interaction with cofactors is highly influenced by posttranslational modifications such as phosphorylation, acetylation and sumoylation (Kang et al., 2006; Khiem et al., 2008; Ma et al., 2005; Zhu and Gulick, 2004).

MEF2 transcription factors bind to a consensus DNA-binding region known as a MEF2 element (5'-YTAWWWWTAR-3') as homodimers or heterodimers, and can, through interactions with cell- and tissue-specific cofactors, function as both positive and negative regulators of gene transcription (Black and Olson, 1998; McKinsey et al., 2002).

A Role for MEF2C in the Neural Crest

Mef2c expression can be detected around embryonic day (E) 8.5 in mice in pre-migratory neural crest precursors adjacent to the neural folds (Edmondson et al., 1994) and later around E9.5 in the craniofacial mesenchyme of the first and second branchial arch as well as frontonasal mass (Fig.2). Despite its early and robust expression in the neural crest, *Mef2c*'s role in this lineage was not previously explored because germline inactivation of *Mef2c* results in early embryonic cardiac lethality prior to neural crest differentiation (Bi et al., 1999; Lin et al., 1998; Lin et al., 1997). In order to circumvent this early lethality, *Mef2c* was inactivated in the neural crest using a conditional gene inactivation approach (Fig. 3) (Verzi et al., 2007). Mice bearing a floxed allele of *Mef2c* were crossed to *Mef2c*^{+/+} mice expressing Cre recombinase under the control of the *Wnt1*

promoter (Fig. 3), and the progeny from this cross were scored for viability at birth (Verzi et al., 2007). Neural crest conditional *Mef2c* knockout mice were born alive and at expected Mendelian frequencies, but began to look cyanotic within a few minutes of birth and soon after died from asphyxiation. Gross and histological examination of neural crest conditional *Mef2c* knockout heads revealed a cleft in the posterior palate (Fig. 4, bottom left panel), which resulted in a significant narrowing of the airway (Fig. 4, bottom right panel) and consequent asphyxiation (Verzi et al., 2007). Skeletal analysis of *Mef2c* neural crest knockout heads also identified defects in several other neural crest-derived craniofacial elements, including loss of the tympanic ring, a severely hypoplastic mandible, malformed or absent temporal and mandibular processes, and hypoplastic zygomatic and frontal bones (Fig. 5) (Verzi et al., 2007). In contrast, the parietal bone, which is not of neural crest origin, was unaffected in these animals (Verzi et al., 2007). This phenotype clearly indicates that *Mef2c* is required for the proper development of cranial neural crest derivatives.

The discovery of this novel role for *Mef2c* during craniofacial development prompted us to investigate the molecular and cellular basis of *Mef2c* function in the cranial neural crest lineage and also determine if *Mef2c* plays a role in other neural crest derivatives such as the peripheral nervous system and melanocytes. The overall goal of this thesis has been to further dissect MEF2C function in the neural crest by identifying the downstream effectors and transcriptional cofactors of MEF2C in the cranial neural crest (Chapter 1 and Chapter 2), and characterizing *Mef2c* function in the melanocyte lineage (Chapter 3).

In Chapter 1, we searched for potential molecular targets of *Mef2c* in the cranial neural crest. Through *in situ* hybridization analyses we show that MEF2C is specifically required for the cranial neural crest expression of the homeodomain transcription factor genes, *Dlx5* and *Dlx6*, and the bHLH transcription factor gene, *Hand2*. These results are strongly supported by the observation that inactivation of one or more of these genes in mice results in a craniofacial phenotype very similar to the phenotype exhibited by neural crest knockouts of *Mef2c* (Beverdam et al., 2002; Depew et al., 2002; Robledo and Lufkin, 2006). *Dlx5*, *Dlx6*, and *Hand2* are downstream transcriptional effectors of Endothelin signaling in the cranial neural crest (Charite et al., 2001; Clouthier et al., 2000; Ruest et al., 2004; Thomas et al., 1998). The observation that the early cranial neural crest expression of these factors is dependent on *Mef2c* suggests that MEF2C function in this lineage may also be dependent on Endothelin signaling.

In Chapter 2, the functional and transcriptional interaction between MEF2C and *Dlx5/6* was further dissected using a combination of bioinformatic, *in vitro* transactivation, and *in vivo* transgenic analyses. We identified a highly conserved enhancer in the *Dlx5/6* locus that directs expression to the early cranial neural crest lineage. In transactivation studies, this enhancer was strongly activated by MEF2C alone, which suggests that *Dlx5* and *Dlx6* may be direct transcriptional targets of MEF2C during craniofacial development. In addition, cotransfection of the enhancer with MEF2C and *Dlx5* resulted in robust synergy implying that *Dlx5* is not only a transcriptional target but also a cofactor of MEF2C. This transcriptional synergy is also supported by a strong

genetic interaction between *Mef2c* and *Dlx5/6* during craniofacial development. We also show that MEF2C and Dlx5 are capable of physically interacting with each other through their DNA binding domains, thus providing a biochemical basis for the functional synergy between these proteins.

The final chapter of this thesis explores MEF2C function in the neural crest-derived melanocyte lineage. Conditional loss of *Mef2c* in the neural crest results in reduced expression of melanocyte genes during development, and a significant reduction in the number of melanocytes at birth.

Overall, the research findings described in this thesis make an invaluable contribution to our understanding of the cellular and molecular interactions governing MEF2C function during the development of two neural crest derivatives – the cranial skeleton and melanocytes. In addition, identification of the functional and biochemical basis of MEF2C-Dlx5/6 interactions lends significant insight into the general transcriptional interplay between MEF2 proteins and homeodomain transcription factors which are co-expressed in several developmental lineages.

Figure Legends

Figure 1: The neural crest gives rise to multiple cell types

Neural crest cells migrate throughout the body and differentiate into many different cell types. Cells in the trunk region form melanocytes and several neuron and glia cell types. Neural crest cells in the cranial (the embryonic head) region give rise to cranial neurons

and glia but also have the potential to form mesenchymal derivatives, such as cartilage, bone and connective tissue. (Knecht and Bronner-Fraser, 2002)

Figure 2: *Mef2c* is expressed in the neural crest-derived craniofacial mesenchyme. Whole mount (A) and sagittal section (B) *in situ* hybridization showing endogenous *Mef2c* expression in E9.5 wild type mouse embryos. The first branchial arch is indicated by red arrowheads in both panels; asterisks mark *Mef2c* expression in the frontonasal mesenchyme. (Verzi et al., 2007)

Figure 3: *Mef2c* was inactivated in the neural crest using a conditional gene inactivation approach.

Figure depicts the mouse crosses set up to specifically inactivate *Mef2c* in the neural crest. (Verzi et al., 2007) (Courtesy: Mike Verzi)

Figure 4: Cleft palate and upper airway constriction in neural crest conditional *Mef2c* knockout mice.

Gross (left panels) and histological (right panels) examination shows cleft palate (arrowhead in left bottom panel) and constriction of the upper airway (arrowhead in right bottom panel) in the *Mef2c* conditional knockouts. (Verzi et al., 2007) (Courtesy: Mike Verzi)

Figure 5: Skeletal analysis of *Mef2c* neural crest knockout heads

Skeleton preparations of neonatal heads, stained with alizarin red (bone) and alcian blue (cartilage), highlight the craniofacial defects seen in neural crest conditional knockouts of *Mef2c* (B,D) in comparison to littermate controls (A,C). Arrowheads mark location of the tympanic ring in a control skull (A) and its absence in the mutant skull (B). Bars of equal size show that the mutant mandible is shorter than the control (A, B). Panels C and D zoom in to highlight other hypoplastic/absent bones including tympanic ring (1), zygomatic bone (2), mandibular processes (3), and temporal bone processes (4). (Verzi et al., 2007) (Courtesy: Mike Verzi)

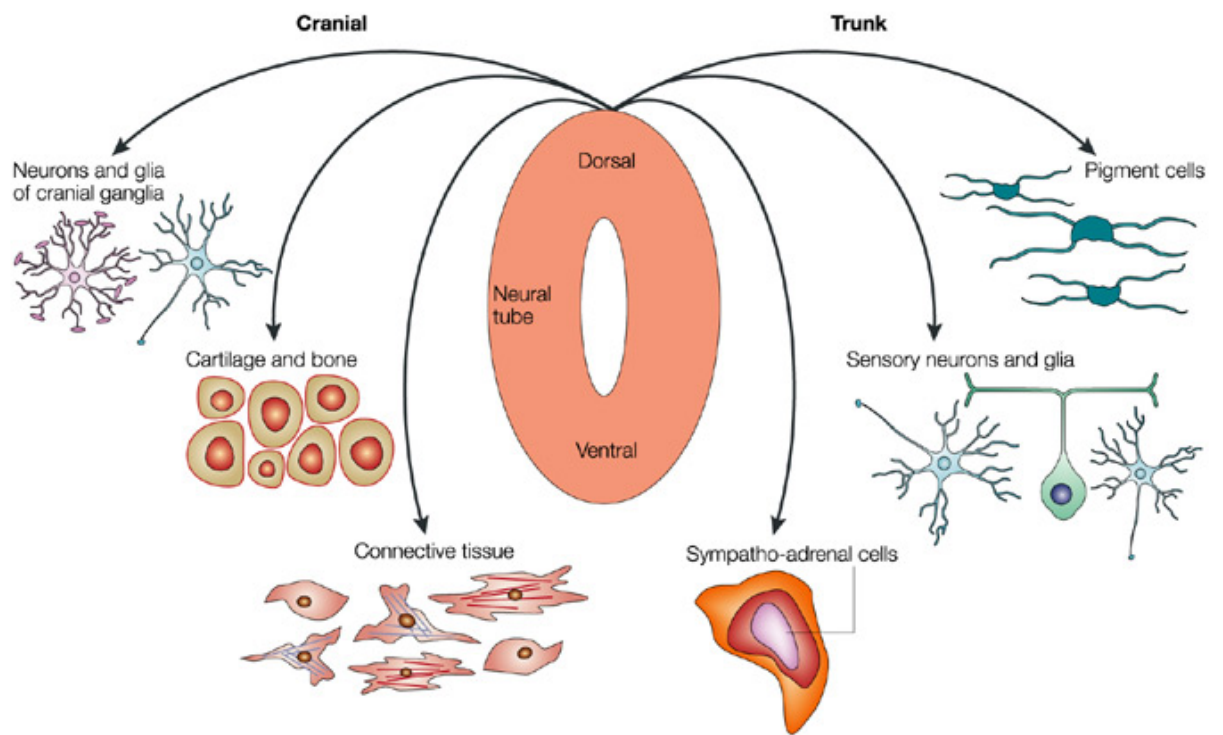


Figure 1: The neural crest gives rise to multiple cell types

(Knecht and Bronner-Fraser, 2002)

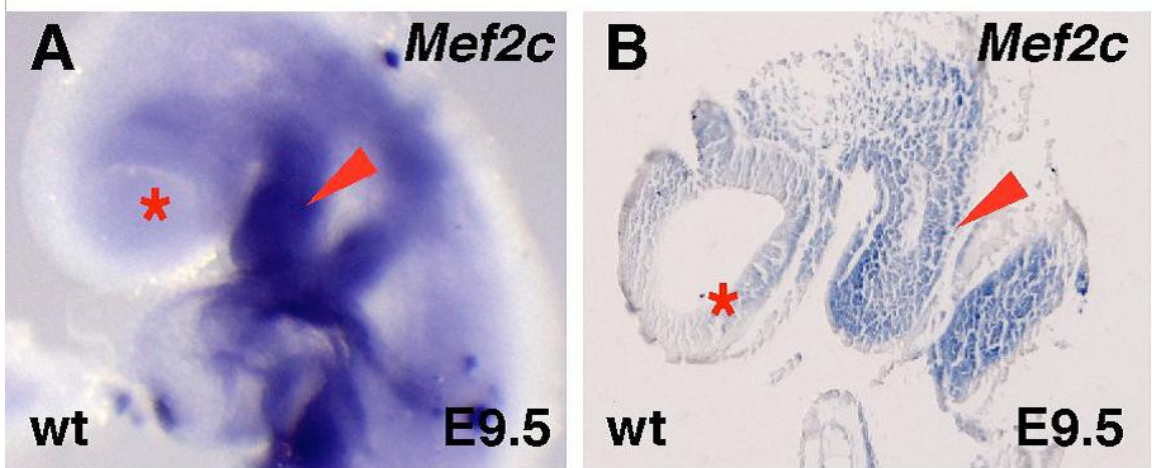


Figure 2: *Mef2c* is expressed in the neural crest-derived craniofacial mesenchyme
(Verzi et al., 2007)

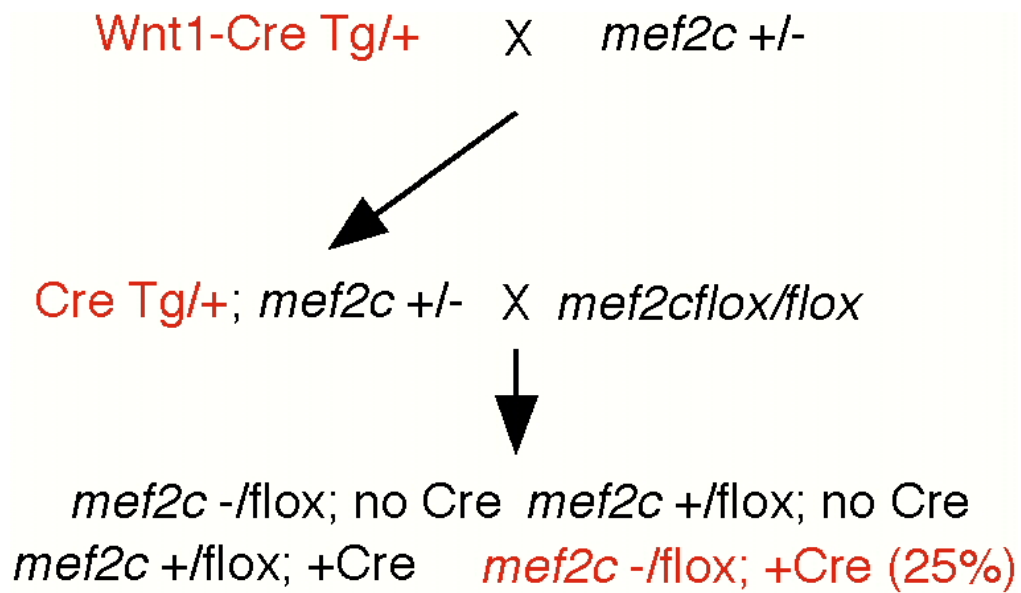


Figure 3: *Mef2c* was inactivated in the neural crest using a conditional gene inactivation approach. (Verzi et al., 2007) (Courtesy: Mike Verzi)

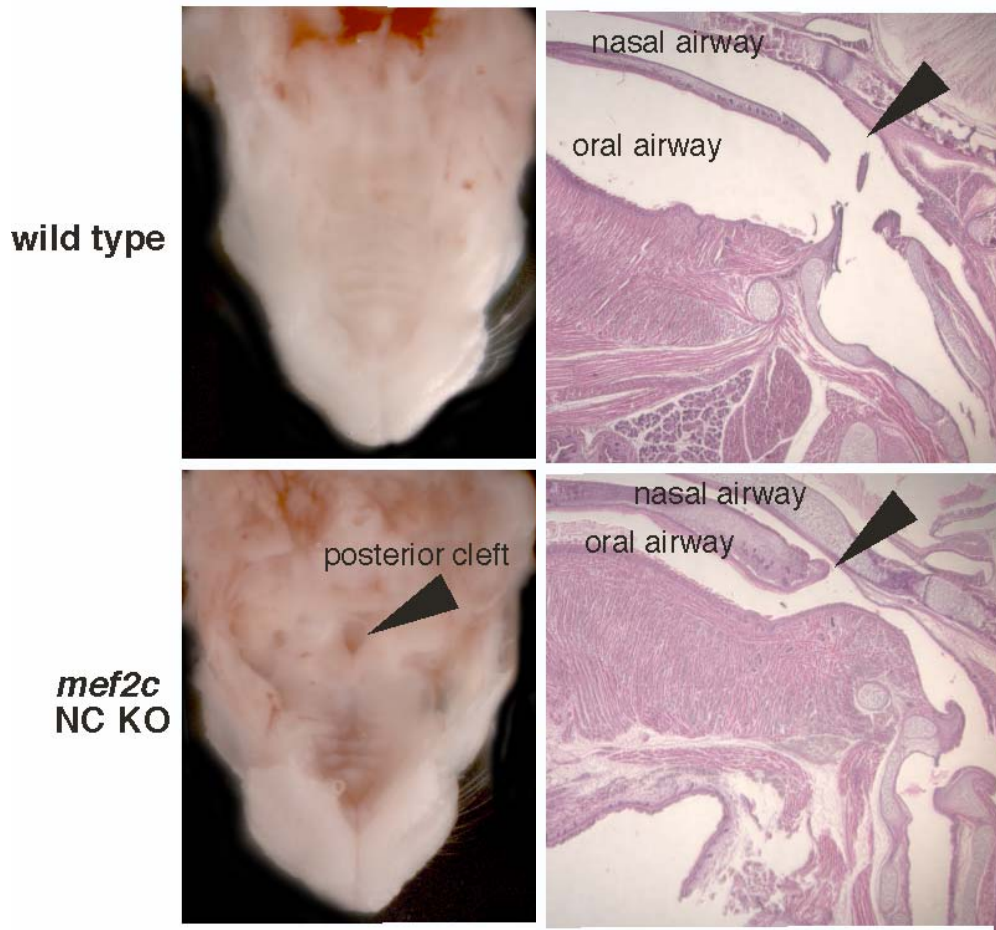


Figure 4: Cleft palate and upper airway constriction in neural crest conditional *Mef2c* knockout mice. (Verzi et al., 2007) (Courtesy: Mike Verzi)

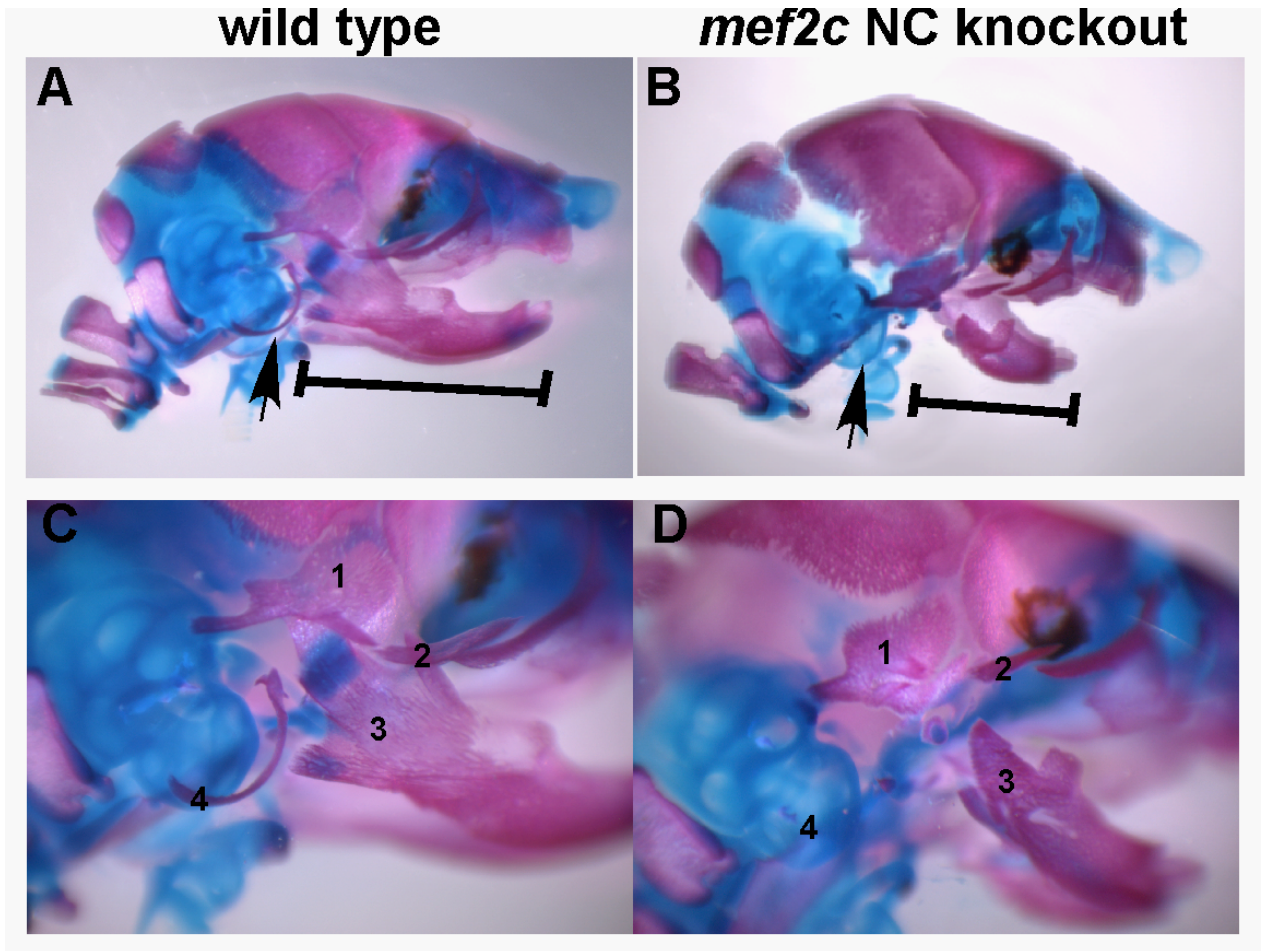


Figure 5: Skeletal analysis of *Mef2c* neural crest knockout heads

(Verzi et al., 2007) (Courtesy: Mike Verzi)

CHAPTER 1

The Transcription factor MEF2C is an upstream regulator of *Dlx5*, *Dlx6* and *Hand2* during craniofacial development

BACKGROUND

Vertebrate craniofacial development is a complex multi-step process that begins with the specification of cranial neural crest progenitors from the dorsal neural tube (Fig.1). Upon specification, these progenitors undergo an epithelial to mesenchymal transition and begin to migrate subectodermally along defined pathways to form the craniofacial mesenchyme, which ultimately differentiates into the cartilage, bone, and connective tissues of the face and neck (Fig.6). The axial level of origin of cranial neural crest cells defines the cell and tissue types to which they eventually contribute (Graham et al., 2004; Lumsden et al., 1991; Osumi-Yamashita et al., 1994; Schilling and Kimmel, 1994; Serbedzija et al., 1992; Trainor and Tam, 1995). Cells originating from the midbrain and rhombomeres 1 and 2 of the hindbrain migrate into the frontonasal mass and first branchial arch, and give rise to most of the bones of the face and skull, including the lower and upper jaw (Fig.6, red) (Graham et al., 2004). A second stream of cells arising primarily at the level of rhombomere 4 of the hindbrain migrates into the second pharyngeal arch and eventually gives rise to the hyoid skeleton (Fig.6, green) (Graham et al., 2004). Finally, cells originating adjacent to post-otic rhombomeres 6 and 7 (Fig.6, blue) contribute to the aortic arches and outflow tract (Graham et al., 2004)

The specification, migration and proper differentiation of cranial neural crest cells is under tight molecular control, and several transcription factors and signaling molecules have been implicated in one or more of these processes. These include the Dlx homeodomain transcription factors, Dlx5 and Dlx6, and the bHLH transcription factor Hand2. *Dlx* homeobox genes are mammalian orthologs of the *Drosophila Distal-less (Dll)* gene and consist of six genes (*Dlx1-6*) that are organized into the *Dlx1/2*, *Dlx3/4*, and *Dlx5/6* bigene clusters. All six *Dlx* genes are expressed in proximodistal restricted patterns within the neural crest derived mesenchyme of the first and second branchial arches (Beverdam et al., 2002; Depew et al., 2002; Panganiban and Rubenstein, 2002; Qiu et al., 1997; Robledo and Lufkin, 2006). *Dlx5* and *Dlx6* are restricted to the distal region of the branchial arches, and germline inactivation of these genes in *cis* in mice results in severe craniofacial defects in first and second arch derivatives, including a homeotic transformation of the lower jaw into the maxilla (Beverdam et al., 2002; Depew et al., 2002; Robledo and Lufkin, 2006). Dlx6 has also been shown to directly activate *Hand2* gene expression in the first and second branchial arches via a conserved branchial arch enhancer element (Charite et al., 2001). Deletion of this *Hand2* enhancer in mice results in defects in cranial neural crest derivatives including the palate and mandible (Yanagisawa et al., 2003)

Branchial arch expression of *Dlx5/6* and *Hand2* is dependent on Endothelin signaling. Endothelins are small 21 amino acid peptides implicated in various biological processes, including craniofacial, cardiac, and peripheral nervous system development

(Yanagisawa and Masaki, 1989). These peptides are proteolytically cleaved into the mature 21-amino acid peptide by endothelin-converting enzymes (ECE-1 and ECE-2) and other proteases (Xu et al., 1994). Once active, Endothelins signal through G-protein-coupled receptors (ET-A and ET-B) to mediate downstream biological processes (Ishikawa et al., 1989; Yanagisawa and Masaki, 1989). Among the three known Endothelin isopeptides (ET-1, ET-2, and ET-3), only ET-1 has been implicated in the development of cranial neural crest derivatives. ET-1 and the protease ECE-1 are expressed in the epithelium and paraxial mesoderm of the first and second branchial arches, while the receptor ET-A is expressed in the neural crest-derived ectomesenchyme of the pharyngeal arches (Barni et al., 1995; Clouthier et al., 1998; Francis-West et al., 1998; Kurihara et al., 1994; Maemura et al., 1996). Mice homozygous for a targeted mutation of *Ednra*, *Edn1*, or *Ece1* are viable to term but die shortly after birth from mechanical asphyxiation due to severe craniofacial malformations in first and second arch derivatives (Clouthier et al., 1998; Kurihara et al., 1994; Yanagisawa et al., 1998a).

The craniofacial defects in *Mef2c* neural crest conditional knockout mice (Fig.4 and Fig.5) (Verzi et al., 2007) are similar to the defects seen in *Edn1*, *Ednra*, *Ece1* and *Dlx5/6* knockout mice (Clouthier et al., 1998; Kurihara et al., 1994; Yanagisawa et al., 1998b). This prompted us to examine the branchial arch-specific expression of the endothelin targets, *Dlx5*, *Dlx6*, and *Hand2*, in *Mef2c* neural crest conditional knockout mice. Indeed, the expression of all three genes was significantly reduced in *Mef2c* neural crest knockout embryos (Verzi et al., 2007). In contrast, the expression of *Prx1*, which is

also required for cranial neural crest development, but is not downstream of Endothelin signaling, was unaffected in *Mef2c* conditional knockout embryos (Verzi et al., 2007). Together, these observations strongly implicate *Mef2c* in the Endothelin signaling pathway as an upstream regulator of *Dlx5*, *Dlx6* and *Hand2*.

RESULTS

***Mef2c* is required for the branchial arch expression of *Dlx5*, *Dlx6*, and *Hand2*.**

The neonatal craniofacial phenotype of *Mef2c* neural crest (NC) knockouts (Fig.4 and Fig.5) was strikingly similar to the phenotype exhibited by mice deficient in *Dlx5/6* and *Hand2*, which are downstream effectors of the Endothelin pathway. Therefore we wanted to determine if *Mef2c* was also a component of the Endothelin pathway of craniofacial development. We assessed the expression of these Endothelin targets in *Mef2c* neural crest knockout embryos by whole mount and section *in situ* hybridization at E9.5, which is the time when *Mef2c* shows robust expression in the neural crest mesenchyme of the branchial arches and frontonasal mass (Fig. 2). As shown in control embryos in Figure 7, *Dlx5* (panel A and G), *Dlx6* (panel C and I), and *Hand2* (panel E and K), show strong expression in the first and second branchial arches at this developmental stage (Verzi et al., 2007). However, the expression of all three genes was almost completely absent in *Mef2c* NC knockout embryos (Fig.7 compare panels A, C, E to B, D, and F, and panels G, I, and K to H, J, and L). In contrast, the branchial arch-specific expression of *Prx1*, which is another important regulator of craniofacial development but not downstream of endothelin signaling, was comparable between

Mef2c NC knockout embryos and their littermate controls (Fig. 7, compare panels M and N) (Verzi et al., 2007). Cellular analyses of the branchial arches revealed no obvious differences in proliferation or apoptosis between *Mef2c* NC knockout embryos and their littermate controls, and fate mapping studies, using the *Rosa26R Cre*-dependent reporter line (Verzi et al., 2007), indicated that neural crest migration into the branchial arches was comparable in these embryos (data not shown). Taken together, these observations strongly suggest that conditional loss of *Mef2c* in the neural crest specifically impacts the *Dlx5/6-Hand2* molecular pathway of craniofacial development, and that the observed reduction in expression of these genes is not due to a general loss of branchial arch integrity.

DISCUSSION

Congenital craniofacial anomalies are among the most common causes of birth defects in infants, signifying the importance of understanding the molecular basis of craniofacial development. Although several transcription factors have been implicated in craniofacial development, little is known about the molecular networks that connect these proteins to upstream signaling cues and downstream effectors. Our research group has identified a novel role for the MADS domain transcription factor MEF2C during vertebrate craniofacial development, where neural crest-specific loss of *Mef2c* results in neonatal lethality due to severe craniofacial defects, including hypoplasia or complete loss of several bones of the cranial skeleton (Fig.4 and Fig.5) (Verzi et al., 2007). The specific aim of the work presented here was to identify the downstream targets of

MEF2C in the craniofacial lineage to gain a better understanding of the molecular network governing MEF2C function in this lineage. We show that *Mef2c* is required for the branchial arch expression of the Dlx homeodomain transcription factors, Dlx5 and Dlx6, and the bHLH transcription factor Hand2. The fact that these transcription factors have been shown to be components of the Endothelin pathway of craniofacial development, and the craniofacial defects exhibited by neural crest knockouts of *Mef2c* closely resemble the defects seen in animals deficient in Endothelin signaling strongly suggests that *Mef2c* may also be a downstream effector of Endothelin signaling during craniofacial development. Interestingly, in addition to the cranial neural crest, *Mef2c* and Endothelin receptors are co-expressed in other developmental lineages, including the heart and the peripheral and enteric nervous systems, and are co-expressed postnatally as well. Thus, an interaction between MEF2 and Endothelin signaling may have broad implications for development and disease.

The observed transcriptional hierarchy between MEF2C, Dlx5/6 and Hand2 raises a number of important questions. *Dlx5* and *Dlx6* are proposed to play redundant roles during craniofacial development, since simultaneous deletion of both genes results in much more severe craniofacial defects, including a homeotic transformation of the lower jaw into upper jaw, than those seen in animals lacking either one of the two genes (Beverdam et al., 2002; Depew et al., 2002). A role for MEF2C as an upstream activator of *Dlx5/6* during craniofacial development suggests that the phenotype in *Mef2c* neural crest knockout mice should be more severe than that observed in *Dlx5/6* double knockout mice. However, *Mef2c* neural crest knockout mice do not exhibit homeotic

transformation of the lower jaw (Fig.4 and Fig.5). A possible explanation for this observation is that, unlike *Dlx5/6*^{-/-} embryos, *Mef2c* neural crest knockout embryos show a significant reduction but not complete loss of *Dlx5/6* expression in the branchial arches. This suggests that either there are additional MEF2-independent regulators of *Dlx5/6* expression in the craniofacial mesenchyme or that *Mef2c* function is partially compensated by the other three MEF2 factors. Functional redundancy between MEF2 factors has also been observed in other developmental lineages (Potthoff and Olson, 2007).

The identification of MEF2C as an upstream activator of *Dlx5*, *Dlx6*, and *Hand2* also prompted us to ask if these genes are direct transcriptional targets of MEF2C. MEF2 and Dlx transcription factors are known to directly regulate gene expression by binding to conserved consensus MEF2 and HOX sites, respectively, within the loci of their targets (Feledy et al., 1999; Molkenin et al., 1996). Several direct targets of *Dlx5/6* have already been identified within the craniofacial mesenchyme, including *Hand2*, *Dlx3*, and *Gbx2* (Charite et al., 2001; Jeong et al., 2008). We used a bioinformatic screen to search for MEF2 dependent enhancers within the *Dlx5/6* and *Hand2* loci. The next chapter of this thesis describes the identification of a highly conserved MEF2-dependent branchial arch enhancer in the *Dlx5/6* locus, and further dissects the genetic, biochemical and cellular interactions between MEF2C and *Dlx5/6* during craniofacial development.

Figure Legends

Figure 6: Cranial neural crest cells migrate along distinct pathways

Cranial neural crest migrates in three streams. The trigeminal stream (red), which emanates from the region overlying the midbrain (mb) and rhombomeres (r) 1 and 2, migrates into the upper jaw primordia, underneath the eye, and into the first pharyngeal arch (PA1), to form the lower jaw. The hyoid stream (green), from rhombomere 4, migrates into the second pharyngeal arch, forming the jaw support. The post-otic stream (purple) emerges from the neural tube adjacent to rhombomeres 6 and 7 and populates the caudal pharyngeal arches (Graham et al., 2004).

Figure 7: *Dlx5*, *Dlx6*, and *Hand2* expression in the first branchial arch requires MEF2C. Whole mount (A-F), and section (G-N) *in situ* hybridization shows that *Dlx5* (A, G vs. B, H), *Dlx6* (C, I vs. D, J), and *Hand2* (E, K vs. F, L) expression is nearly absent in the branchial arches of *Mef2c* neural crest knockout embryos at E9.5. In contrast, *Prx1* expression is comparable between controls (M) and *Mef2c* neural crest knockouts (N).

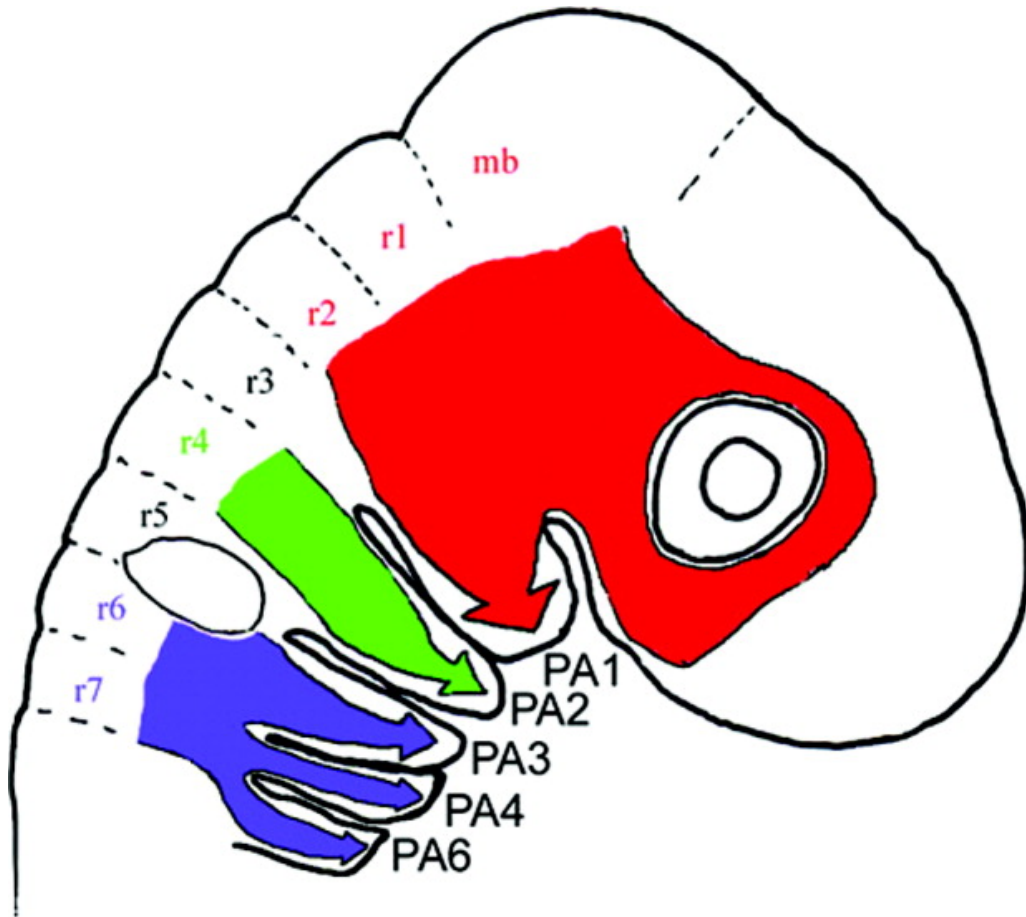


Figure 6: Cranial neural crest cells migrate along distinct pathways

(Couly et al., 2002; Graham et al., 2004)

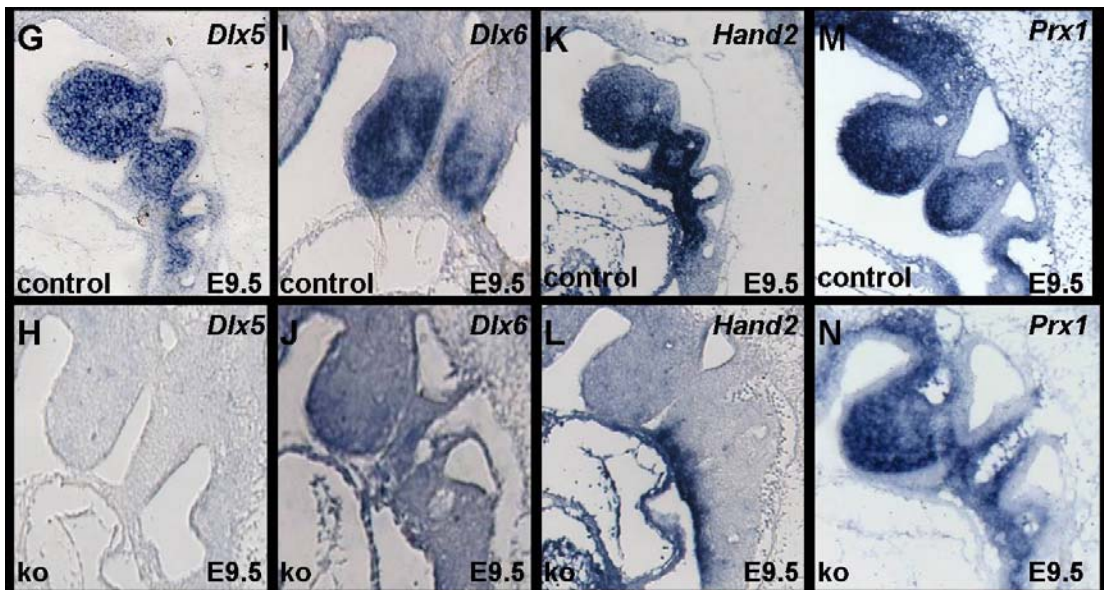
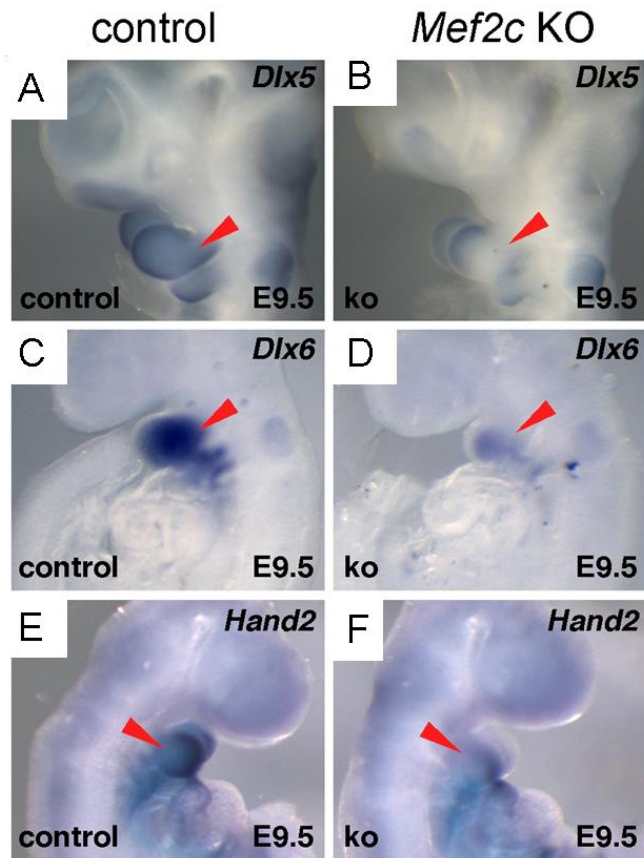


Figure 7: *Dlx5*, *Dlx6*, and *Hand2* expression in the first branchial arch require MEF2C (Verzi et al., 2007)

CHAPTER 2

Genetic and functional interaction between MEF2C and Dlx5/6 is essential for craniofacial development.

INTRODUCTION

Craniofacial malformations constitute the majority of congenital birth defects in humans (CDC, 2006). Among these, clefts of the lip and palate are the most common, occurring in as many as 1 in every 600 newborns (CDC, 2006). So far, treatment of palate defects is limited to expensive and invasive surgeries, underlining the importance of understanding the cellular and molecular basis of palate development.

Vertebrate palate development begins with the formation of bilateral palatal shelves on the medial wall of the maxillary process, which occurs around E11.5 in mice. Between E12.5 and E13.5, the palatal shelves proliferate extensively and extend vertically along the sides of the tongue. Subsequently, by E14.5, the two shelves elevate above the tongue and begin to elongate medially toward the midline. Palate formation is finally complete when the medial edges of the opposing palatal shelves come in contact with each other to allow fusion by E15.5 (Greene and Pratt, 1976; Okano et al., 2006).

The proper development of the palate, and the rest of the cranial skeleton, is highly influenced by the timely proliferation, migration and osteogenic differentiation of

mesenchymal precursors. Even minor perturbations in these cellular processes can affect palate growth, and result in partial or complete cleft of the palate (Gritli-Linde, 2007). Several families of transcription factors have been identified to play crucial roles in the development of the palate and other bones of the cranial skeleton (Francis-West et al., 1998; Gritli-Linde, 2007). However, little is known about how these factors structurally and functionally interact with each other to interpret upstream signaling cues and orchestrate developmental decisions.

The previous chapter of this thesis discussed the requirement of the MADS domain transcription factor MEF2C for the proper development of cranial neural crest derivatives (Fig.4 and Fig.5) (Verzi et al., 2007). Neural crest-specific loss of *Mef2c* in mice causes severe defects in the cranial skeleton, including a hypoplastic mandible and cleft palate, which results in neonatal lethality due to mechanical asphyxiation (Fig.4 and Fig.5) (Verzi et al., 2007). On a molecular level, loss of *Mef2c* specifically disrupts the expression of downstream components of the Endothelin pathway, resulting in significant loss in the expression of the *Dlx* homeodomain transcription factor genes *Dlx5* and *Dlx6*, and the bHLH transcription factor gene *Hand2* (Fig.7) (Verzi et al., 2007).

In this chapter, the functional interaction between MEF2C and *Dlx5/6* is further dissected. We identify a highly conserved MEF2-dependent branchial arch enhancer within the *Dlx5/6* locus that is synergistically activated by MEF2C and *Dlx5*, suggesting that *Dlx5* is not only a transcriptional target but also a cofactor of MEF2C (Verzi et al., 2007). In addition to this transcriptional synergy, *Mef2c* and *Dlx5/6* interact genetically

(Verzi et al., 2007). Mice heterozygous for either *Mef2c* or *Dlx5/6* alone are viable and fertile, but mice heterozygous for both *Mef2c* and *Dlx5/6* (*Dlx5/6*^{+/-}; *Mef2c*^{+/-}) exhibit perinatal lethality. Skeleton preparations of *Dlx5/6*^{+/-}; *Mef2c*^{+/-} heads revealed hypoplasia of the pterygoid bones and a cleft in the posterior palate, strongly suggesting that these genes interact during craniofacial development (Verzi et al., 2007). Histological analysis of palate development indicated that palatal shelf specification and descent was normal, but the subsequent elevation and closure of the palatal shelves was significantly delayed in *Dlx5/6*^{+/-}; *Mef2c*^{+/-} animals, indicating that these stages of palatogenesis may be sensitive to the dosage of these transcription factors. *Dlx5/6*^{+/-}; *Mef2c*^{+/-} animals also show reduced osteogenic differentiation within the palatal shelves, which supports the notion that MEF2C and Dlx5/6 coregulate targets involved in bone differentiation. In addition to this genetic and transcriptional synergy, we also uncover a strong physical interaction between MEF2C and Dlx5, mediated through their DNA binding domains. Taken together, these results lend significant insight into our understanding of the cellular and biochemical basis of the functional interaction between *Mef2c* and *Dlx5/6* during craniofacial development. The Dlx5-MEF2C interaction during craniofacial development also provides a valuable tool for probing similar interactions between MADS-family transcription factors and homeobox proteins in other developmental lineages.

RESULTS

An evolutionarily conserved enhancer in the *Dlx5/6* locus is bound and activated by MEF2C

Since *Dlx5/6* and *Hand2* expression was reduced in the branchial arches of *Mef2c* neural crest knockout embryos, we hypothesized that MEF2C might directly regulate their expression through tissue-specific enhancers. To identify potential enhancers, all the conserved non-coding regions within the *Hand2* and *Dlx5/6* loci were screened for MEF2 binding elements using the VISTA genome analysis software (Frazer et al., 2004). We identified an evolutionarily conserved 1300-bp fragment immediately upstream of the *Dlx6* coding sequence (Fig. 8A) that contained four highly conserved MEF2 binding sites (Fig. 8B, MEF2-1, MEF2-2, MEF2-3 and MEF2-4) (Verzi et al., 2007). To determine whether these putative MEF2 sites represented *bona fide cis*-acting elements, radiolabeled probes containing each of these sites were tested for MEF2C binding *in vitro* by EMSA (Fig 9 and data not shown). MEF2C bound robustly to radiolabeled probes representing MEF2-3 (Fig. 9A, lane 2) and MEF2-4 (Fig. 9A, lane 8), and weakly to MEF2-1 (data not shown) and MEF2-2 (data not shown). The observed interaction with each MEF2 site was specific since excess unlabeled probe efficiently competed for MEF2C binding with the radiolabeled probe (Fig.9A, lanes 3 and 9). On the other hand, mutant versions of the probes failed to compete for MEF2C binding (Fig.9A, lanes 4 and 10). A *bona fide* control MEF2 element from the *Myogenin* promoter (Dodou et al., 2003), but not a mutant version of this probe, also efficiently competed for binding to each of these MEF2 sites (Fig. 9A, lanes 5 and 11 vs. lanes 6 and 12).

Since the MEF2 sites within the *Dlx5/6* enhancer were bound robustly by MEF2C, we tested whether the enhancer could be *trans*-activated by MEF2C *in vitro*.

When 3T3 fibroblast cells were co-transfected with pRK5-MEF2C-VP16 and a control *lacZ* reporter plasmid under the control of a minimal TK promoter, no reporter activity was detected (Fig.9B, lane 2). Co-transfection of a *Dlx5/6 lacZ* reporter plasmid (*Dlx5/6-TK*) with a pRK5 plasmid lacking MEF2C-VP16 also showed no reporter activity (Fig.9B, lane 3). However, co-transfection of the cells with pRK5-MEF2C-VP16 and *Dlx5/6-TK* resulted in 12-fold activation of the reporter (Fig.9B, lane 4), which was dependent on the MEF2 sites, since mutation of these sites almost completely abolished MEF2 *trans*-activation of the reporter (Fig.9B, lane 6) (Verzi et al., 2007). Taken together, the results of the binding assay and *trans*-activation studies strongly suggest that the MEF2 elements within the *Dlx5/6* enhancer are *bona fide* MEF2C sites, and implicate MEF2C as a direct transcriptional regulator of *Dlx5/6*.

The *Dlx5/6* enhancer directs expression to the first and second branchial arches during embryonic development

Since the *Dlx5/6* enhancer showed strong MEF2C-dependent activation *in vitro*, we next tested its activity *in vivo*. The 1300-bp fragment was cloned into the *Hsp68-lacZ* reporter plasmid, and the resulting construct was used to generate transgenic embryos. As depicted in Figure 10, this *Dlx5/6* enhancer directed strong *lacZ* expression to the craniofacial mesenchyme of the first and second branchial arches as well as frontonasal mass at E9.5 (Verzi et al., 2007). This expression was very similar to the endogenous *Dlx5* and *Dlx6* expression in the arches (Fig. 7), which supports the notion that this is a *bona fide* *Dlx5/6* enhancer. Taken together, the MEF2-dependent activation of this enhancer *in vitro*, and its activity in the craniofacial mesenchyme, strongly suggests that

MEF2C directly regulates *Dlx5/6* expression within the developing craniofacial mesenchyme via this *Dlx5/6* enhancer.

The *Dlx5/6* branchial arch enhancer is cooperatively activated by MEF2C and Dlx5

In addition to the four conserved MEF2 sites, the *Dlx5/6* enhancer also contains multiple potential homeodomain protein (HOX) binding sites (Fig. 8). Since previous studies have identified auto- and cross-regulation among *Dlx* genes (Sumiyama and Ruddle, 2003), we wanted to determine if the *Dlx5/6* enhancer was activated by Dlx proteins. To test this notion, the *Dlx5/6-lacZ* reporter plasmid was cotransfected with a Dlx5 expression plasmid in 3T3 cells (Fig. 11). Cotransfection with Dlx5 resulted in a robust 50-fold activation of the *Dlx5/6* reporter (Fig. 11, lane 5), strongly implicating auto-regulation as a potential mode of positive feedback control of *Dlx5/6* expression.

The close proximity of the MEF2 and HOX elements in the *Dlx5/6* enhancer prompted us to determine if the enhancer may be coactivated by MEF2C and Dlx5. Indeed, co-transfection of MEF2C-VP16 and Dlx5 expression plasmids resulted in a synergistic 400-fold activation of the *Dlx5/6* reporter (Fig. 11, lane 6), but had no effect on the activity of the control reporter lacking the *Dlx5/6* enhancer region (Fig. 11, lane 2) (Verzi et al., 2007). Based on these findings, it may be hypothesized that MEF2C participates in a feed-forward transcriptional circuit with Dlx5 and Dlx6, by first activating their expression, and then cooperating with them to further reinforce their expression in the craniofacial mesenchyme.

MEF2C and Dlx5 physically interact through their DNA binding domains

The transcriptional synergy between MEF2C and Dlx5 on the *Dlx5/6* enhancer suggested that the proteins might also physically interact. To test for physical interaction between Dlx5 and MEF2C, we performed GST pull-down assays using recombinant GST-MEF2C and *in vitro* translated [³⁵S] methionine-labeled Dlx5 (Fig.12). Full length GST-MEF2C (GST-MEF2C-FL) robustly bound [³⁵S] methionine-labeled full length Dlx5 (Dlx5-FL) (Fig.12, lane 1). A similar interaction was also observed between GST-MEF2C and a smaller homeodomain DNA binding (Dlx5-DBD) fragment of Dlx5 (Fig.12, lane 5). However, GST-MEF2C failed to interact with an N-terminal fragment of Dlx5 (Dlx5-N) lacking the homeodomain (Fig.12, lane 3). The interactions were specific since none of the Dlx5 proteins interacted with GST alone (Fig.12, lane 2, 4 and 6). To confirm that the absence of binding between GST-MEF2C and Dlx5-N was specifically due to a lack of interaction between these proteins, and not due to inefficient expression of the Dlx5-N fragment, equal fractions (20% of the input used in the pulldown) of the [³⁵S] methionine-labeled Dlx5 proteins were run alongside the pull down lysates. As shown in Fig.12 (lanes 13, 14, and 15), all three proteins were expressed at comparable levels.

Since the DNA binding domain of Dlx5 bound MEF2C efficiently, we next determined whether the DNA binding domain (DBD) of MEF2C was also sufficient to mediate interaction with Dlx5. Indeed, recombinant GST-tagged MEF2C-DBD (GST-MEF2C-DBD) efficiently bound Dlx5-FL (Fig.12, lane 7) and Dlx5-DBD (Fig.12, lane 11) but not the N-terminal region of Dlx5 (Fig.12, lane 9). In control reactions, there was

no interaction between any of the Dlx5 proteins and GST alone (Fig.12, lanes 8, 10, and 12). This robust physical interaction between Dlx5 and MEF2C, taken together with the transcriptional synergy between these proteins, further supports the feed-forward transcriptional model in which Dlx5 and Dlx6 are not just transcriptional targets but also cofactors of MEF2C.

Genetic interaction between *Mef2c* and *Dlx5/6* results in neonatal lethality in compound heterozygous mice

Based on the physical interaction and transcriptional synergy between MEF2C and Dlx5, we wanted to determine if the genes interact. The *Dlx5* and *Dlx6* loci are closely linked in the genome so that the two genes have been deleted together in a single gene targeting event (Robledo and Lufkin, 2006). Both *Dlx5/6*^{+/-} and *Mef2c*^{+/-} animals are viable and fertile, and exhibit no obvious defects at birth (Lin et al., 1997; Robledo and Lufkin, 2006). To test for genetic interaction between *Mef2c* and *Dlx5/6*, we crossed *Dlx5/6*^{+/-} mice with *Mef2c*^{+/-} mice, and assessed the viability of their progeny at birth (Table 1). As expected, wild type, *Dlx5/6*^{+/-} and *Mef2c*^{+/-} animals were born alive, and appeared healthy at birth. In contrast, almost 100% of *Dlx5/6*^{+/-}; *Mef2c*^{+/-} pups appeared sick and cyanotic at birth, with little or no milk in their stomach, and subsequently died before P1 (Table 1) (Verzi et al., 2007). The fact that loss of one copy of both *Dlx5/6* and *Mef2c* results in neonatal lethality strongly suggests that interaction between these loci is required for normal development.

Mice heterozygous for both *Mef2c* and *Dlx5/6* have hypoplastic palatal and pterygoid bones

The coexpression of *Dlx5/6* and *Mef2c* in the cranial neural crest prompted us to determine if double heterozygosity at these loci affects craniofacial development. *Mef2c* and *Dlx5/6* are each essential for the proper development of several cranial neural crest-derived craniofacial elements including the zygoma, tympanic ring, pterygoid complex, frontal, mandibular, hyoid and temporal bones, and the palate (Fig. 5) (Acampora et al., 1999; Beverdam et al., 2002; Depew et al., 2002; Robledo and Lufkin, 2006; Robledo et al., 2002). In addition, *Dlx5/6*^{-/-} also exhibit defects in non-neural crest-derived parietal, interparietal and supraoccipital structures, which often results in open fontanelles and exencephaly at birth (Acampora et al., 1999; Robledo and Lufkin, 2006; Robledo et al., 2002). Based on a preliminary histological examination on P0, *Dlx5/6*^{+/-}; *Mef2c*^{+/-} animals appeared to have a shorter secondary palate (Fig. 13, indicated by a red asterisk) in comparison to their wild type control littermates. This phenotype is similar (although less severe) to the palate defect exhibited by knockout of *Dlx5/6* (Beverdam et al., 2002; Depew et al., 2002; Jeong et al., 2008) and the neural crest-specific knockout of *Mef2c* (Fig.4).

To gain a better understanding of this palate defect, and identify other potential craniofacial defects, skeletons of wild type, *Dlx5/6*^{+/-}, *Mef2c*^{+/-} and *Dlx5/6*^{+/-}; *Mef2c*^{+/-} neonates were stained with alcian blue and alizarin red for cartilage and bone respectively. The overall cranial skeleton morphology was comparable between wild type, *Dlx5/6*^{+/-}, and *Mef2c*^{+/-} animals, except for subtle hyoid and gonial bone patterning

defects in *Dlx5/6*^{+/-} animals, and these have also been reported previously (Beverdam et al., 2002; Depew et al., 2002; Jeong et al., 2008; Robledo and Lufkin, 2006; Robledo et al., 2002). The secondary palate was completely closed, and similar in length and morphology in these single heterozygous and wild type control animals (Fig.14, panels A, B, and C). By contrast, all 23 *Mef2c*^{+/-}; *Dlx5/6*^{+/-} mice reported in Table 1 had a significantly shorter secondary palate, as shown in panel D, and quantified in panel E of Figure 14. In addition, the pterygoid processes of the basosphenoid complex were hypoplastic and misshapen in 100% of these animals (indicated by arrowheads in Fig. 14D), although other elements of the basosphenoid complex were comparable in size and morphology to controls. Interestingly, the pterygoid and palate are both derivatives of the maxillary mesenchyme, and the formation of these pterygoid processes is closely linked to palatogenesis. As a consequence defects of the palate are often accompanied by abnormalities in pterygoid bones. The specific impact on these two structures therefore prompted us to assess the different stages of palatogenesis in *Dlx5/6*^{+/-}; *Mef2c*^{+/-} animals.

Palatal shelf elevation and closure is delayed in *Dlx5/6*^{+/-}; *Mef2c*^{+/-} animals

Palatogenesis begins with the formation of bilateral palatal shelves on the medial wall of the maxillary process, which occurs around embryonic day (E) 11.5 in mice (Okano et al., 2006). Between E12.5 and E13.5, these palatal shelves extend vertically in a downward direction along the sides of the tongue (Greene and Pratt, 1976; Okano et al., 2006). This period of palate growth is characterized by extensive proliferation and osteogenic differentiation, which continues as the shelves subsequently elevate above the tongue and begin to elongate medially toward the midline around E14.5. The medial

edges of the opposing palatal shelves eventually fuse with each other by E15.5 to form the mature palate (Okano et al., 2006).

To identify potential abnormalities in palatal shelf specification, descent, elevation or fusion, which might explain the palate defect seen in *Dlx5/6^{+/-}; Mef2c^{+/-}* neonates, we performed histological analyses on the palates of wild type, *Dlx5/6^{+/-}*, *Mef2c^{+/-}* and *Dlx5/6^{+/-}; Mef2c^{+/-}* embryos at various developmental stages (Fig. 15). The initial specification of the bilateral palatal shelves from the maxillary mesenchyme was comparable between *Dlx5/6^{+/-}; Mef2c^{+/-}* animals and their littermate controls at E12.5 (Figure 15, compare panel D to A-C). *Dlx5/6^{+/-}; Mef2c^{+/-}* embryos also exhibited no obvious defects in palatal shelf descent or elongation between E13.5 and E14.5 (Fig.15 compare panel H to panels E-G and panel L to panels I-K). However, the subsequent elevation and closure of these palatal shelves, which naturally occurs between E14.5-E15.5, was significantly delayed in mice heterozygous for both *Dlx5/6* and *Mef2c*, resulting in a significant cleft in the posterior palates of E15.5 embryos (Fig.15P). In comparison, the palatal shelves of wild type, *Dlx5/6^{+/-}*, and *Mef2c^{+/-}* embryos were completely closed by E15.5 (Fig.15, panels M-O).

Skeletal analysis of E16.5 heads also shows the cleft palate in *Dlx5/6^{+/-}; Mef2c^{+/-}* palates, in contrast to the normal closed palates of wild type, *Dlx5/6^{+/-}*, and *Mef2c^{+/-}* embryos (Fig.16, compare panel D to panels A-C). The distance (in pixels) between the palatal shelves was quantified using NIH ImageJ, and clearly highlights the delayed closure of *Dlx5/6^{+/-}; Mef2c^{+/-}* palates (Fig.16E).

Reduced osteogenic differentiation at the site of palate closure in *Dlx5/6*^{+/-}; *Mef2c*^{+/-} animals

Delays in palatal shelf elevation and closure often result from misregulation of one or more of the cellular processes underlying palate growth. These include the timely migration of neural crest precursors into the palatal shelves, optimal proliferation within the shelves, and the proper differentiation of these mesenchymal cells into osteoblasts (Ferguson, 1987; Gritli-Linde, 2007). MEF2 factors have previously been shown to regulate proliferation and differentiation of several cell lineages (Khiem et al., 2008; Potthoff and Olson, 2007). In addition, both *Mef2c* and *Dlx5/6* have been implicated in osteogenic differentiation of the axial skeleton (Acampora et al., 1999; Arnold et al., 2007; Robledo and Lufkin, 2006). Conditional deletion of *Mef2c*, or the expression of a dominant-negative mutant of MEF2C, in developing cartilage, both severely disrupt chondrocyte hypertrophy and endochondral ossification of all long bones (Arnold et al., 2007). On the other hand, the expression of a superactivating form of MEF2C (MEF2C-VP16) promotes precocious chondrocyte hypertrophy and ossification of endochondral bones (Arnold et al., 2007). Neural crest-specific knockout of *Mef2c* also causes delays in cranial skeleton differentiation (Verzi et al., 2007).

We assessed rates of proliferation, migration and apoptosis in E11.5-E15.5 embryos, but found no obvious difference between *Dlx5/6*^{+/-}; *Mef2c*^{+/-} embryos and their littermate controls (data not shown).

To determine if the palate defect exhibited by *Dlx5/6*^{+/-}; *Mef2c*^{+/-} animals was due to abnormal osteogenic differentiation, we assessed mineralization and osteoid formation in Goldner's trichrome stained coronal sections from wild type, *Dlx5/6*^{+/-}, *Mef2c*^{+/-}, and *Dlx5/6*^{+/-}; *Mef2c*^{+/-} posterior palates at E15.5 (Fig. 17). Wild type, *Dlx5/6*^{+/-}, and *Mef2c*^{+/-} embryos showed considerable osteoid formation (purple/brown) throughout the palate, and some mineralization (green) at the periphery of the palate (Fig. 17, panels A-C). In comparison, *Dlx5/6*^{+/-}; *Mef2c*^{+/-} palates appeared to have less or delayed formation of osteoid matrix and mineralization (Fig. 17D), although osteogenic differentiation in other regions of the head was comparable to littermate controls (data not shown). This observation, supported by previously proposed roles for Dlx5/6 and MEF2C in osteogenic differentiation of the axial skeleton (Acampora et al., 1999; Arnold et al., 2007; Robledo and Lufkin, 2006), strongly suggests that a delay in osteogenic differentiation may, at least in part, account for the palate defect seen in *Dlx5/6*^{+/-}; *Mef2c*^{+/-} animals.

DISCUSSION

Craniofacial development, facilitated by the exquisitely timed specification, migration, and differentiation of various embryonic cell populations, is under tight transcriptional control (Francis-West et al., 1998). However, little is known about how transcription factors functionally interact with each other and upstream signaling molecules to regulate these developmental processes. In this chapter, I have focused on the functional interaction between the transcription factors MEF2C, Dlx5, and Dlx6,

which belong to a common signaling pathway in which *Dlx5* and *Dlx6* are downstream targets of MEF2C within the craniofacial mesenchyme (Fig. 7, Chapter 1) (Verzi et al., 2007).

The work presented here shows that *Dlx5/6* are direct transcriptional targets of MEF2C through an evolutionarily conserved branchial arch enhancer. In addition, *Dlx5/6* can synergize with MEF2C on a physical, transcriptional and genetic level. Based on these findings, we propose a novel model in which *Dlx5* and *Dlx6* function as transcriptional targets and interacting partners of MEF2C, by cooperating with MEF2C to reinforce their own expression, and to co-regulate downstream targets within the craniofacial mesenchyme (Fig. 18).

The craniofacial phenotype exhibited by *Dlx5/6*^{+/-}; *Mef2c*^{+/-} animals suggests that MEF2C and *Dlx5/6* specifically co-regulate secondary palate growth, and loss of this regulation in *Mef2c*^{+/-}; *Dlx5/6*^{+/-} animals results in a significant delay in elevation and subsequent closure of palatal shelves. Based on the coexpression of these genes in the craniofacial mesenchyme of the branchial arches and frontonasal mass at E9.5 (Fig. 2 and 7), it may be hypothesized that specific early patterning genes are exquisitely sensitive to the dosage of these two transcription factors. Using a candidate-based approach, we did not see a significant change in the expression of known branchial arch targets of *Dlx5/6* (Jeong et al., 2008), or *Mef2c*, including *Hand2*, by *in situ* hybridization (data not shown). However, subtle changes in the expression of these genes, above the threshold of detection by *in situ* hybridization, could account for the observed palate defect.

Alternatively, the observed palate defect could be due to misregulation of a distinct set of targets requiring coactivation by MEF2C and Dlx5 or Dlx6.

It should also be noted that *Mef2c* and *Dlx5/6* continue to be expressed during later osteogenic differentiation of the craniofacial skeleton, although the function of these genes during these later stages of craniofacial development is as yet unknown (Arnold et al., 2007; Robledo et al., 2002). However, *Mef2c* and *Dlx5/6* have each been implicated in endochondral bone differentiation of the axial skeleton (Acampora et al., 1999; Arnold et al., 2007; Potthoff and Olson, 2007; Robledo et al., 2002), and MEF2C directly activates collagen 10a1 (*Col10a1*) expression, a specific marker of chondrocyte hypertrophy, and indirectly or directly regulates *Runx2*, a transcription factor necessary for chondrocyte hypertrophy (Arnold et al., 2007). Taken together with the observed defect in osteogenic differentiation within the secondary palate in *Dlx5/6*^{+/-}; *Mef2c*^{+/-} mice, it may be hypothesized that MEF2C and Dlx5/6 co-regulate genes involved in osteogenic differentiation during later stages of craniofacial development.

Ongoing experiments will use bioinformatic screens, microarray analyses, and candidate-based real time PCR approaches to identify potential early patterning and late differentiation targets specifically misregulated in *Dlx5/6*^{+/-}; *Mef2c*^{+/-} embryos. Identification of novel downstream effectors of *Mef2c* and *Dlx5/6* should lend valuable insight into the molecular networks facilitating craniofacial development. We may also gain a better understanding of the overlapping and unique functions of *Mef2c* and *Dlx5/6* within the cranial skeleton.

In addition to the robust genetic interaction between MEF2C and Dlx5/6, we also showed that MEF2C physically associates with Dlx5 *in vitro*, and that this physical interaction is mediated through their DNA binding domains. This is an important finding because it provides a strong biochemical basis for the transcriptional synergy between MEF2C and Dlx5 on the *Dlx5/6* branchial arch enhancer (Fig. 12). Interestingly, mutation of the MEF2 elements in the Dlx5/6 enhancer does not abolish the transcriptional synergy between MEF2C and Dlx5 (data not shown), even though these sites are essential for activation by MEF2C alone (Fig. 9). This result also supports the notion that the transcriptional synergy is mediated through a physical association between these proteins.

The interaction between Dlx5 and MEF2C may be essential for assembling transcriptional complexes on the *Dlx5/6* enhancer through the recruitment of specific cofactors, and may allow us to identify novel tissue-restricted regulators of the cranial neural crest lineage. Alternatively, the physical association between MEF2C and Dlx5 may be required for recognition and activation of specific targets, since homeodomain proteins are notorious for their promiscuous DNA binding specificity. If so, then the interaction between these proteins could be used to identify other coregulated targets through biochemical pull down assays like ChIP-on-chip (Aparicio et al., 2004).

Interestingly, MEF2 proteins also colocalize with homeodomain proteins in other developmental lineages. For instance, MEF2C and the homeodomain protein Nkx2.5 are

both critical regulators of the cardiac lineage (Black, 2007; Bruneau, 2002; Lin et al., 1997; Srivastava and Olson, 2000). In addition to being coexpressed in the developing heart (Lin et al., 1997; Lints et al., 1993), they regulate common downstream cardiac targets like ANF (Durocher et al., 1996; Zang et al., 2004), and have been shown to genetically and functionally interact during heart development (Vincentz et al., 2008). Mammalian two hybrid and co-immunoprecipitation assays show that MEF2C can physically associate with Nkx2.5, however, the domains mediating this interaction are unknown (Vincentz et al., 2008). Based on our data, it would be useful to determine if the interaction between MEF2C and Nkx2.5 is also mediated through the DNA-binding domains. If so, the MEF2C-Dlx5 physical association can serve as a robust model to identify the specific residues with the DNA-binding domains that mediate protein-protein interaction vs. DNA-binding, and determine the functional implications of mutations in these residues in the cardiac as well as craniofacial lineage.

Transcription factors are often expressed in several developmental lineages, but their cellular roles in different lineages, and functional interactions with cofactors, are often conserved. For instance, MEF2C is expressed in the heart, skeletal muscle, and cranial skeleton, but in each of these lineages, it specifically controls the terminal differentiation program and appears to be dispensable for initial specification (Potthoff and Olson, 2007). The results presented in this chapter also strongly suggest that *Mef2c* and *Dlx5/6* coregulate the osteogenic differentiation of the palate. Interestingly, both *Mef2c* and *Dlx5/6* have been implicated in endochondral differentiation of the axial skeleton, but a functional interaction between these proteins has not been explored in this

lineage (Arnold et al., 2007; Robledo et al., 2002). Therefore, it would be interesting to determine if endochondral differentiation of the axial skeleton is also subject to co-regulation by these two transcription factors.

Figure Legends

Figure 8: An evolutionarily conserved enhancer in the *Dlx5/6* locus contains several consensus MEF2 sites

(A) Schematic representation of the *Dlx5/6* locus shows the location of a highly conserved fragment, depicted here as a blue box, immediately upstream of the *Dlx6* gene.

(B) ClustalW alignment of the mouse, human, and chicken sequences from the conserved region of the *Dlx5/6* enhancer shows four conserved consensus MEF2 elements, highlighted in blue, and several conserved Hox/Dlx binding sites, highlighted by yellow boxes. MEF2-1 and MEF2-2 sites contain potential Hox/Dlx binding elements, and the region of overlap is highlighted in green (Verzi et al., 2007).

Figure 9: The *Dlx5/6* enhancer is bound and activated by MEF2C

A) Consensus MEF2 sites within the *Dlx5/6* enhancer were tested by electrophoretic mobility shift analysis (EMSA) for MEF2C binding. MEF2C was transcribed and translated *in vitro*, and incubated with radiolabeled double stranded oligos spanning either the MEF2-3 site (lanes 2-6) or MEF2-4 (lanes 7-12) site. MEF2C bound both MEF2-3 (lane 2) and MEF2-4 (lane 8) robustly, and this binding was efficiently competed by excess amounts of unlabeled probe (D3 and D4, lanes 3 and 9), but not by

oligos in which the MEF2-3 and MEF2-4 sites were mutated (mD3 in lane 4, and mD4 in lane 10). Excess amounts of control oligos (C), containing the *myogenin* MEF2 binding site (Dodou et al., 2003), also efficiently competed for both MEF2-3 (lane 5) and MEF2-4 (lane 11). In contrast, control oligos in which the MEF2 site was mutated (mC) failed to compete for MEF2C binding to either MEF2-3 (lane 6) or MEF2-4 (lane 12).

Unprogrammed lysate lacking MEF2C showed no binding to either probe (lane 1 and 6).

B) Cotransfection of a MEF2C-VP16 expression plasmid with the *Dlx5/6-TK-lacZ* reporter into 3T3 cells results in a robust 12-fold activation of the reporter (lane 4), which is dependent on the MEF2 sites within the *Dlx5/6* enhancer, since mutation of these sites abolishes this activation (lane 6). MEF2C-VP16 showed no *trans*-activation of the parent reporter (lane 2) (Verzi et al., 2007).

Figure 10: The *Dlx5/6* enhancer directs expression to the craniofacial mesenchyme during embryonic development.

Whole mount image of an X-gal stained E9.5 transgenic embryo shows *lacZ* expression, under the control of the *Dlx5/6* enhancer, in the craniofacial mesenchyme of the first and second branchial arches. The arrowhead indicates branchial arch expression of the *Dlx5/6-lacZ* transgene (Verzi et al., 2007).

Figure 11: The *Dlx5/6* branchial arch enhancer is synergistically activated by MEF2C and Dlx5

Cotransfection of a MEF2C or Dlx5 expression plasmid into 3T3 cells results in a 3-fold (lane 4) and 50-fold (lane 5) respective activation of the *Dlx5/6-TK-lacZ* reporter.

Cotransfection of the *Dlx5/6* reporter with both Dlx5 and MEF2C expression plasmids results in a robust synergistic activation of over 400-fold (lane 6). In contrast, the addition of both expression plasmids has no effect on the activity of the parent reporter (lane 2) (Verzi et al., 2007).

Figure 12: MEF2C and Dlx5 physically interact through their DNA binding domains
GST pulldown assays using full length GST-tagged MEF2C (GST-MEF2C-FL) and *in vitro* translated [³⁵S] methionine-labeled Dlx5 proteins show that GST-MEF2C-FL robustly binds full length Dlx5 (Dlx5-FL) (lane 1), as well as the homeodomain DNA binding (Dlx5-DBD) fragment of Dlx5 (lane 5), but not an N-terminal fragment of Dlx5 (Dlx5-N) which lacks the homeodomain (lane 3). A GST-tagged fragment of MEF2C, containing just the MADS-MEF2 DNA binding domain (GST-MEF2C-DBD) also interacts with [³⁵S] methionine-labeled full length Dlx5 (lane 7) as well as its DNA binding domain (lane 11), but not Dlx5-N (lane 9). The interaction between GST-MEF2C-FL as well as GST-MEF2C-DBD and the Dlx5 proteins is specific, since Dlx5 protein shows no interaction with GST alone (lane 2, 4, 6, 8, 10, and 12). As a control, 20% of the [³⁵S] methionine-labeled Dlx5 protein used in the pulldown was run alongside the pull down lysates to confirm uniform protein expression (lanes 13, 14, and 15).

Figure 13: Mice heterozygous for both *Mef2c* and *Dlx5/6* exhibit palate defects
Sagittal sections of wild type (A) and *Dlx5/6*^{+/-};*Mef2c*^{+/-} (B) heads collected on P0 show that, in comparison to the wild type control, *Dlx5/6*^{+/-};*Mef2c*^{+/-} mice have an incomplete palate (red asterisk and arrowhead) (Verzi et al., 2007).

Figure 14: *Dlx5/6^{+/-}; Mef2c^{+/-}* animals have hypoplastic palatal and pterygoid bones. Skeleton preparations of wild type (A), *Dlx5/6^{+/-}* (B), *Mef2c^{+/-}* (C) and *Dlx5/6^{+/-};Mef2c^{+/-}* (D) heads, collected on P0, reveal palate and pterygoid defects in *Dlx5/6^{+/-};Mef2c^{+/-}* animals. In comparison to their littermates, *Dlx5/6^{+/-};Mef2c^{+/-}* animals have a significantly shorter palate (P) (quantified in panel E, n=7, *P<0.001), causing the underlying presphenoid bone to be partially visible (D, red asterisk). In addition, the two pterygoid (pt) processes, indicated by black arrowheads, are hypoplastic and misshapen in these mice.

Figure 15: Palatal shelf elevation and closure is defective in *Dlx5/6^{+/-}; Mef2c^{+/-}* animals. Coronal sections from wild type (A, E, I, M), *Dlx5/6^{+/-}* (B, F, J, N), *Mef2c^{+/-}* (C, G, K, O) and *Dlx5/6^{+/-};Mef2c^{+/-}* (D, H, L, P) heads were collected from E12.5-E15.5 to assess the various stages of palate development. Palatal shelf (ps) specification at E12.5 (A-D) is comparable between all four genotypes. Similarly, palate descent between E13.5 (E-H) and E14.5 (I-L) is normal in all the animals. However, palate elevation and fusion, which is complete by E15.5 in wild type (M), *Dlx5/6^{+/-}* (N), and *Mef2c^{+/-}* (O) embryos, is delayed in *Dlx5/6^{+/-};Mef2c^{+/-}* (P) embryos, resulting in a cleft of the posterior palate.

Figure 16: Skeletal analysis shows cleft plate in *Dlx5/6^{+/-}; Mef2c^{+/-}* mice at E16.5. Skeleton preparations of wild type (A), *Dlx5/6^{+/-}* (B), *Mef2c^{+/-}* (C) and *Dlx5/6^{+/-};Mef2c^{+/-}* (D) embryos, collected at E16.5, reveal that in comparison to their littermate controls, *Dlx5/6^{+/-};Mef2c^{+/-}* (D) embryos exhibit a cleft (red asterisk) of the secondary palate (p).

(E) Graph depicts the distance between palatal shelves of E16.5 wild type (n=9), *Dlx5/6*^{+/-} (n=7), *Mef2c*^{+/-} (n=3), and *Dlx5/6*^{+/-};*Mef2c*^{+/-} (n=3) mice, quantified using NIH ImageJ.

*P<0.001

Figure 17: Reduced osteogenic differentiation at the site of palate closure in *Dlx5/6*^{+/-};*Mef2c*^{+/-} embryos.

Coronal sections of the anterior palates of *Dlx5/6*^{+/-};*Mef2c*^{+/-} (D) embryos and their littermate controls, taken at E15.5, were stained with Goldner's Trichrome to assess osteogenic differentiation within the palate. Wild type (A), *Dlx5/6*^{+/-} (B), and *Mef2c*^{+/-} (C) palates exhibited extensive mineralization (green) and osteoid matrix formation (purple), extending from the periphery towards the center of the palate. In comparison, *Dlx5/6*^{+/-};*Mef2c*^{+/-} palates were significantly less mineralized, suggesting that osteogenic differentiation was defective or delayed.

Figure 18: *Dlx5* functions as a transcriptional target and cofactor of MEF2C during craniofacial development.

We propose a feed-forward transcriptional model in which *Dlx5* and *Dlx6*, known effectors of Endothelin signaling, function as direct transcriptional targets and interacting cofactors of MEF2C within the craniofacial mesenchyme. Upon activation by MEF2C, *Dlx5* cooperates with MEF2C to reinforce expression of *Dlx5/6*, and to coregulate craniofacial development.

Table 1: Genetic interaction between *Mef2c* and *Dlx5/6* results in neonatal lethality in compound heterozygous mice

Mef2c^{+/-} mice were crossed to *Dlx5/6*^{+/-} mice, and the total number of progeny was scored on P0. For each genotype born, animals that appeared healthy and had milk in their stomach were scored as alive and viable (Alive on P0). Animals either dead, dying, or clearly cyanotic, with little or no milk in their stomach, were scored as dead/dying on P0. Nearly all wild type, *Mef2c*^{+/-}, and *Dlx5/6*^{+/-} mice were viable at birth. By contrast, almost all (22/23) *Dlx5/6*^{+/-}; *Mef2c*^{+/-} mice died or were clearly cyanotic on P0, indicating a strong genetic interaction between *Dlx5/6* and *Mef2c* (Verzi et al., 2007)

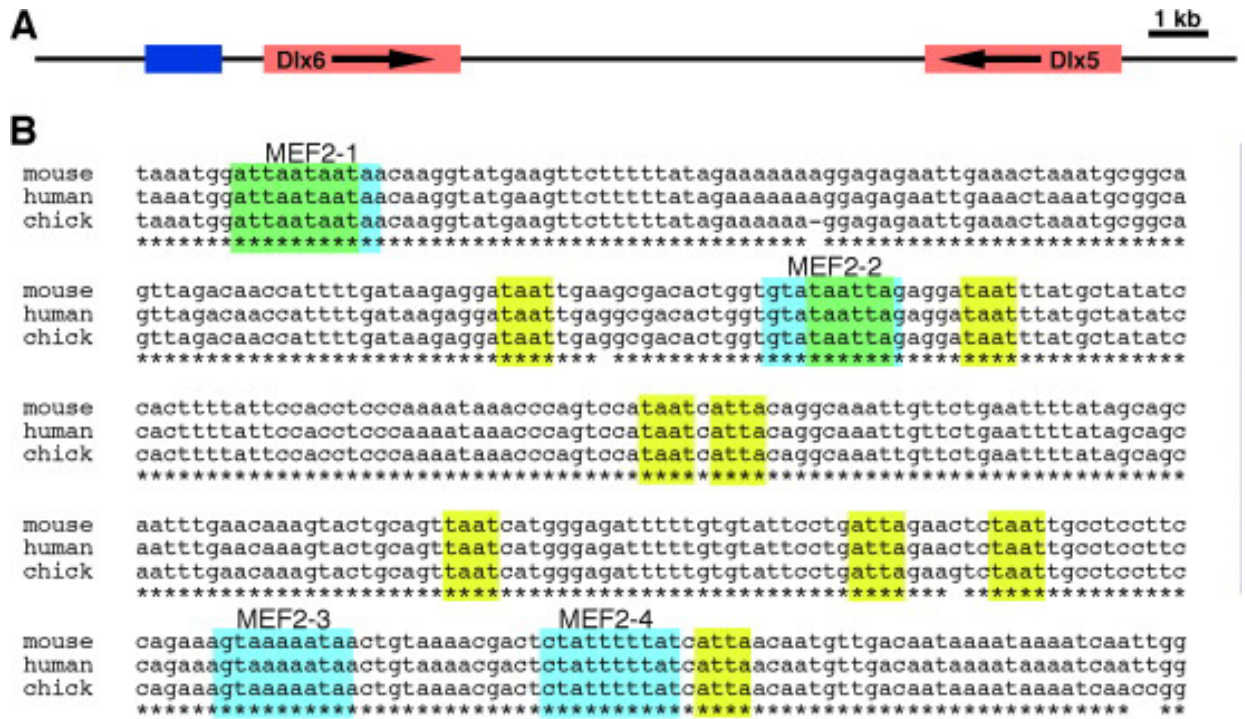
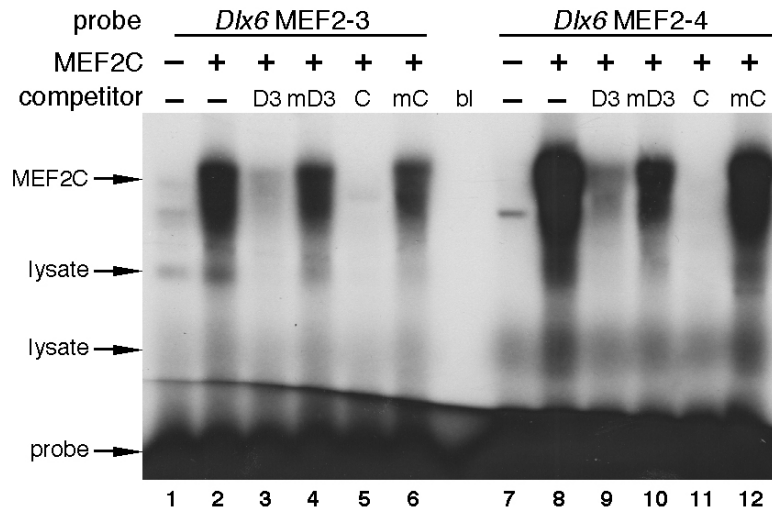
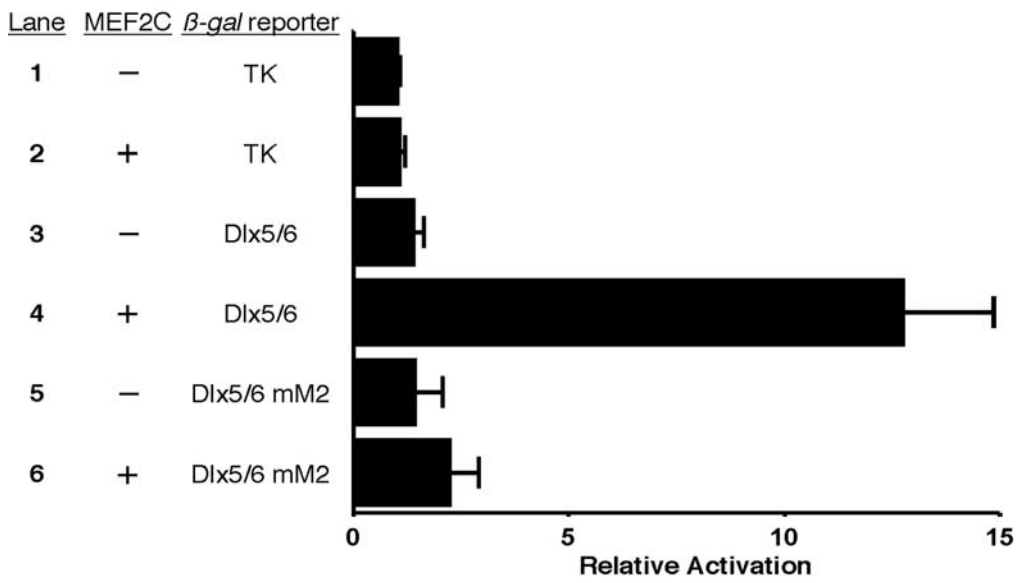


Figure 8: An evolutionarily conserved enhancer in the *Dlx5/6* locus contains several consensus MEF2 sites. (Verzi et al., 2007)



A



B

Figure 9: The *Dlx5/6* enhancer is bound and activated by MEF2C (Verzi et al., 2007)



Figure 10: The *Dlx5/6* enhancer directs expression to the craniofacial mesenchyme during embryonic development (Verzi et al., 2007)

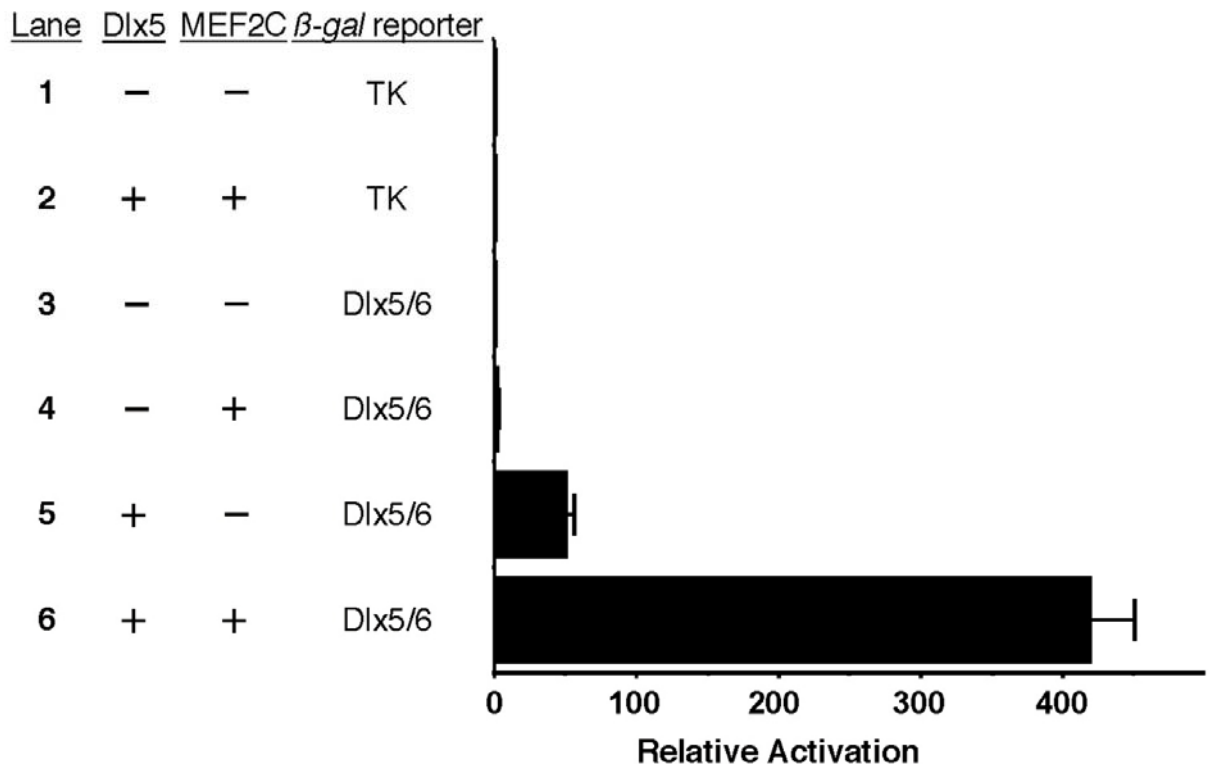


Figure 11: The *Dlx5/6* branchial arch enhancer is synergistically activated by MEF2C and Dlx5 (Verzi et al., 2007)

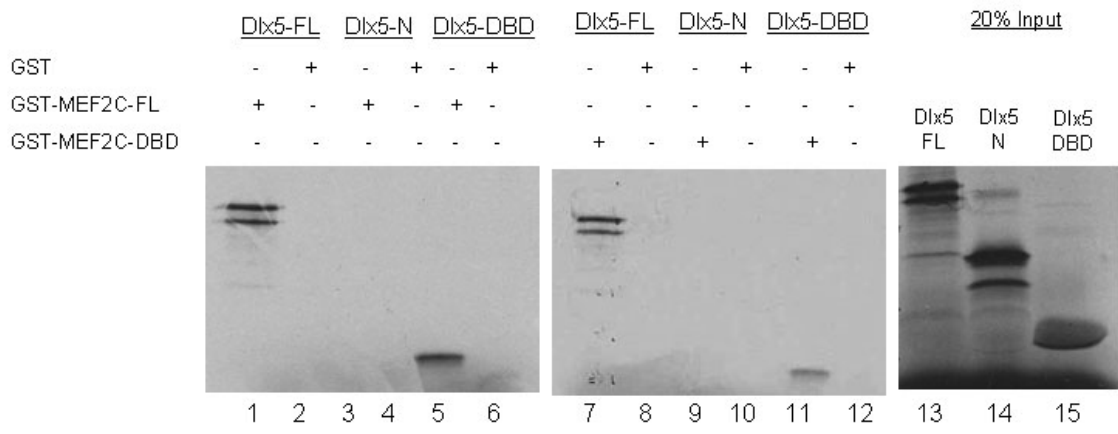


Figure 12: MEF2C and Dlx5 physically interact through their DNA binding domains

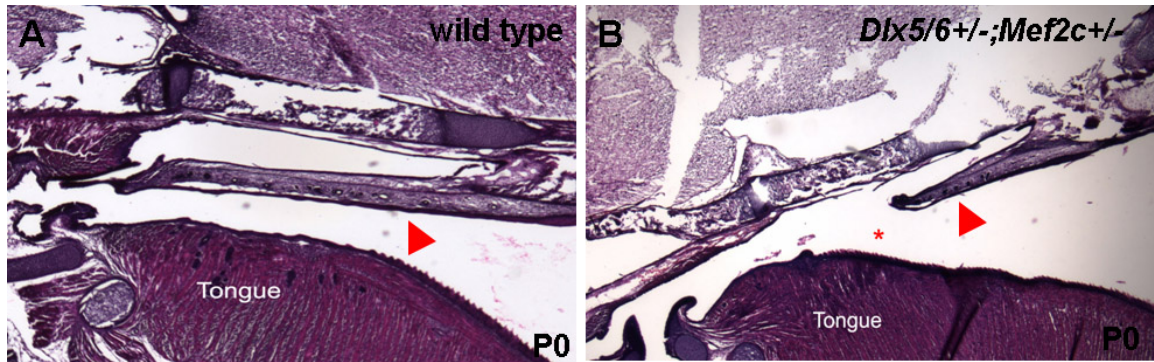
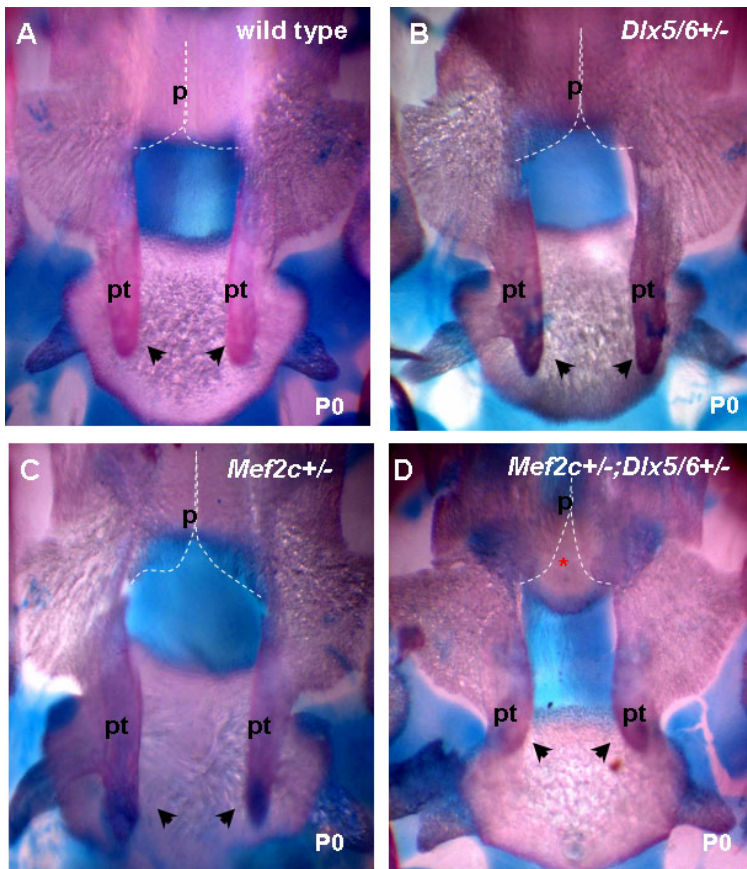


Figure 13: Mice heterozygous for both *Mef2c* and *Dlx5/6* exhibit palate defects (Verzi et al., 2007)



E

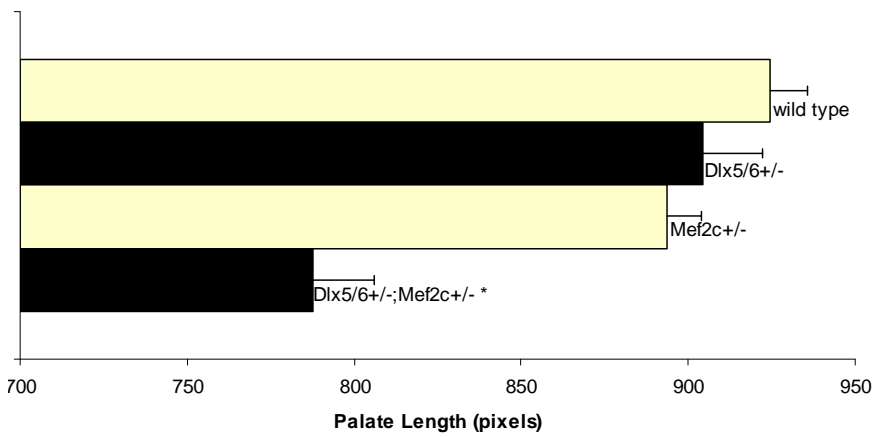
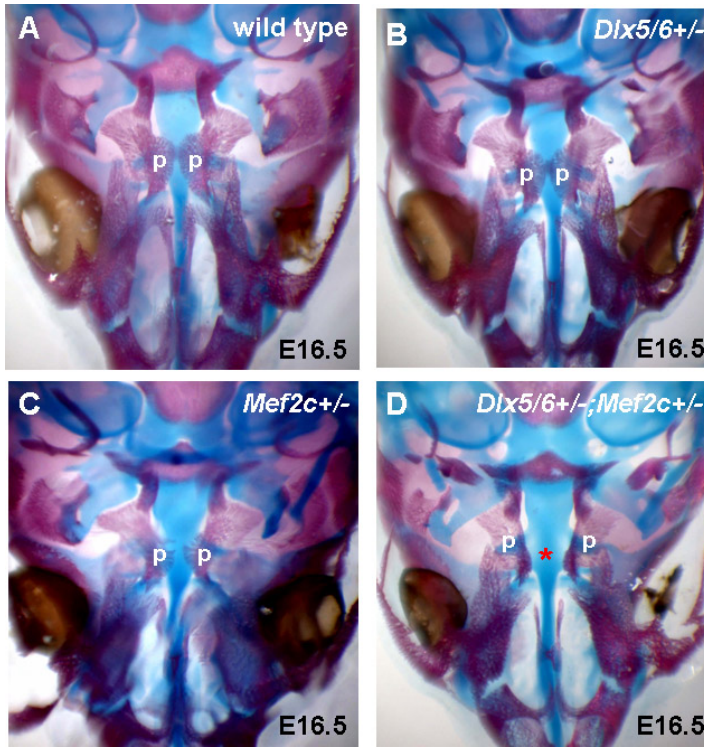


Figure 14: *Dlx5/6*^{+/-}; *Mef2c*^{+/-} animals have hypoplastic palatal and pterygoid bones



Figure 15: Palatal shelf elevation and closure is delayed in *Dlx5/6*^{+/-}; *Mef2c*^{+/-} animals



E

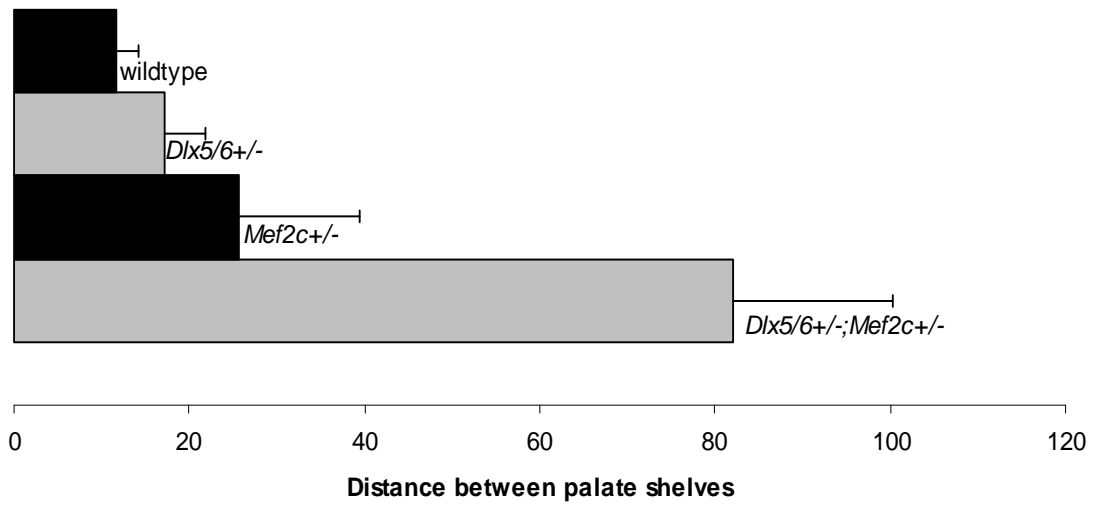


Figure 16: Skeletal analysis shows cleft palate in *Dlx5/6*^{+/-}; *Mef2c*^{+/-} mice at E16.5

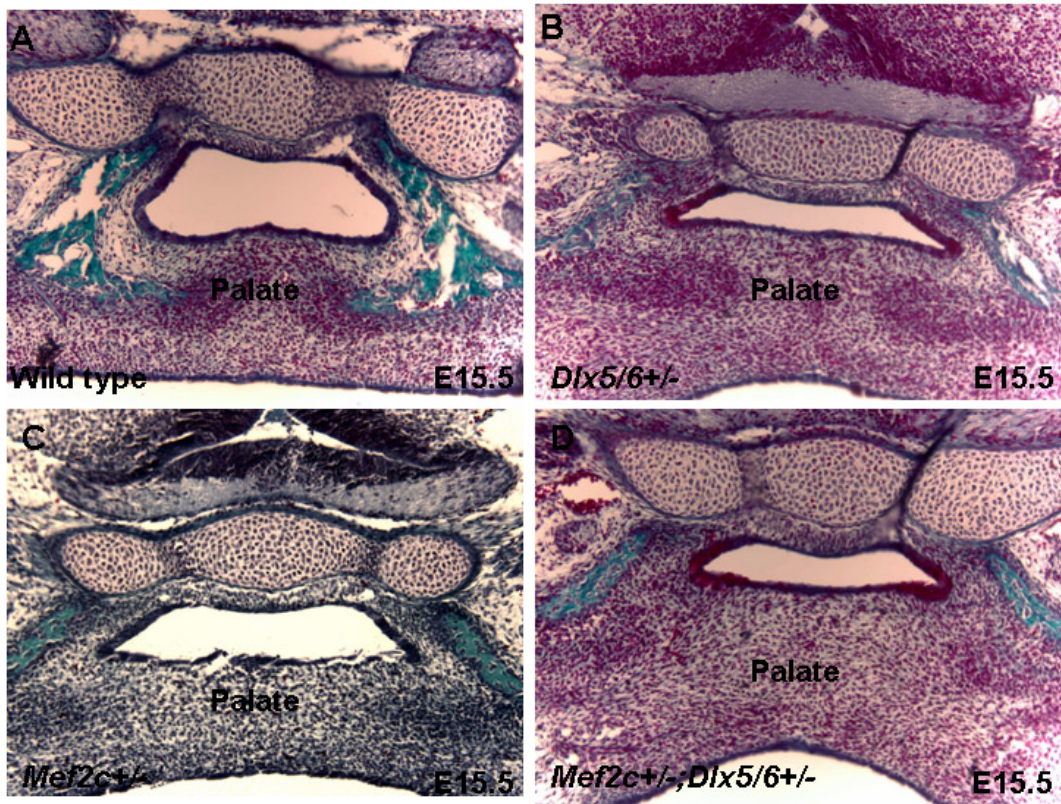


Figure 17: Reduced osteogenic differentiation at the site of palate closure in *Dlx5/6*^{+/-}; *Mef2c*^{+/-} embryos

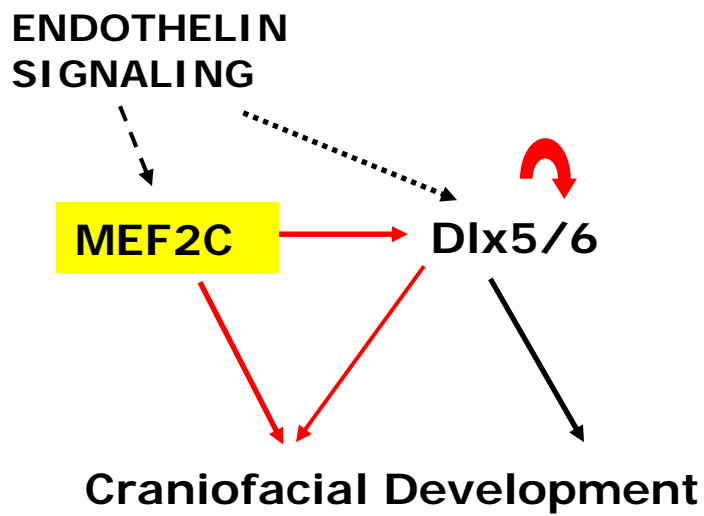


Figure 18: Dlx5 functions as a transcriptional target and cofactor of MEF2C during craniofacial development

	Expected	Observed	Alive on P0	Dead/dying on P0
Wild type	35	34	34	0
<i>Mef2c</i> ^{+/-}	35	45	44	1
<i>Dlx5/6</i> ^{+/-}	35	38	36	2
<i>Dlx5/6</i> ^{+/-} ; <i>Mef2c</i> ^{+/-}	35	23	1	22

Table 1: Genetic interaction between *Mef2c* and *Dlx5/6* results in neonatal lethality in compound heterozygous mice (Verzi et al., 2007)

CHAPTER 3

The MADS Box Transcription Factor MEF2C Regulates Melanocyte Development

in vivo

BACKGROUND

Melanocytes are the pigment cells of the skin, hair and choroid. Like the bones and cartilage of the craniofacial skeleton, melanocytes are also derivatives of the multipotent neural crest (Le Douarin, 1999). In contrast, pigment cells in the retinal pigmented epithelium originate from the neural epithelium of the optic cup (Lin and Fisher, 2007).

Melanocytes contain specialized lysosomal related organelles called melanosomes, within which the pigment melanin is synthesized (Boissy et al., 2006; Turner et al., 1975). Through their dendrite-like projections, mature melanocytes transfer these melanosomes to their adjacent keratinocytes, where they contribute to skin pigmentation (Boissy, 2003). The number, size, composition and distribution of melanosomes within keratinocytes changes in response to signaling cues, and results in differences in pigmentation (Boissy, 2003)s.

Melanosomes contain two main types of melanin — red/yellow pheomelanin and brown/black eumelanin (Lin and Fisher, 2007). The synthesis of both of these melanins

requires the initial tyrosinase-dependent hydroxylation of the monophenol L-tyrosine to the *o*-diphenol 3,4-dihydroxyphenylalanine (DOPA) and the oxidation of DOPA to the *o*-quinone DOPAquinone (Garcia-Borrón and Solano, 2002; Sturm et al., 2001). After the synthesis of DOPAquinone, the melanogenic pathways diverge to form either eumelanin or pheomelanin (Ebanks et al., 2009). Other crucial enzymes in the melanogenic pathway include tyrosinase-related proteins TRP1 and dopachrome tautomerase (DCT) (Jiao et al., 2006).

The formation of mature pigment-producing melanocytes from their neural crest precursors involves complex and exquisite coordination of several biological processes, thus making the melanocyte lineage an excellent model to understand the development of the neural crest into its many derivatives (Le Douarin, 1999)

The first step in melanocyte development is the specification of non-pigmented melanocyte precursors called melanoblasts at the dorsal neural tube (Baker and Bronner-Fraser, 1997; Knecht and Bronner-Fraser, 2002). Upon specification, these melanoblasts detach from the neuroepithelium, and begin to travel along characteristic dorsal-lateral pathways to various destinations, including the dermis and epidermis, the inner ear, and the choroids of the eye. During the course of this migration, melanoblasts, in response to intrinsic and environmental cues, proliferate extensively, and begin to differentiate into mature pigment producing melanocytes (Baker and Bronner-Fraser, 1997; Knecht and Bronner-Fraser, 2002; Le Douarin, 1999; Steel and Barkway, 1989; Trainor, 2005).

The biological processes regulating melanocyte development, including melanoblast specification, migration, proliferation, survival and differentiation, are tightly regulated, and even minor perturbations in one or more of these functions results in pigmentation disorders (Goding, 2000a). Several proteins have been identified to play crucial roles in the proper development of melanocytes, and gene inactivation studies have lent valuable insight into the function of these molecules in the melanocyte lineage (Goding, 2000a). An early and critical determinant of the neural crest lineage, and a well-established regulator of melanocyte development, is the HMG domain transcription factor Sox10 (Britsch et al., 2001; Potterf et al., 2001). *Sox10* is expressed in early premigratory neural crest cells, as well as in the migrating melanocytes, and peripheral and enteric nervous system precursors (Britsch et al., 2001; Potterf et al., 2001). However, Sox10 expression declines during the terminal differentiation of these various precursors (Kim et al., 2003). This dynamic expression of *Sox10* correlates with its many functions in these lineages, including the regulation of multipotency, proliferation, apoptosis, survival and lineage commitment (Britsch et al., 2001; Kim et al., 2003; Paratore et al., 2001; Sonnenberg-Riethmacher et al., 2001). Human mutations in *SOX10* have been linked to Waardenburg syndromes, a group of neurocristopathies that include hypopigmentation, deafness, and aganglionic colon as major phenotypes (Baxter et al., 2004; Spritz et al., 2003). *Sox10* null mice completely lack pigmentation and fail to develop a functional peripheral nervous system, and even heterozygous loss of *Sox10* results in hypopigmentation and distal bowel aganglionosis, signifying the importance of Sox10 during melanocyte and PNS development (Herbarth et al., 1998; Lane and Liu, 1984; Southard-Smith et al., 1999; Southard-Smith et al., 1998).

An important direct downstream effector of Sox10 in the melanocyte lineage is the basic helix-loop-helix-leucine zipper (bHLH-LZ) transcription factor Mitf (Bondurand et al., 2000; Lee et al., 2000; Potterf et al., 2000; Verastegui et al., 2000). *Mitf* is the earliest marker of commitment to the melanocyte lineage and a direct regulator of genes involved in melanocyte differentiation (Hodgkinson et al., 1993; Lister et al., 1999; Nakayama et al., 1998; Opdecamp et al., 1997). These include, among others, the melanogenic enzyme *Dct*, and *Pmel 17*, which encodes a melanosome structural protein and has also been implicated in melanin biosynthesis (Kobayashi et al., 1994; Solano et al., 2000). In humans, heterozygous mutations in *Mitf* cause auditory-pigmentary syndromes, such as Waardenburg syndrome type 2 and Tietz syndrome (Tassabehji et al., 1994a), and mice bearing null alleles of the *Mitf* gene exhibit a complete loss of neural crest-derived melanocytes and associated deafness (Moore, 1995).

The transcriptional interactions that facilitate melanocyte development are complex and non-linear. Sox10 and *Mitf* function in a feed forward transcriptional pathway, in which Sox10 directly activates Mitf through a melanocyte-specific promoter, and then cooperates with Mitf to activate downstream melanocyte genes (Goding, 2000b). In addition to Sox10, *Mitf* is regulated by several other factors, including Pax3, CREB, and Lef1 (Goding, 2000b; Vance and Goding, 2004). These factors respond to distinct upstream cues to either independently, synergistically, or antagonistically regulate *Mitf* expression in melanocytes (Goding, 2000b). Interestingly, *Mitf* overexpression fails to completely rescue pigmentation in *Sox10*-deficient mouse

melanoblasts (Goding, 2000b), indicating that there are additional as yet unidentified regulators of the melanocyte lineage.

The previous chapters of this thesis have described the expression and function of MEF2C in the cranial neural crest. To identify the upstream transcriptional regulators of *Mef2c* in the neural crest, all of the conserved non-coding sequences within the *Mef2c* locus were screened for enhancer activity in transgenic mouse embryos. This approach led to the identification of a highly conserved enhancer that exhibited activity in the developing neural crest and its derivatives, including craniofacial mesenchyme, peripheral nervous system and melanocytes (Fig.19). The robust activity of this *Mef2c* enhancer in melanocytes and the peripheral nervous system suggested that, in addition to the cranial neural crest, MEF2C might also play a role in trunk neural crest-derived lineages. Interestingly, transgenic analysis showed that the melanocyte and peripheral nervous system-specific activity of this enhancer was dependent on Sox10. In addition, Sox10 and MEF2C synergistically activated the enhancer in transient transfections, suggesting a positive feed-forward transcriptional program where MEF2C functions as a transcriptional target as well as cofactor of Sox10. Based on this transcriptional synergy between MEF2C and Sox10, and the robust activity of the *Mef2c* neural crest enhancer in melanocytes and the peripheral nervous system (Fig.19), we hypothesized that *Mef2c* could play a role in these tissues downstream of Sox10, and investigated its function in these lineages. Since germline inactivation of *Mef2c* in mice results in early cardiac lethality by E10, prior to the development of these neural crest derivatives, we examined the neural crest conditional knockouts of *Mef2c* (Fig.3, 4, and 5) which survive until

birth, for melanocyte and peripheral nervous system defects. No obvious peripheral nervous system defects were observed, but neural crest specific loss of *Mef2c* resulted in reduced expression of several melanocyte genes during development, and a significant reduction in the number of melanocytes at birth. The discovery of this unanticipated role for *Mef2c* in melanocytes, taken together with the observation that the *Mef2c* neural crest enhancer is directly activated by Sox10, strongly suggests that *Mef2c* is a direct transcriptional target of Sox10 in the melanocyte lineage.

RESULTS

Mice deficient in *Mef2c* exhibit pigmentation defects at birth

Since germline inactivation of *Mef2c* in the mouse causes cardiac lethality by E10 (Lin et al., 1997), neural crest-specific knockouts of *Mef2c* (Fig. 3), which survive until birth but die shortly after due to mechanical asphyxiation (Fig.4 and Fig.5), were assessed for melanocyte and peripheral nervous system defects. *Mef2c* neural crest knockout animals exhibited no obvious defects in peripheral or enteric innervation on P0 (data not shown). However, we did observe a significant reduction in the number of melanocytes in both epidermis and dermis in *Mef2c* neural crest knockout mice when we stained skin from the anterior region of the back with dihydroxyphenylalanine (DOPA) (Fig.20). Further analysis of the skin by electron microscopy showed that, in addition to fewer melanocytes, *Mef2c* neural crest knockout mice also had fewer melanosomes per melanocyte, suggesting that melanocyte function was also compromised in these mice (Fig.21). Although the craniofacial defects in *Mef2c* neural crest knockout mice caused

lethality at birth and prevented an analysis of the pigmentation defect beyond P0, these results clearly demonstrate that *Mef2c* function in the neural crest is required for proper melanocyte development.

***Mef2c* is required for proper expression of several melanocyte genes during development**

We next examined the embryonic expression of the melanocyte genes, *Mitf*, *Dct* and *Pmel 17*, in *Mef2c* neural crest conditional knockout embryos. At E12.5, the periocular (Fig. 22D-F) and trunk (data not shown) expression of all three genes was slightly reduced in *Mef2c* neural crest knockout embryos compared to control embryos (Fig. 22A-C). These observations indicate that MEF2C is an early and critical regulator of the melanocyte lineage.

***Mef2c* is not required for *Sox10* expression in trunk neural crest derivatives**

The reduction in melanocyte expression in *Mef2c* neural crest knockout embryos and neonates was similar, albeit less severe, to the pigmentation defects in *Sox10*-null mice (Hakami et al., 2006; Potterf et al., 2001). *Sox10* null embryos show complete lack of melanocyte marker expression as early as E11, although early neural crest specification at the dorsal neural tube is unaffected (Kapur, 1999; Potterf et al., 2001; Southard-Smith et al., 1998). We also have strong evidence to suggest that the transcriptional activity of the neural crest enhancer of *Mef2c* in melanocytes and the peripheral nervous system was dependent on *Sox10* (data not shown). Based on these two observations, we reasoned that *Mef2c* might function downstream of *Sox10* during trunk

neural crest development. To test this hypothesis, *Sox10* expression was assessed in *Mef2c* neural crest knockout embryos at E12.5 (Fig. 23), which is the stage when we observed reduced expression of *Mitf*, *Dct* and *Pmel17* in these embryos (Fig. 23). We were unable to detect *Sox10* expression in melanocytes in either control or *Mef2c* neural crest knockout embryos, consistent with previous reports that *Sox10* expression in melanocytes is not detectable (Hou et al., 2006). However, we observed comparable levels of *Sox10* expression in cranial and enteric ganglia in *Mef2c* neural crest knockout and control embryos (Fig. 23, panel A and B), suggesting that *Sox10* does not function downstream of MEF2C in those neural crest-derived lineages, and supporting the notion that *Sox10* might function upstream of MEF2C in neural crest-derived tissues.

DISCUSSION

The complex interplay between environmental cues, signaling molecules, and transcription factors, underlying the development and differentiation of melanocytes, makes it one of the most fascinating models of the neural crest lineage. Here we have identified the transcription factor MEF2C as a novel regulator of melanocyte development. *Mef2c* is a known regulator of several developmental lineages, including skeletal and cardiac muscle, central nervous and immune system, axial and craniofacial skeleton (Black and Olson, 1998; Kang et al., 2006; Lin et al., 1998; Lin et al., 1997; Potthoff and Olson, 2007).

Interestingly, in several of these lineages, MEF2C directly interacts with its upstream regulators or downstream effectors in feed forward transcriptional networks to potentiate developmental decisions. For example, in the skeletal muscle lineage, *Mef2c* is a direct transcriptional target of members of the MyoD family of basic helix-loop-helix (bHLH) proteins. Upon activation by MyoD, MEF2C functions as a cofactor of MyoD family members to activate downstream muscle differentiation genes in a cooperative manner (Black and Olson, 1998; Dodou et al., 2003; Wang et al., 2001). Similarly, during cardiac morphogenesis, MEF2 factors, upon activation by early cardiac core factors such as Nkx2.5 and GATA4, synergize with these factors to reinforce the cardiac differentiation program (Morin et al., 2000; Vincentz et al., 2008). In the craniofacial mesenchyme, MEF2C synergizes with its direct downstream target *Dlx5* to facilitate proper craniofacial development (Chapter 1 and 2). In each of these examples, MEF2C directly interacts with lineage-determining factors to facilitate the proper differentiation of distinct lineages.

Here, we show that *Mef2c* is an early and essential regulator of the melanocyte lineage, such that loss of *Mef2c* in this lineage not only affects melanocyte number and function, but also affects the expression of very early melanoblast markers like *Mitf*. The observations that the melanocyte phenotype in *Mef2c* neural crest knockout animals is similar, although less severe, to *Sox10* deficient animals, and that MEF2C and Sox10 share common melanocyte targets (*Mitf*, *Dct*, and *pMel17*), while *Sox10* expression in trunk neural crest derivatives is unaffected in *Mef2c* neural crest knockouts, together strongly support the notion that MEF2C and Sox10 function in a common transcriptional

pathway of melanocyte development. Furthermore, our data support a role for *Mef2c* as a downstream target of Sox10. The transactivation and transgenic analyses of the *Mef2c* neural crest enhancer provide further evidence that MEF2C is a direct transcriptional target and cofactor of Sox10. We also tested for genetic synergy between the *Mef2c* and *Sox10* loci by inter-crossing mice heterozygous for either *Mef2c* or *Sox10* and looking for exacerbation of the melanocyte phenotype in mice heterozygous for both *Sox10* and *Mef2c* (data not shown). However, since the crosses were maintained in a mixed outbred background, where even haploinsufficiency for *Sox10* alone results in a high degree of variability in phenotype penetrance and severity, we were unable to detect any obvious changes in the melanocyte phenotype. Nevertheless, the transcriptional interaction between Sox10 and MEF2C at the *Mef2c* locus, in combination with the *in vivo* evidence, strongly suggests that *Mef2c* and *Sox10* function in a feed-forward transcriptional pathway of melanocyte development.

The identification of this potential transcriptional interaction between MEF2C and Sox10 is also significant because, in addition to the melanocyte lineage, Sox10 and MEF2C are co-expressed in other neural crest derivatives, including the cranial and enteric ganglia. It would therefore be useful to determine if the development of these lineages is also impacted by functional interplay between these two transcription factors. There are also significant therapeutic implications to this assessment, since human mutations in *SOX10* have been associated with a severe form of Waardenburg syndrome Type IV, which, in addition to hypopigmentation and hearing loss, includes the aganglionic colon symptoms of Hirschsprung disease (Herbarth et al., 1998; Southard-

Smith et al., 1999). Besides *SOX10*, mutations in many of its known cofactors, including the c-RET tyrosine kinase receptor, Pax3, and the Endothelin B receptor also cause Hirschsprung disease (Hofstra et al., 1996; Lang et al., 2000; Paratore et al., 2001; Tanaka et al., 1998). Interestingly, only 50% of human patients exhibiting symptoms of Hirschsprung disease have mutations in known disease loci, and even in cases with known genetic causes, the severity or the symptoms are highly variable, which is likely due to genetic modifiers (Heanue and Pachnis, 2007; Southard-Smith et al., 1999). We did not observe any obvious peripheral nervous system defects in heterozygous *Mef2c* mice, and neonatal lethality due to craniofacial malformations in *Mef2c* neural crest conditional knockout mice prevented assessment of innervation defects in these animals postnatally. However, loss of *Mef2c* function in the neural crest does result in hypopigmentation at birth, which is characteristic of many forms of Waardenburg disease (Tassabehji et al., 1994b; Verastegui et al., 2000). Based on this, and on the observation that MEF2C is both a transcriptional target and partner of Sox10, it would be interesting to determine if *Mef2c* acts as a candidate modifier of Sox10 in mouse models of a variety of neurocristopathies.

The identification of MEF2C as a developmental regulator of the melanocyte lineage also makes it a potential candidate for playing a role in melanoma. Research efforts strongly suggest that the cellular processes that dictate normal melanocyte growth closely resemble the proliferation and metastasis of melanoma (Vance and Goding, 2004). In addition, several transcription factors, including Sox10 and Mitf, which have been implicated during melanocyte development, are misregulated in skin cancers (Vance

and Goding, 2004). The signaling pathways that regulate the expression and function of these transcription factors during melanocyte development are also actively involved in melanomas (Davies et al., 2002; Widlund et al., 2002). One signaling pathway of particular interest in this regard is the MAP-kinase pathway. In melanocytes, MAPK signaling plays a significant role in maintaining Mitf function and stability, but studies have also shown that deregulation of the MAPK pathway accounts for 70% of melanomas (Davies et al., 2002). There is also a wealth of research from several developmental lineages including T cells, B lymphocytes, and fibroblasts, implicating MAPK signaling upstream and downstream of MEF2 transcription factors (de Angelis et al., 2005; Han et al., 1997; Kato et al., 1997; Khiem et al., 2008; Yang et al., 1999). It would be interesting, and of potential therapeutic benefit, to determine if *Mef2c* is involved in melanoma, and if the MAPK pathway interacts with MEF2C in this lineage.

Figure Legends

Figure 19: Highly conserved enhancer within the *Mef2c* locus directs expression to neural crest lineages.

A) Schematic representation of the *Mef2c* locus showing the location of the neural crest enhancer, *Mef2c*-F1 (green box). The enhancer region was cloned into the HSP68-*lacZ* reporter construct, and assayed for function in transgenic mice. Previously identified enhancers are depicted as red bars, and exons are indicated with vertical black lines. B-G) *Mef2c*-F1 directs expression to several neural crest derivatives including the craniofacial mesenchyme (B), cranial and enteric ganglia (black arrowheads) (C, D, and F), and

melanocytes (red arrowheads) (E and G). In addition to the neural crest, this enhancer also directs expression to the developing heart. (Courtesy: Mike Verzi)

Figure 20: Reduced number of melanocytes in *Mef2c* neural crest knockout neonates

Skin from the backs of neonatal control (A and C) and *Mef2c* neural crest KO (B and D) mice was harvested, processed for DOPA staining, and examined by light microscopy. *Mef2c* neural crest KO skin contains fewer melanocytes (indicated by red arrows and arrowheads) in both the epidermis (B) and dermis (D), in comparison to the normal distribution of melanocytes in control epidermis (A) and dermis (C). Quantification of melanocyte distribution per unit volume of skin shows significantly reduced number of melanocytes in *Mef2c* neural crest knockout dermis tissue (n=9), in comparison to controls (n=7). $P < 0.0001$

Figure 21: Fewer melanosomes per melanocyte in *Mef2c* neural crest knockout neonates

Transmission electron microscopy of dermis tissue from dorsal back skin shows that *Mef2c* neural crest knockout mice have fewer melanosomes (B and D, highlighted by arrows in panel B) per melanocyte than their control littermates (A and D, highlighted by arrows in panel A). Panels C and D zoom in on a single melanocyte to highlight the difference in melanosome number.

Figure 22: *Mef2c* is required for the proper expression of several melanocyte genes during development

Whole mount *in situ* hybridization at E12.5 shows that the expression of three melanocyte markers, *Dct* (A and D), *Pmel17* (B and E), and *Mitf* (C and F) is significantly reduced in the peri-ocular region in neural crest knockouts of *Mef2c* (D, E, and F) in comparison to littermate controls (A, B, and C). Melanocytes are indicated by red arrowheads.

Figure 23: *Sox10* expression in the peripheral nervous system is not dependent on MEF2C

Whole mount *in situ* analysis at E12.5 shows no obvious difference in *Sox10* expression in the cranial and enteric ganglia of control (A, B, and C) and *Mef2c* neural crest knockout (D, E, and F) embryos. Panels B and E show a dorsal view of the embryos in A and D. Panels C and F zoom in on the region around the right hindlimb to demonstrate the comparable levels of *Sox10* expression in this region.

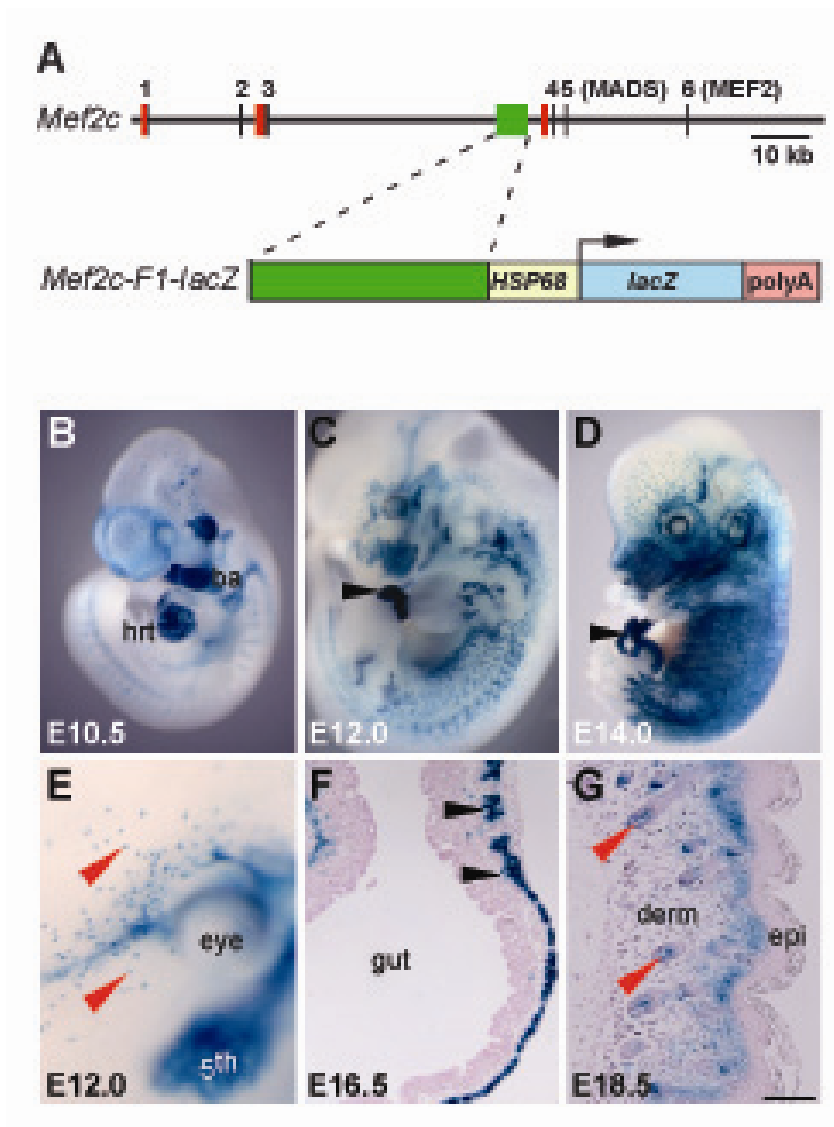


Figure 19: Highly conserved enhancer within the *Mef2c* locus directs expression to neural crest lineages (Courtesy: Mike Verzi)

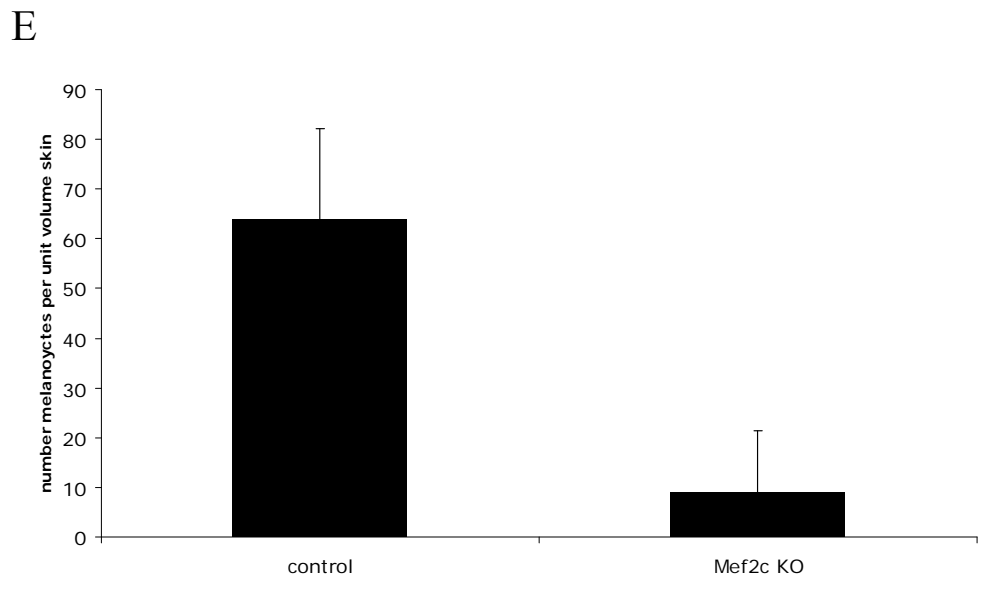
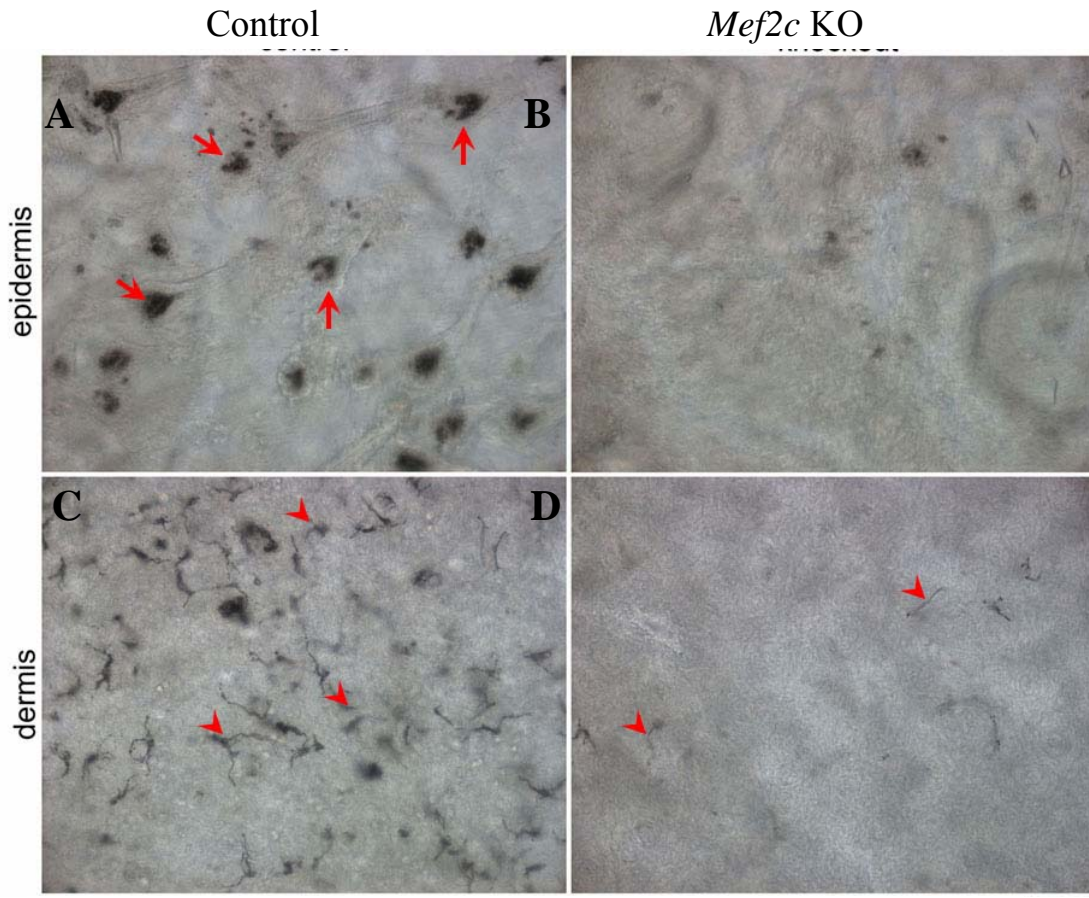


Figure 20: Reduced number of melanocytes in *Mef2c* neural crest knockout neonates

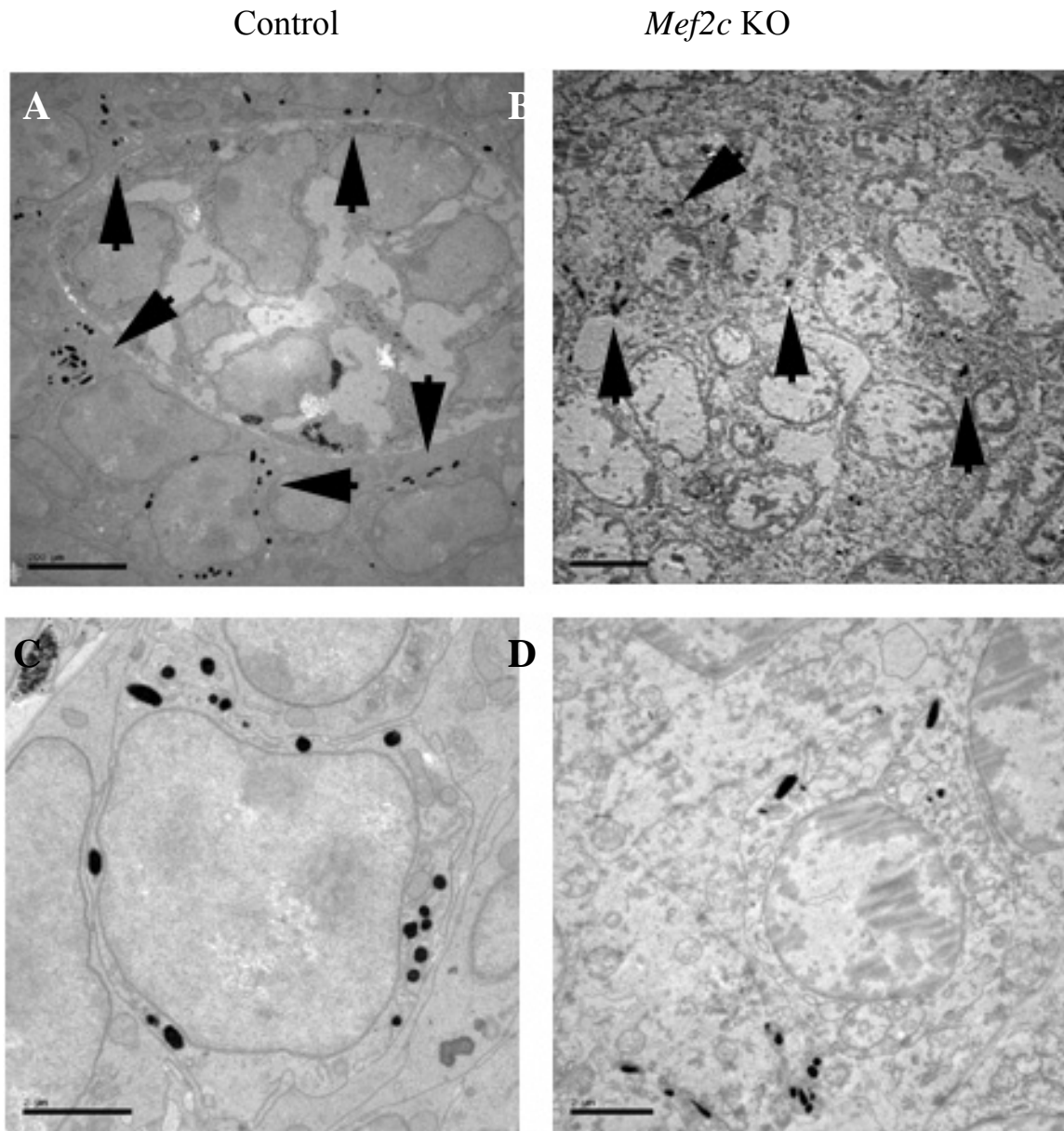


Figure 21: Fewer melanosomes per melanocyte in *Mef2c* neural crest knockout neonates

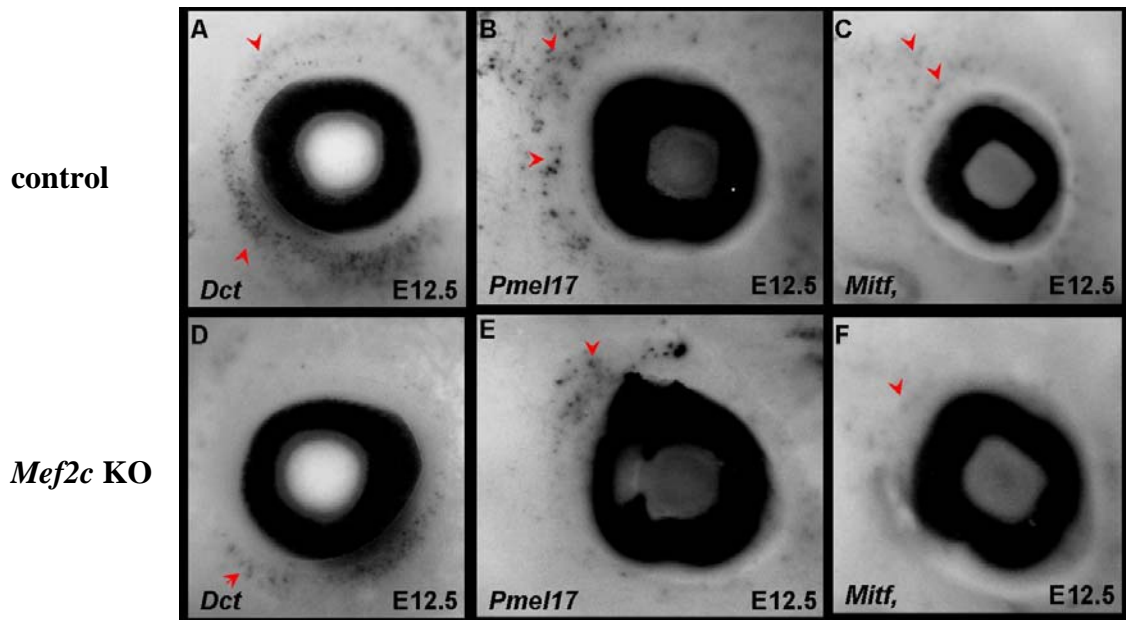


Figure 22: *Mef2c* is required for the proper expression of several melanocyte genes during development

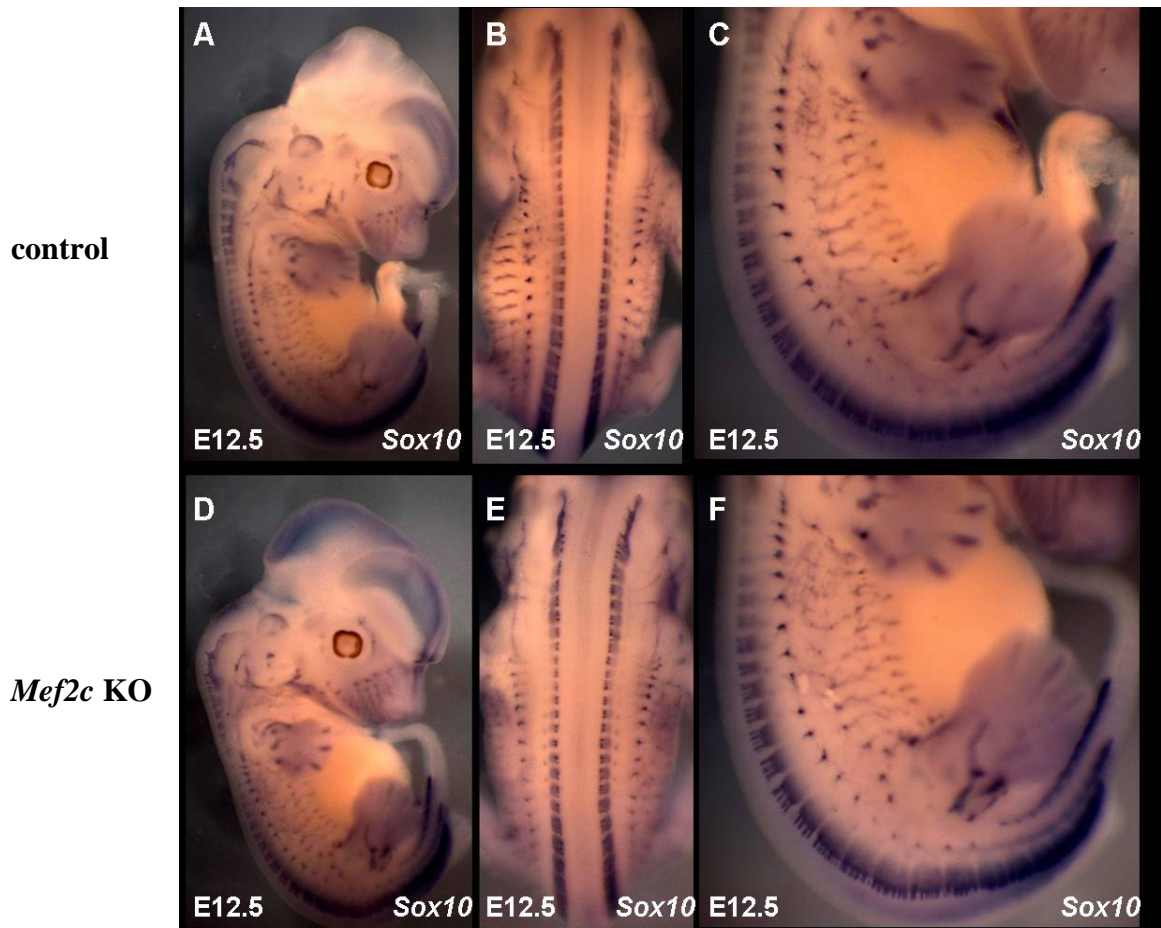


Figure 23: *Sox10* expression in the peripheral nervous system is not dependent on MEF2C

METHODS

IMMUNOHISTOCHEMISTRY AND *IN SITU* HYBRIDIZATION

Whole mount *in situ* hybridization was performed according to standard methods using digoxigenin-labeled antisense probes as described previously (Rojas et al., 2005). Briefly, embryos were fixed overnight in 4% paraformaldehyde, then washed twice with PBT (1x phosphate-buffered saline (PBS) + 0.1% Tween20) and dehydrated through a series of PBT (1x PBS+0.1% Tween20)-methanol washes. Embryos were then rehydrated through a reciprocal series of PBT-methanol washes and treated at room temperature with 20 µg/ml proteinase K for 30 minutes. After proteinase K treatment, embryos were rinsed with 2 mg/ml glycine in PBT for 15 minutes, followed by two successive 5 minute washes in PBT at room temperature. Embryos were then fixed in 4% paraformaldehyde and 0.2% glutaraldehyde for 20 minutes at room temperature, rinsed three times in PBT, and incubated in hybridization solution (50% formamide, 1% SDS, 5 xSSC, 50 µg/ml yeast tRNA, 50 µg/ml heparin) for at least one hour at 70°C. Digoxigenin-labeled antisense or sense RNA probes were added to the hybridization solution at a concentration of 100 ng/ml.

CELL CULTURE AND TRANSFECTIONS

All the transfections presented in this thesis were done in 3T3 fibroblast cells. The cells were maintained in Dulbecco's Modified Eagle Medium (DMEM) supplemented with 10% fetal calf serum. All transfections were performed in 12 well plates using Fugene 6 (Roche) according to manufacturer's instructions. Each transfection contained

0.7 μg of reporter plasmid and 0.7 μg of expression plasmid. In transfections with 2 expression plasmids, the amount of each expression plasmid was adjusted to 0.35 μg each. In transfections without an expression construct, the parent expression plasmid was added to keep the total amount of DNA in each transfection constant at 1.4 μg . Cells were cultured for 48 hours after transfection, harvested and assayed by using the Luminescent β -gal Detection System (Clontech), as described previously (Dodou et al., 2003). MEF2C-VP16 is in the pRK-5 mammalian expression vector (BD PharMingen) and contains the Herpesvirus VP16 transcriptional activation domain fused in frame to the C terminus of the MEF2C coding sequence. The Dlx5 expression plasmid, in pcDNA3, was obtained from Dr. Renny Franceschi's lab (University of Michigan) and contains a FLAG-epitope fused to the N-terminal region the entire coding sequence of Dlx5.

TRANSGENIC ANALYSIS AND GENOTYPING

Transgenic mice were generated by oocyte microinjection by using standard procedures as described previously (Dodou et al., 2003). Transgenic and knockout alleles were detected by Southern blot.

B-GALACTOSIDASE STAINING

β -Galactosidase expression in *lacZ* transgenic embryos or tissues was detected by X-gal staining, as described previously (Dodou et al., 2003). Transverse and sagittal sections from X-gal-stained embryos and tissues were cut at a thickness of 8 μm and counterstained with Neutral Fast Red, as described previously (Anderson et al., 2004).

ELECTROPHORETIC MOBILITY SHIFT ASSAYS

Electrophoretic mobility shift assays were performed as described previously (Dodou et al., 2003). Briefly, *Mef2c* cDNA was transcribed and translated using the TNT Quick Coupled Transcription/Translation System according to manufacturers protocols (Promega). Double-stranded oligonucleotides were labeled with ^{32}P -dCTP, using Klenow to fill in the overhanging 5' ends, and purified on a nondenaturing polyacrylamide-TBE gel. Binding reactions were pre-incubated at room temperature in 1x binding buffer [40 mM KCl, 15 mM HEPES (pH 7.9), 1 mM EDTA, 0.5 mM DTT, 5% glycerol] containing recombinant protein, 1 μg of poly dI-dC, and competitor DNA for 10 minutes prior to probe addition. Reactions were incubated for an additional 20 minutes at room temperature after probe addition and electrophoresed on a 6% nondenaturing polyacrylamide gel. The sequences of the control MEF2 binding site have been described previously (Dodou et al., 2003; Peirano et al., 2000). The sense-strand sequences of the *Dlx5/6* oligos used in EMSA are as follows:

1. **Dlxmef3F**: 5'-gggCCTTCCAGAAAGTAAAAATAACTGTAAAACGAC-3'
2. **Dlxmef3R**: 5'-gggGTCGTTTTACAGTTATTTTTACTTTCTGGAAGG-3'
3. **Dlxmef4F**: 5'-gggGTAAAACGACTCTATTTTTATCATTAACAATGTTG-3'
4. **Dlxmef4R**: 5'-gggCAACATTGTTAATGATAAAAATAGAGTCGTTTTAC-3'
5. **Dlxmutmef3F**: 5'-gggCCTTCCAGAAAGTTACAAATAACTGTAAAAC-3'
6. **Dlxmutmef3R**: 5'-gggGTTTTACAGTTATTTGTACTTTCTGGAAGG-3'
7. **Dlxmutmef4F**: 5'-gggAAAACGACTCTATTTTGATCATTAACAAT-3'
8. **Dlxmutmef4R**: 5'-gggATTGTTAATGATCAAAAATAGAGTCGTTTT-3'

GST PULL DOWN

GST pull down assays were performed as described previously (Dodou et al., 2003). Briefly, the BL21 CodonPlus strain of *E. coli* was transformed with either pGEX2T-MEF2C-FL (full length MEF2C), pGEX2T-MEF2C-DBD comprising the DNA binding MADS/MEF2 domain of MEF2C (amino acids 1-86), or pGEX2T alone. Cells were induced for protein expression and lysed by sonication after which the lysates were incubated with Glutathione Sepharose 4B beads for 30 minutes according to the manufacturer's instructions (Amersham). Protein-bound beads were then washed extensively in PBS, and incubated with *in vitro* translated [³⁵S] methionine-labeled Dlx5 proteins, in HEMG buffer (100mM KCl, 40mM HEPES (pH 7.4), 0.2mM EDTA, 0.1% NP-40, 1.5 mM DTT, 10% glycerol, and freshly supplemented 5% glycine and 1% BSA) at 4°C for 2 h with gentle rocking. Beads were then washed 3X in HEMG buffer with BSA and glycine, and 2 times in HEMG buffer alone. Samples were resolved by SDS-PAGE and subjected to autoradiography. The mouse Dlx5 proteins used for this assay included full length Dlx5 (Dlx5-FL), an N-terminal fragment of Dlx5 (Dlx5-N) spanning amino acids 1-136, and the DNA-binding homeodomain (Dlx5-HD) of Dlx5 spanning amino acids 128-195.

SKELETON AND CARTILAGE PREPARATIONS

Skeleton and cartilage preparations were performed according to standard procedures (Hogan, 1994). Briefly, neonatal pups or E16.5 mouse embryos were skinned, eviscerated and dehydrated in 95% ethanol, then sequentially stained using alcian blue (in

acid ethanol) and alizarin red (in 2% potassium hydroxide) for cartilage and bone respectively. Following staining, the preparations were cleared in 1% potassium hydroxide (KOH) and transferred to glycerol for storage and imaging.

GOLDNER TRICHROME STAINING

For histological analysis, embryos of different developmental stages were fixed in 4% paraformaldehyde (PFA) at 4 °C overnight, dehydrated through a graded ethanol series, and embedded in paraffin. Paraffin-embedded tissues were then sectioned coronally, and subjected to Hematoxylin/Eosin or Goldner's Trichrome staining. Goldner's trichrome staining was performed as previously described (Wu et al., 2008). Briefly, sections were first stained with Hematoxylin, rinsed in distilled water, and then stained for 5 minutes each in: 1) ponceau/acid fuchsin (0.75 g ponceau 2R [ponceau xylydine] [P2395-25G; Sigma-Aldrich], 0.25 g acid fuchsin, 0.1 g azophloxine [11640-25G; Sigma-Aldrich], 2mL acetic acid to 1L in distilled water); 2) orange G (20 g orange G [861286-25G; Sigma-Aldrich] and 40 g phosphomolybdic acid diluted to 1 l with distilled water); and 3) light green (2 g light green SF [L1886-25G; Sigma-Aldrich], 2 ml glacial acetic acid, to 1 l with distilled water) with rinses in 1% acetic acid between each step, and a 5 minute treatment with 1% acetic acid at the end of the staining procedure.

DOPA STAINING AND ELECTRON MICROSCOPY

DOPA staining and EM analyses on dorsal skin samples isolated from neonatal pups were performed as previously described (Nguyen and Wei, 2007). For DOPA staining, the tissue was placed in 2 M NaBr for 2 h at room temperature. The epidermis

and dermis were separated and washed twice in 0.1 M phosphate buffer pH 6.8. The tissue was then incubated at 37°C for 2 h in DOPA solution (0.5 mg 3,4-dihydroxy-L-phenylalanine (Sigma, St Louis, MO) per ml of 0.1 M phosphate buffer, pH 6.8). After staining with DOPA, the tissue was washed twice with PBS, and post-fixed for 15 minutes in 4% paraformaldehyde (Sigma) at room temperature followed by a PBS rinse. The tissue was stored at 4°C in PBS/10% glycerol (Fisher Scientific, Fair Lawn, NJ) and mounted in the same solution for examination by light microscopy. Whole mount skin samples were visualized and photographed using a Zeiss Axioplan2 Imaging microscope with the 20X objective. Sequential focal planes were photographed through the entire depth of the skin tissue creating “z-stacks”. In each animal, the 3 z-stacks with the highest DOPA-stained cell densities were chosen for analysis. For each z-stack, cells in each focal plane were counted, and the total for the 3 analyzed z-stacks was averaged. Reported is the average number of cells per z-stack per animal. The number of animals of each genotype assessed were as follows: n=7 for control, and n=9 for *Mef2c* neural crest KO.

For EM analysis, back skin was fixed in modified Karnovsky's fixative (2% paraformaldehyde/ 2% glutaraldehyde/ 0.1M cacodylate buffer, pH 7.3/ 0.06% CaCl₂). The tissue was then washed twice in 0.1M cacodylate buffer, postfixed in reduced osmium (1.5% potassium ferrocyanide/2% osmium tetroxide) for 2 h, rinsed in H₂O, dehydrated with increasing ethanol concentrations, and embedded in Epon resin overnight. Epon blocks were later sectioned on a Leica EM UC6 microtome and mounted onto formvar coated grids. Grids were stained in 10% uranyl acetate/50% methanol and

viewed on a Zeiss 10A electron microscope at 60kV. Images were captured on Gatan Bioscan 792 camera using DigitalMicrograph 3.4 software. Using the digital images, melanosome density per unit area of melanocyte cytoplasm was determined by measuring the cytoplasmic area using NIH ImageJ (<http://rsbweb.nih.gov/ij/index.html>) and counting DOPA stained melanosomes within the cytoplasmic area. n=3 cells counted/strain for control and KO strains. Only 1 control and 1 KO was assessed in this initial EM analysis.

PLASMIDS

1. Dlx5/6-Hsp68LacZ

Fwd primer: 5' CCACCACACAAGCTTGCTACCCACAC 3'

Rev primer: 5' TGTG TTCAGAAGCAGGGGCCCTAG 3'

This construct was initially cloned into the HindIII site of an Hsp68LacZ vector which lacked the Hsp promoter. Subsequently, the insert was pulled out as a ClaI/EcoRI fragment, blunted and cloned in reverse orientation into the SmaI site of Hsp68-LacZ to create plasmid Dlx5/6-Hsp68LacZ(reverse).

2. Dlx5/6-TKBgalbasic

The ClaI/EcoRI Dlx5/6 insert described above was blunt ligated in reverse orientation to TKBgalbasic, cut with XmaI and NheI and blunted.

3. Dlx5/6mutmef2X (in TKBgalbasic and Hsp68LacZ)

MEF2 site 3 and 4 mutations were made in the context of Dlx5/6-Hsp68LacZ (reverse) using Hsp100R and T3 external primers and the following mutation primers:

Dlx5/6 Mutation Primers:

>Dlxmutmef3fwd

5' CCTTCCAGAAAGTACAAATAACTGTAAAAC 3'

>Dlxmutmef3rev

5' GTTTTACAGTTATTTGTACTTTCTGGAAGG 3'

>Dlxmutmef4fwd

5' AAAACGACTCTATTTTGATCATTAACAAT 3'

>Dlxmutmef4rev

5' ATTGTTAATGATCAAAATAGAGTCGTTTT 3'

4. Dlx5/6mutmef4X (in TKBgalbasic)

MEF2 site 1 and 2 were mutated using Dlx5/6mutmef2X-TA (in pCR2.1TOPO) as a template, M13F and M13R as external primers, and the following mutagenic primers:

Dlx6Mef1mutfwd

5'GCAAATAATAAATGGATGCATAATAACAAGG 3'

Dlx6Mef1mutrev

5'GAACTTCATACCTTGTTATTATGCATCCATT 3'

Dlx6Mef2mutfwd

5'GCGACACTGGTGTATAGCTAGAGGATAATTTA 3'

Dlx6Mef2mutrev

5'TAAATTATCCTCTAGCTATACACCAGTGTCGC 3'

5. pSG424-Dlx5 clones for mammalian 2 hybrid assays

Dlx5 cDNA (full length as well as the different domains were cloned into pSG424 to generate GAL4 fusion proteins). The primers used to generate each of these proteins are listed below. All primers were designed to introduce EcoR1 and HindIII restriction sites 5' of the insert and an EcoR1 site 3' of the insert. pcDNA3-FlagDlx5 (Franceschi Lab, University of Michigan) was used as the PCR template for all constructs unless otherwise noted. PCR amplified products were first subcloned into pCR2.1TOPO, then digested with EcoR1 and inserted in frame into the EcoR1 site of pSG424. The HindIII site was introduced so that the GAL4 domain can be pulled out in the future if needed.

Primers:

Dlx5Gal4#1

5' ATCACTGAATTCAAGCTTATGGACTATAAGGACGATGA 3'

Dlx5Gal4#2(128)

5' ATCACTGAATTCAAGCTTATGGTGAATGGCAAACC 3'

Dlx5Gal4#2-1

5' ATGGACTATAAGGACGATGACGACAAGGAGCCAGAGGTGAGGATGGTG 3'

Dlx5Gal4#3

5' GGATAGAATTCAACTTTCTTTGGTTTACC 3'

Dlx5Gal4#4

5' CGTTAGAATTCCATGATCTTCTTGATCTTGGATC 3'

Dlx5Gal4#5

5' GGATAGAATTCATAAAGCGTCCCGGAGGCCAGT 3'

A. pSG424Dlx5(1) – full length Dlx5 was amplified using primers Dlx5Gal4#1 and Dlx5Gal4#5. Construct has a 5' FLAG tag.

B. pSG424Dlx5(2) – N terminal region of Dlx5 (1-136) amplified using primers Dlx5Gal4#1 and Dlx5Gal4#3. Construct has a 5' FLAG tag.

C. pSG424Dlx5(3) – N terminal + Homeodomain region of Dlx5 (1-195) amplified using primers Dlx5Gal4#1 and Dlx5Gal4#4. Construct has a 5' FLAG tag.

D. pSG424Dlx5(4) – Homeodomain region of Dlx5 (128-195) amplified using primers Dlx5Gal4#2 and Dlx5Gal4#4.

E. pSG424Dlx5(5) – Homeodomain + C-terminal region of Dlx5 (128-289) amplified using primers Dlx5Gal4#2 and Dlx5Gal4#5

F. pSG424Dlx5(B1/5) – Extended homeodomain + C-terminal region of Dlx5 (123-289) was amplified using a two step PCR protocol. First, primers Dlx5Gal4#2-1 and Dlx5Gal4#5 were used to amplify an intermediate piece which was TA cloned. This TA clone was then used as a template with Dlx5Gal4#1 and Dlx5Gal4#5 to generate the final construct which includes a small, highly conserved region 5' of the homeodomain. Construct also has a 5' FLAG tag.

6. pGEX2T-Dlx5

Full length Dlx5 cloned into pGEX2T to generate a GST-FLAG-Dlx5 fusion protein. The primers used to amplify Dlx5 cDNA from pcDNA3-FlagDlx5 (Franceschi Lab, University of Michigan) are shown below. The 5' primer introduces a Sma1 site for in frame insertion as a Sma1/EcoR1 fragment into pGEX2T.

Dlx5flagSmaFwd

5' GATCCCCGGGCACCATGGACTATAAGGACGATG 3'

Dlx5cDNArev

5' TAGAATAGGGCCCCTCTAGACT 3'

7. pRK5-Dlx5

Full length Dlx5 was pulled out of pcDNA3-FlagDlx5 (Franceschi Lab, University of Michigan) as a SacI digest, blunted and cloned into pRK5 digested with SmaI. Clones were screened for directionality.

8. pCITE-DlxHD

This construct contains the homeodomain (HD) region of Dlx5 (128-195) inserted in frame into pCITE 2A. The HD region was digested out of pSG424Dlx5(4) as an EcoRI fragment and inserted into the EcoRI site of pCITE 2a.

9. pCITE-DlxNterm

This construct contains the N-terminal region of Dlx5 (1-136) digested out of pSG424Dlx5(2) as an EcoRI fragment and inserted into the EcoRI site of pCITE 2A. The construct also has a 5' FLAG tag.

10. DCT enhancer constructs

The *DCT* enhancer is 780bp and located approximately 40Kb upstream of DCT. The following primers were used to amplify the enhancer region from mouse DNA, which was then cloned into pCR2.1 TOPO:

DCT5'enhancerfwd

5' GACACCCAAGGAAATGCAGTTGCCTGAAAGC 3'

DCT5'enhancerrev

5' CAGCGTTTGTGAGACAACTTGTCAGGAG 3'

- A) **DCT-TKBgalbasic** was blunt cloned as an EcoR1 fragment from *DCT-TA* (above) in TKBgalbasic cut with Xma1/Nhe1 and blunted. The reverse clone (*DCT-TK#19*) showed robust activity in transfections.
- B) **DCT-Hsp68LacZ**. The *DCT-TA* EcoR1 blunt insert was cloned into the Sma1 site of *Hsp68-LacZ*. Clones were screened and a reverse clone was selected for sequencing and injection.
- C) **DCTmutMEF-TKBgalbasic**. The two MEF2 sites in the *DCT* enhancer were mutated using the following primers and *DCT-TA* (in pCR2.1TOPO) as a template. The SOE product was TA cloned, verified by sequencing and subsequently digested with EcoR1 and blunt ligated to TKBgalbasic (Xma1/Nhe1 blunted).

DCT_Mef1mutFprimer

5' CCTGCAAAATTAAAGCTAGAATCAATA 3'

DCT_Mef1mutRprimer

5' GTATTGATTCTAGCTTTAATTTTGCAGG 3'

DCT_Mef2mutFprimer

5' CTAATCTTTAAGTTTTAATGCGCTGTCCAC 3'

DCT_Mef2mutRprimer

5' GTGGACAGCGCATTAAACTTAAAGATTAG 3'

D) **DCTmutMEF-Hsp68LacZ**. The above described mutMEF2 Soe product, digested with EcoR1 and blunted, was cloned into Hsp68LacZ cut with Sma1. Clone #15 in the reverse orientation was selected for sequencing and injection.

E) **DCTmutSOX-TKBgalbasic**. This construct was designed exactly as described above for *DCTmutMEF-TKBgalbasic*, except using the following primers:

DCT_Sox1mutFprimer

5' AATTAGAATCAGTACGATGAATACTCACTATGC 3'

DCT_Sox1mutRprimer

5' GCATAGTGAGTATTCATCGTACTGATTCTAATT 3'

DCT_Sox2mutFprimer

5' CTGTCCACAATTTATAAACCATCAAG 3'

DCT_Sox2mutRprimer

5' CTTGATGGTTTATAAATTGTGGACAG 3'

F) **DCTsmall-TKBgalbasic.** A minimal conserved region (392bp) within the *DCT* enhancer was amplified by PCR using the following primer and *DCT-TA* (in pCR2.1TOPO) as a template. The PCR product was TA cloned, digested with EcoR1 and blunt ligated to TKBgalbasic (Xma1/Nhe1 blunted).

DCT5'smallfwd

5' GGCTTTCAGACACTGTGCCATTTCTGC 3'

DCT5'smallrev

5' GGAGCCGATGCTGCTTCTCGCCCTCTG 3'

IN SITU PLASMIDS

Gene	Parent vector	Inse rt Size (bp)	Antisense	Sense	Reference/Source
Dlx6		350	EcoR1/SP6		John Rubenstein (UCSF)
Msx1	pCRIITOP0	320	BamH1/T7	EcoRV/SP6	Deepak Srivastava (UCSF)
Msx2	pCRIITOP0	420	EcoRV/SP6	BamH1/T7	Deepak Srivastava (UCSF)
Goosecoid	pBS KS(-)	905	BamH1/T3	HincII/T7	Gail Martin (UCSF)
Dlx5	pBS KS(-)	1600	Sal1/T3		John Rubenstein (UCSF)
Shh	pBS SK+	640	HindIII/T3		Gail Martin (UCSF)

Prx1	pBS SK+		BamH1/T7		James F. Martin (Texas A&M University)
Osteocalcin			BamH1/T3		Rich Schneider (UCSF)
Runx2			EcoR1/T7		Rich Schneider (UCSF)
eHand	pBS SKII+	1900	Not1/T7	Sal1/T3	Deepak Srivastava (UCSF)
dHand	pcDNA1	1100	EcoR1/SP6	Not1/T7	Deepak Srivastava (UCSF)
Mef2c_PA	pBS SK+	208	HindIII/T3	BamH1/T7	Original clone in pCRII from Eric Olson (UT Southwestern) had GATA6 cDNA as well, so I subcloned the 208bp piece into pBS.
Sox9 (rat)	pcDNA3	1500	HindIII/SP6	Xho1/T7	Holly Ingraham (UCSF)
Alx4	pBS KS(-)	650	EcoRV/T7	BamH1/T3	Gail Martin (UCSF)
Dlx3	pBS KS(-)	1100	Not1/T3	Xho1/T7	Maria Morasso (NIH)
Pitx2	dBEST		Xho1/T3		James F. Martin (Texas A&M University)
Gbx2			HindIII/T7		Gail Martin (UCSF)
Zac1	pCRIITOP0	255	Spe1/T7	EcoRV/SP6	Generated using the following primers: Fwd: 5'GCTGATGCAAGAGAAT ATGCAGGC3' Rev:

					5'ATCGGCTCCAAAGGCTC CAAAGGCTC3'
Cited1	pCRIITOP	380	EcoRV/SP6	Spe1/T7	Generated using the following primers: Fwd: 5'AGGATGTCAACCAGGA GATGAACTCTCTG3' Rev: 5'GACAGATCCCGGAGAC CCTCCCACTACCAGAG3'
Unc5c	pCRIITOP	723	BamH1/T7	EcoRV/SP6	Generated using the following primers: Fwd: 5'GCCTATTTAATTGTGGC TGGGGTATCCTCAGG3' Rev: 5'CAACTGGCTCCTCTTTC TTTCCAATAATC3'
Tbx22	pCRIITOP	320	EcoRV/SP6	BamH1/T7	Generated using the following primers: Fwd: 5'GGGCCATATCATTCTGC AGTC3'

					Rev: 5'GTGTGTCTGTGACAAAA GTTT3'
Alx3	pCRIITOP	310	Spe1/T7	EcoRV/SP6	Generated using the following primers: Fwd: 5'TCAGCTGCAGAACTCCC TGTGGCCCAGTCCAG3' Rev: 5'CGTGGTCCAGTTCAGCA GGCCAGGGGGCTC3'
Hgf1	pCRIITOP	395	EcoRV/SP6	BamH1/T7	Generated using the following primers: Fwd: 5'AGGGAGATTATGGTGG CCCACTCATTTGT3' Rev: 5'GATATGTTACTGCACTT GCAGGTACCTTAATTCAC 3'
Rgs5	pCRIITOP	367	Spe1/T7	EcoRV/SP6	Generated using the following primers: Fwd:

					<p>5'AGGTGAACATTGACCAC TTCACTAAAGACATC3'</p> <p>Rev:</p> <p>5'GTGAGGGCTCTTAGACA ACAGATCCACATAAC3'</p>
Vegf	pCRIITOP	374	EcoRV/SP6	HindIII/T7	<p>Generated using the following primers:</p> <p>Fwd:</p> <p>5'ATCGGAGCTGGGAGAA GTGCTAGCTCGGGCCTG3'</p> <p>Rev:</p> <p>5'TTGGCATGGTGGAGGTA CAGCAGTAAAGC3'</p>
MitfUTR	pCR2.1TOP	255			<p>Generated using the following primers:</p> <p>Fwd:</p> <p>5'CGGAGCATGCGTGTTAG CGAGCCTGCCTTG3'</p> <p>Rev:</p> <p>5'CAGTTCACAGATACTGC ACGCTGAAGGT3'</p>
<i>DCT</i> UTR	pCR2.1TOP	196	BamH1/T7		<p>Generated using the following primers:</p>

					<p>Fwd: 5'CAGAGGAAGAAGCTCC AGTTTGGTCCACAA3'</p> <p>Rev: 5'TCAGGCCAGGTAGGAG CATGCTAGGCTTC3'</p>
Sox10	pBS		Xho1/T3	Not1/T7	Obtained from Mike Verzi
DCTimage	pYX-Asc	694	Not1/T7	EcoRV/T3	Image Clone ID. 30539879
Mitfimage	pCR BluntII TOPO		EcoRV/SP6	HindIII/T7	Image Clone ID. 40047441
Dlx2	AmpR	600	EcoR1/T3		Juhee Jeong (John Rubenstein, UCSF)
Dlx1	AmpR	250	BamH1/T7		Juhee Jeong (John Rubenstein, UCSF)
Dlx4	pBS SK+	900	EcoR1/T7	HindIII/T3	Juhee Jeong (John Rubenstein, UCSF)

REFERENCES

- Acampora, D., Merlo, G. R., Paleari, L., Zerega, B., Postiglione, M. P., Mantero, S., Bober, E., Barbieri, O., Simeone, A., Levi, G., 1999. Craniofacial, vestibular and bone defects in mice lacking the Distal-less-related gene *Dlx5*. *Development*. 126, 3795-809.
- Anderson, J. P., Dodou, E., Heidt, A. B., De Val, S. J., Jaehnig, E. J., Greene, S. B., Olson, E. N., Black, B. L., 2004. HRC is a direct transcriptional target of MEF2 during cardiac, skeletal, and arterial smooth muscle development in vivo. *Mol Cell Biol*. 24, 3757-68.
- Aparicio, O., Geisberg, J. V., Struhl, K., 2004. Chromatin immunoprecipitation for determining the association of proteins with specific genomic sequences in vivo. *Curr Protoc Cell Biol*. Chapter 17, Unit 17 7.
- Arnold, M. A., Kim, Y., Czubyrt, M. P., Phan, D., McAnally, J., Qi, X., Shelton, J. M., Richardson, J. A., Bassel-Duby, R., Olson, E. N., 2007. MEF2C transcription factor controls chondrocyte hypertrophy and bone development. *Dev Cell*. 12, 377-89.
- Baker, C. V., Bronner-Fraser, M., 1997. The origins of the neural crest. Part I: embryonic induction. *Mech Dev*. 69, 3-11.
- Barni, T., Maggi, M., Fantoni, G., Serio, M., Tollaro, I., Gloria, L., Vannelli, G. B., 1995. Identification and localization of endothelin-1 and its receptors in human fetal jaws. *Dev Biol*. 169, 373-7.
- Baxter, L. L., Hou, L., Loftus, S. K., Pavan, W. J., 2004. Spotlight on spotted mice: a review of white spotting mouse mutants and associated human pigmentation disorders. *Pigment Cell Res*. 17, 215-24.
- Beverdam, A., Merlo, G. R., Paleari, L., Mantero, S., Genova, F., Barbieri, O., Janvier, P., Levi, G., 2002. Jaw transformation with gain of symmetry after *Dlx5/Dlx6* inactivation: mirror of the past? *genesis*. 34, 221-7.
- Bi, W., Drake, C. J., Schwarz, J. J., 1999. The transcription factor MEF2C-null mouse exhibits complex vascular malformations and reduced cardiac expression of angiopoietin 1 and VEGF. *Dev Biol*. 211, 255-67.
- Black, B. L., 2007. Transcriptional pathways in second heart field development. *Semin Cell Dev Biol*. 18, 67-76.
- Black, B. L., Olson, E. N., 1998. Transcriptional control of muscle development by myocyte enhancer factor-2 (MEF2) proteins. *Annu Rev Cell Dev Biol*. 14, 167-96.
- Boissy, R., Huizing, M., Gahl, W. Eds.), 2006. Biogenesis of melanosomes. Blackwell Publishing Ltd, Oxford, UK.
- Boissy, R. E., 2003. Melanosome transfer to and translocation in the keratinocyte. *Exp Dermatol*. 12 Suppl 2, 5-12.
- Bondurand, N., Pingault, V., Goerich, D. E., Lemort, N., Sock, E., Le Caignec, C., Wegner, M., Goossens, M., 2000. Interaction among SOX10, PAX3 and MITF, three genes altered in Waardenburg syndrome. *Hum Mol Genet*. 9, 1907-17.

- Bour, B. A., O'Brien, M. A., Lockwood, W. L., Goldstein, E. S., Bodmer, R., Taghert, P. H., Abmayr, S. M., Nguyen, H. T., 1995. *Drosophila* MEF2, a transcription factor that is essential for myogenesis. *Genes Dev.* 9, 730-41.
- Britsch, S., Goerich, D. E., Riethmacher, D., Peirano, R. I., Rossner, M., Nave, K. A., Birchmeier, C., Wegner, M., 2001. The transcription factor Sox10 is a key regulator of peripheral glial development. *Genes Dev.* 15, 66-78.
- Bruneau, B. G., 2002. Transcriptional regulation of vertebrate cardiac morphogenesis. *Circ Res.* 90, 509-19.
- CDC, *Improved National Prevalence Estimates for 18 Selected Major Birth Defects - United States, 1999-2001. Morbidity and Mortality Weekly Report, Vol. volume 54 2006, pp. 1301-1305.*
- Chai, Y., Jiang, X., Ito, Y., Bringas, P., Han, J., Rowitch, D. H., Soriano, P., McMahon, A. P., Sucov, H. M., 2000. Fate of the mammalian cranial neural crest during tooth and mandibular morphogenesis. *Development.* 127, 1671-1679.
- Charite, J., McFadden, D. G., Merlo, G., Levi, G., Clouthier, D. E., Yanagisawa, M., Richardson, J. A., Olson, E. N., 2001. Role of Dlx6 in regulation of an endothelin-1-dependent, dHAND branchial arch enhancer. *Genes Dev.* 15, 3039-49.
- Clouthier, D. E., Hosoda, K., Richardson, J. A., Williams, S. C., Yanagisawa, H., Kuwaki, T., Kumada, M., Hammer, R. E., Yanagisawa, M., 1998. Cranial and cardiac neural crest defects in endothelin-A receptor-deficient mice. *Development.* 125, 813-24.
- Clouthier, D. E., Williams, S. C., Yanagisawa, H., Wieduwilt, M., Richardson, J. A., Yanagisawa, M., 2000. Signaling pathways crucial for craniofacial development revealed by endothelin-A receptor-deficient mice. *Dev Biol.* 217, 10-24.
- Couly, G., Creuzet, S., Bennaceur, S., Vincent, C., Le Douarin, N. M., 2002. Interactions between Hox-negative cephalic neural crest cells and the foregut endoderm in patterning the facial skeleton in the vertebrate head. *Development.* 129, 1061-73.
- Danielian, P. S., Muccino, D., Rowitch, D. H., Michael, S. K., McMahon, A. P., 1998. Modification of gene activity in mouse embryos in utero by a tamoxifen-inducible form of Cre recombinase. *Curr Biol.* 8, 1323-6.
- Davies, H., Bignell, G. R., Cox, C., Stephens, P., Edkins, S., Clegg, S., Teague, J., Woffendin, H., Garnett, M. J., Bottomley, W., Davis, N., Dicks, E., Ewing, R., Floyd, Y., Gray, K., Hall, S., Hawes, R., Hughes, J., Kosmidou, V., Menzies, A., Mould, C., Parker, A., Stevens, C., Watt, S., Hooper, S., Wilson, R., Jayatilake, H., Gusterson, B. A., Cooper, C., Shipley, J., Hargrave, D., Pritchard-Jones, K., Maitland, N., Chenevix-Trench, G., Riggins, G. J., Bigner, D. D., Palmieri, G., Cossu, A., Flanagan, A., Nicholson, A., Ho, J. W., Leung, S. Y., Yuen, S. T., Weber, B. L., Seigler, H. F., Darrow, T. L., Paterson, H., Marais, R., Marshall, C. J., Wooster, R., Stratton, M. R., Futreal, P. A., 2002. Mutations of the BRAF gene in human cancer. *Nature.* 417, 949-54.

- de Angelis, L., Zhao, J., Andreucci, J. J., Olson, E. N., Cossu, G., McDermott, J. C., 2005. Regulation of vertebrate myotome development by the p38 MAP kinase-MEF2 signaling pathway. *Dev Biol.* 283, 171-9.
- De Val, S., Anderson, J. P., Heidt, A. B., Khiem, D., Xu, S. M., Black, B. L., 2004. Mef2c is activated directly by Ets transcription factors through an evolutionarily conserved endothelial cell-specific enhancer. *Dev Biol.* 275, 424-34.
- Depew, M. J., Lufkin, T., Rubenstein, J. L., 2002. Specification of jaw subdivisions by Dlx genes. *Science.* 298, 381-5.
- Dodou, E., Verzi, M. P., Anderson, J. P., Xu, S. M., Black, B. L., 2004. Mef2c is a direct transcriptional target of ISL1 and GATA factors in the anterior heart field during mouse embryonic development. *Development.* 131, 3931-42.
- Dodou, E., Xu, S. M., Black, B. L., 2003. mef2c is activated directly by myogenic basic helix-loop-helix proteins during skeletal muscle development in vivo. *Mech Dev.* 120, 1021-32.
- Dupin, E., Creuzet, S., Le Douarin, N. M., 2006. The contribution of the neural crest to the vertebrate body. *Adv Exp Med Biol.* 589, 96-119.
- Durocher, D., Chen, C. Y., Ardati, A., Schwartz, R. J., Nemer, M., 1996. The atrial natriuretic factor promoter is a downstream target for Nkx-2.5 in the myocardium. *Mol Cell Biol.* 16, 4648-55.
- Ebanks, J. P., Wickett, R. R., Boissy, R. E., 2009. Mechanisms regulating skin pigmentation: the rise and fall of complexion coloration. *Int J Mol Sci.* 10, 4066-87.
- Edmondson, D. G., Lyons, G. E., Martin, J. F., Olson, E. N., 1994. Mef2 gene expression marks the cardiac and skeletal muscle lineages during mouse embryogenesis. *Development.* 120, 1251-63.
- Farlie, P. G., McKeown, S. J., Newgreen, D. F., 2004. The neural crest: basic biology and clinical relationships in the craniofacial and enteric nervous systems. *Birth Defects Res C Embryo Today.* 72, 173-89.
- Feledy, J. A., Morasso, M. I., Jang, S. I., Sargent, T. D., 1999. Transcriptional activation by the homeodomain protein distal-less 3. *Nucleic Acids Res.* 27, 764-70.
- Ferguson, M. W., 1987. Palate development: mechanisms and malformations. *Ir J Med Sci.* 156, 309-15.
- Francis-West, P., Ladher, R., Barlow, A., Graveson, A., 1998. Signalling interactions during facial development. *Mech Dev.* 75, 3-28.
- Frazer, K., Pachter, L., Poliakov, A., Rubin, E., Dubchak, I., 2004. VISTA: computational tools for comparative genomics. *Nucleic Acids Res.* 1.
- Garcia-Borrón, J. C., Solano, F., 2002. Molecular anatomy of tyrosinase and its related proteins: beyond the histidine-bound metal catalytic center. *Pigment Cell Res.* 15, 162-73.
- Goding, C. R., 2000a. Melanocyte development and malignant melanoma. *Forum (Genova).* 10, 176-87.
- Goding, C. R., 2000b. Mitf from neural crest to melanoma: signal transduction and transcription in the melanocyte lineage. *Genes Dev.* 14, 1712-28.

- Graham, A., Begbie, J., McGonnell, I., 2004. Significance of the cranial neural crest. *Dev Dyn.* 229, 5-13.
- Greene, R. M., Pratt, R. M., 1976. Developmental aspects of secondary palate formation. *J Embryol Exp Morphol.* 36, 225-45.
- Gritli-Linde, A., 2007. Molecular control of secondary palate development. *Dev Biol.* 301, 309-26.
- Hakami, R. M., Hou, L., Baxter, L. L., Loftus, S. K., Southard-Smith, E. M., Incao, A., Cheng, J., Pavan, W. J., 2006. Genetic evidence does not support direct regulation of EDNRB by SOX10 in migratory neural crest and the melanocyte lineage. *Mech Dev.* 123, 124-34.
- Han, J., Jiang, Y., Li, Z., Kravchenko, V. V., Ulevitch, R. J., 1997. Activation of the transcription factor MEF2C by the MAP kinase p38 in inflammation. *Nature.* 386, 296-9.
- Heanue, T. A., Pachnis, V., 2007. Enteric nervous system development and Hirschsprung's disease: advances in genetic and stem cell studies. *Nat Rev Neurosci.* 8, 466-479.
- Herbarth, B., Pingault, V., Bondurand, N., Kuhlbrodt, K., Hermans-Borgmeyer, I., Puliti, A., Lemort, N., Goossens, M., Wegner, M., 1998. Mutation of the Sry-related Sox10 gene in Dominant megacolon, a mouse model for human Hirschsprung disease. *Proc Natl Acad Sci U S A.* 95, 5161-5.
- His, W., 1868. Untersuchungen ueber die erste Anlage der Wirtbeltierleibes die erste Entwicklung des Hunchens im Ei. Leipzig. Vogel,.
- Hodgkinson, C. A., Moore, K. J., Nakayama, A., Steingrimsson, E., Copeland, N. G., Jenkins, N. A., Arnheiter, H., 1993. Mutations at the mouse microphthalmia locus are associated with defects in a gene encoding a novel basic-helix-loop-helix-zipper protein. *Cell.* 74, 395-404.
- Hofstra, R. M. W., Osinga, J., Tan-Sindhunata, G., Wu, Y., Kamsteeg, E.-J., Stulp, R. P., Ravenswaaij-Arts, C. v., Majoor-Krakauer, D., Angrist, M., Chakravarti, A., Meijers, C., Buys, C. H. C. M., 1996. A homozygous mutation in the endothelin-3 gene associated with a combined Waardenburg type 2 and Hirschsprung phenotype (Shah-Waardenburg syndrome). *Nat Genet.* 12, 445-447.
- Hogan, B. C., F; Lacy, E (Ed.) 1994. Manipulating the mouse embryo: A laboratory manual. Cold Spring Harbor Laboratory
- Hou, L., Arnheiter, H., Pavan, W. J., 2006. Interspecies difference in the regulation of melanocyte development by SOX10 and MITF. *Proc Natl Acad Sci U S A.* 103, 9081-5.
- Ishikawa, T., Yanagisawa, M., Goto, K., Masaki, T., 1989. [Endothelin: a novel endothelium-derived peptide]. *Nippon Rinsho.* 47, 2121-30.
- Jeong, J., Li, X., McEvelly, R. J., Rosenfeld, M. G., Lufkin, T., Rubenstein, J. L., 2008. Dlx genes pattern mammalian jaw primordium by regulating both lower jaw-specific and upper jaw-specific genetic programs. *Development.* 135, 2905-16.
- Jiao, Z., Zhang, Z. G., Hornyak, T. J., Hozeska, A., Zhang, R. L., Wang, Y., Wang, L., Roberts, C., Strickland, F. M., Chopp, M., 2006. Dopachrome

- tautomerase (Dct) regulates neural progenitor cell proliferation. *Dev Biol.* 296, 396-408.
- Kang, J., Gocke, C. B., Yu, H., 2006. Phosphorylation-facilitated sumoylation of MEF2C negatively regulates its transcriptional activity. *BMC Biochem.* 7, 5.
- Kapur, R. P., 1999. Early death of neural crest cells is responsible for total enteric aganglionosis in Sox10(Dom)/Sox10(Dom) mouse embryos. *Pediatr Dev Pathol.* 2, 559-69.
- Kato, Y., Kravchenko, V. V., Tapping, R. I., Han, J., Ulevitch, R. J., Lee, J. D., 1997. BMK1/ERK5 regulates serum-induced early gene expression through transcription factor MEF2C. *EMBO J.* 16, 7054-66.
- Khiem, D., Cyster, J. G., Schwarz, J. J., Black, B. L., 2008. A p38 MAPK-MEF2C pathway regulates B-cell proliferation. *Proc Natl Acad Sci U S A.* 105, 17067-72.
- Kim, J., Lo, L., Dormand, E., Anderson, D. J., 2003. SOX10 maintains multipotency and inhibits neuronal differentiation of neural crest stem cells. *Neuron.* 38, 17-31.
- Knecht, A. K., Bronner-Fraser, M., 2002. Induction of the neural crest: a multigene process. *Nat Rev Genet.* 3, 453-61.
- Kobayashi, T., Urabe, K., Orlow, S. J., Higashi, K., Imokawa, G., Kwon, B. S., Potterf, B., Hearing, V. J., 1994. The Pmel 17/silver locus protein. Characterization and investigation of its melanogenic function. *J Biol Chem.* 269, 29198-205.
- Kurihara, Y., Kurihara, H., Suzuki, H., Kodama, T., Maemura, K., Nagai, R., Oda, H., Kuwaki, T., Cao, W. H., Kamada, N., et al., 1994. Elevated blood pressure and craniofacial abnormalities in mice deficient in endothelin-1. *Nature.* 368, 703-10.
- Lane, P. W., Liu, H. M., 1984. Association of megacolon with a new dominant spotting gene (Dom) in the mouse. *J Hered.* 75, 435-9.
- Lang, D., Chen, F., Milewski, R., Li, J., Lu, M. M., Epstein, J. A., 2000. Pax3 is required for enteric ganglia formation and functions with Sox10 to modulate expression of c-ret. *J. Clin. Invest.* 106, 963-971.
- Le Douarin, N., 1969. Particularites du noyau interphasique chez la Caille japonaise (*Corurnix coturnix japonica*). Utilisation de ces partiucularites comme "marque biologique" dans des recherches sur les interactions tissularies et les migrations cellulaires au cours l'ontogenese *Bulletin Biologique de la France et de la Belgique* 103, 435-452.
- Le Douarin, N., 1973. A biological labeling technique and its use in experimental embryology. *Developmental Biology* 30, 217-222.
- Le Douarin, N., 1980. Migration and differentiation of neural crest cells. *Curr Top Dev Biol.* 16, 31-85.
- Le Douarin, N., 1999. *The Neural Crest*. Cambridge University Press, Cambridge, UK.
- Le Douarin, N. M., Dupin, E., 2003. Multipotentiality of the neural crest. *Curr Opin Genet Dev.* 13, 529-36.
- Lee, M., Goodall, J., Verastegui, C., Ballotti, R., Goding, C. R., 2000. Direct regulation of the Microphthalmia promoter by Sox10 links Waardenburg-

- Shah syndrome (WS4)-associated hypopigmentation and deafness to WS2. *J Biol Chem.* 275, 37978-83.
- Lilly, B., Zhao, B., Ranganayakulu, G., Paterson, B. M., Schulz, R. A., Olson, E. N., 1995. Requirement of MADS domain transcription factor D-MEF2 for muscle formation in *Drosophila*. *Science.* 267, 688-93.
- Lin, J. Y., Fisher, D. E., 2007. Melanocyte biology and skin pigmentation. *Nature.* 445, 843-50.
- Lin, Q., Lu, J., Yanagisawa, H., Webb, R., Lyons, G. E., Richardson, J. A., Olson, E. N., 1998. Requirement of the MADS-box transcription factor MEF2C for vascular development. *Development.* 125, 4565-74.
- Lin, Q., Schwarz, J., Bucana, C., Olson, E. N., 1997. Control of mouse cardiac morphogenesis and myogenesis by transcription factor MEF2C. *Science.* 276, 1404-7.
- Lints, T. J., Parsons, L. M., Hartley, L., Lyons, I., Harvey, R. P., 1993. Nkx-2.5: a novel murine homeobox gene expressed in early heart progenitor cells and their myogenic descendants. *Development.* 119, 969.
- Lister, J. A., Robertson, C. P., Lepage, T., Johnson, S. L., Raible, D. W., 1999. nacre encodes a zebrafish microphthalmia-related protein that regulates neural-crest-derived pigment cell fate. *Development.* 126, 3757-67.
- Lumsden, A., Sprawson, N., Graham, A., 1991. Segmental origin and migration of neural crest cells in the hindbrain region of the chick embryo. *Development.* 113, 1281-91.
- Ma, K., Chan, J. K., Zhu, G., Wu, Z., 2005. Myocyte enhancer factor 2 acetylation by p300 enhances its DNA binding activity, transcriptional activity, and myogenic differentiation. *Mol Cell Biol.* 25, 3575-82.
- Maemura, K., Kurihara, H., Kurihara, Y., Oda, H., Ishikawa, T., Copeland, N. G., Gilbert, D. J., Jenkins, N. A., Yazaki, Y., 1996. Sequence analysis, chromosomal location, and developmental expression of the mouse preproendothelin-1 gene. *Genomics.* 31, 177-84.
- McKinsey, T. A., Zhang, C. L., Olson, E. N., 2002. MEF2: a calcium-dependent regulator of cell division, differentiation and death. *Trends Biochem Sci.* 27, 40-7.
- Molkentin, J. D., Black, B. L., Martin, J. F., Olson, E. N., 1996. Mutational analysis of the DNA binding, dimerization, and transcriptional activation domains of MEF2C. *Mol Cell Biol.* 16, 2627-36.
- Moore, K. J., 1995. Insight into the microphthalmia gene. *Trends Genet.* 11, 442-8.
- Morin, S., Charron, F., Robitaille, L., Nemer, M., 2000. GATA-dependent recruitment of MEF2 proteins to target promoters. *EMBO J.* 19, 2046-55.
- Nakayama, A., Nguyen, M. T., Chen, C. C., Opdecamp, K., Hodgkinson, C. A., Arnheiter, H., 1998. Mutations in microphthalmia, the mouse homolog of the human deafness gene MITF, affect neuroepithelial and neural crest-derived melanocytes differently. *Mech Dev.* 70, 155-66.
- Naya, F. J., Black, B. L., Wu, H., Bassel-Duby, R., Richardson, J. A., Hill, J. A., Olson, E. N., 2002. Mitochondrial deficiency and cardiac sudden death in mice lacking the MEF2A transcription factor. *Nat Med.* 8, 1303-9.

- Nguyen, T., Wei, M. L., 2007. Hermansky-Pudlak HPS1/pale ear gene regulates epidermal and dermal melanocyte development. *J Invest Dermatol.* 127, 421-8.
- Okano, J., Suzuki, S., Shiota, K., 2006. Regional heterogeneity in the developing palate: morphological and molecular evidence for normal and abnormal palatogenesis. *Congenit Anom (Kyoto).* 46, 49-54.
- Opdecamp, K., Nakayama, A., Nguyen, M. T., Hodgkinson, C. A., Pavan, W. J., Arnheiter, H., 1997. Melanocyte development in vivo and in neural crest cell cultures: crucial dependence on the Mitf basic-helix-loop-helix-zipper transcription factor. *Development.* 124, 2377-86.
- Osumi-Yamashita, N., Ninomiya, Y., Doi, H., Eto, K., 1994. The contribution of both forebrain and midbrain crest cells to the mesenchyme in the frontonasal mass of mouse embryos. *Dev Biol.* 164, 409-19.
- Panganiban, G., Rubenstein, J. L., 2002. Developmental functions of the Distal-less/Dlx homeobox genes. *Development.* 129, 4371-86.
- Paratore, C., Goerich, D. E., Suter, U., Wegner, M., Sommer, L., 2001. Survival and glial fate acquisition of neural crest cells are regulated by an interplay between the transcription factor Sox10 and extrinsic combinatorial signaling. *Development.* 128, 3949-61.
- Peirano, R. I., Goerich, D. E., Riethmacher, D., Wegner, M., 2000. Protein zero gene expression is regulated by the glial transcription factor Sox10. *Mol Cell Biol.* 20, 3198-209.
- Potterf, S. B., Furumura, M., Dunn, K. J., Arnheiter, H., Pavan, W. J., 2000. Transcription factor hierarchy in Waardenburg syndrome: regulation of MITF expression by SOX10 and PAX3. *Hum Genet.* 107, 1-6.
- Potterf, S. B., Mollaaghababa, R., Hou, L., Southard-Smith, E. M., Hornyak, T. J., Arnheiter, H., Pavan, W. J., 2001. Analysis of SOX10 function in neural crest-derived melanocyte development: SOX10-dependent transcriptional control of dopachrome tautomerase. *Dev Biol.* 237, 245-57.
- Potthoff, M. J., Olson, E. N., 2007. MEF2: a central regulator of diverse developmental programs. *Development.* 134, 4131-40.
- Qiu, M., Bulfone, A., Ghattas, I., Meneses, J. J., Christensen, L., Sharpe, P. T., Presley, R., Pedersen, R. A., Rubenstein, J. L., 1997. Role of the Dlx homeobox genes in proximodistal patterning of the branchial arches: mutations of Dlx-1, Dlx-2, and Dlx-1 and -2 alter morphogenesis of proximal skeletal and soft tissue structures derived from the first and second arches. *Dev Biol.* 185, 165-84.
- Ranganayakulu, G., Zhao, B., Dokidis, A., Molkenin, J. D., Olson, E. N., Schulz, R. A., 1995. A series of mutations in the D-MEF2 transcription factor reveal multiple functions in larval and adult myogenesis in *Drosophila*. *Dev Biol.* 171, 169-81.
- Robledo, R. F., Lufkin, T., 2006. Dlx5 and Dlx6 homeobox genes are required for specification of the mammalian vestibular apparatus. *genesis.* 44, 425-37.
- Robledo, R. F., Rajan, L., Li, X., Lufkin, T., 2002. The Dlx5 and Dlx6 homeobox genes are essential for craniofacial, axial, and appendicular skeletal development. *Genes Dev.* 16, 1089-101.

- Rojas, A., De Val, S., Heidt, A. B., Xu, S. M., Bristow, J., Black, B. L., 2005. Gata4 expression in lateral mesoderm is downstream of BMP4 and is activated directly by Forkhead and GATA transcription factors through a distal enhancer element. *Development*. 132, 3405-17.
- Ruest, L. B., Xiang, X., Lim, K. C., Levi, G., Clouthier, D. E., 2004. Endothelin-A receptor-dependent and -independent signaling pathways in establishing mandibular identity. *Development*. 131, 4413-23.
- Schilling, T. F., Kimmel, C. B., 1994. Segment and cell type lineage restrictions during pharyngeal arch development in the zebrafish embryo. *Development*. 120, 483-94.
- Serbedzija, G. N., Bronner-Fraser, M., Fraser, S. E., 1992. Vital dye analysis of cranial neural crest cell migration in the mouse embryo. *Development*. 116, 297-307.
- Shore, P., Sharrocks, A. D., 1995. The MADS-box family of transcription factors. *Eur J Biochem*. 229, 1-13.
- Solano, F., Martinez-Esparza, M., Jimenez-Cervantes, C., Hill, S. P., Lozano, J. A., Garcia-Borron, J. C., 2000. New insights on the structure of the mouse silver locus and on the function of the silver protein. *Pigment Cell Res*. 13 Suppl 8, 118-24.
- Sonnenberg-Riethmacher, E., Mieke, M., Stolt, C. C., Goerich, D. E., Wegner, M., Riethmacher, D., 2001. Development and degeneration of dorsal root ganglia in the absence of the HMG-domain transcription factor Sox10. *Mech Dev*. 109, 253-65.
- Southard-Smith, E. M., Angrist, M., Ellison, J. S., Agarwala, R., Baxevanis, A. D., Chakravarti, A., Pavan, W. J., 1999. The Sox10(Dom) mouse: modeling the genetic variation of Waardenburg-Shah (WS4) syndrome. *Genome Res*. 9, 215-25.
- Southard-Smith, E. M., Kos, L., Pavan, W. J., 1998. Sox10 mutation disrupts neural crest development in Dom Hirschsprung mouse model. *Nat Genet*. 18, 60-4.
- Spritz, R. A., Chiang, P. W., Oiso, N., Alkhateeb, A., 2003. Human and mouse disorders of pigmentation. *Curr Opin Genet Dev*. 13, 284-9.
- Srivastava, D., Olson, E. N., 2000. A genetic blueprint for cardiac development. *Nature*. 407, 221-6.
- Steel, K. P., Barkway, C., 1989. Another role for melanocytes: their importance for normal stria vascularis development in the mammalian inner ear. *Development*. 107, 453-63.
- Sturm, R. A., Teasdale, R. D., Box, N. F., 2001. Human pigmentation genes: identification, structure and consequences of polymorphic variation. *Gene*. 277, 49-62.
- Sumiyama, K., Ruddle, F. H., 2003. Regulation of Dlx3 gene expression in visceral arches by evolutionarily conserved enhancer elements. *Proc Natl Acad Sci U S A*. 100, 4030-4.
- Tanaka, H., Moroi, K., Iwai, J., Takahashi, H., Ohnuma, N., Hori, S., Takimoto, M., Nishiyama, M., Masaki, T., Yanagisawa, M., Sekiya, S., Kimura, S., 1998. Novel mutations of the endothelin B receptor gene in patients with

- Hirschsprung's disease and their characterization. *J Biol Chem.* 273, 11378-83.
- Tassabehji, M., Newton, V. E., Read, A. P., 1994a. Waardenburg syndrome type 2 caused by mutations in the human microphthalmia (MITF) gene. *Nat Genet.* 8, 251-5.
- Tassabehji, M., Newton, V. E., Read, A. P., 1994b. Waardenburg syndrome type 2 caused by mutations in the human microphthalmia (MITF) gene. *Nat Genet.* 8, 251-255.
- Thomas, T., Kurihara, H., Yamagishi, H., Kurihara, Y., Yazaki, Y., Olson, E. N., Srivastava, D., 1998. A signaling cascade involving endothelin-1, dHAND and *msx1* regulates development of neural-crest-derived branchial arch mesenchyme. *Development.* 125, 3005-14.
- Trainor, P. A., 2005. Specification of neural crest cell formation and migration in mouse embryos. *Semin Cell Dev Biol.* 16, 683-93.
- Trainor, P. A., Tam, P. P., 1995. Cranial paraxial mesoderm and neural crest cells of the mouse embryo: co-distribution in the craniofacial mesenchyme but distinct segregation in branchial arches. *Development.* 121, 2569-82.
- Turner, W. A., Taylor, J. D., Tchen, T. T., 1975. Melanosome formation in the goldfish: the role of multivesicular bodies. *J Ultrastruct Res.* 51, 16-31.
- Vance, K. W., Goding, C. R., 2004. The transcription network regulating melanocyte development and melanoma. *Pigment Cell Res.* 17, 318-25.
- Verastegui, C., Bille, K., Ortonne, J. P., Ballotti, R., 2000. Regulation of the microphthalmia-associated transcription factor gene by the Waardenburg syndrome type 4 gene, *SOX10*. *J Biol Chem.* 275, 30757-60.
- Verzi, M. P., Agarwal, P., Brown, C., McCulley, D. J., Schwarz, J. J., Black, B. L., 2007. The transcription factor *MEF2C* is required for craniofacial development. *Dev Cell.* 12, 645-52.
- Verzi, M. P., McCulley, D. J., De Val, S., Dodou, E., Black, B. L., 2005. The right ventricle, outflow tract, and ventricular septum comprise a restricted expression domain within the secondary/anterior heart field. *Dev Biol.* 287, 134-45.
- Vincentz, J. W., Barnes, R. M., Firulli, B. A., Conway, S. J., Firulli, A. B., 2008. Cooperative interaction of *Nkx2.5* and *Mef2c* transcription factors during heart development. *Dev Dyn.* 237, 3809-19.
- Wang, D. Z., Valdez, M. R., McAnally, J., Richardson, J., Olson, E. N., 2001. The *Mef2c* gene is a direct transcriptional target of myogenic bHLH and MEF2 proteins during skeletal muscle development. *Development.* 128, 4623-4633.
- Widlund, H. R., Horstmann, M. A., Price, E. R., Cui, J., Lessnick, S. L., Wu, M., He, X., Fisher, D. E., 2002. Beta-catenin-induced melanoma growth requires the downstream target Microphthalmia-associated transcription factor. *J Cell Biol.* 158, 1079-87.
- Wu, M., Li, J., Engleka, K. A., Zhou, B., Lu, M. M., Plotkin, J. B., Epstein, J. A., 2008. Persistent expression of *Pax3* in the neural crest causes cleft palate and defective osteogenesis in mice. *J Clin Invest.* 118, 2076-87.

- Xu, D., Emoto, N., Giaid, A., Slaughter, C., Kaw, S., deWit, D., Yanagisawa, M., 1994. ECE-1: a membrane-bound metalloprotease that catalyzes the proteolytic activation of big endothelin-1. *Cell*. 78, 473-85.
- Yanagisawa, H., Clouthier, D. E., Richardson, J. A., Charite, J., Olson, E. N., 2003. Targeted deletion of a branchial arch-specific enhancer reveals a role of dHAND in craniofacial development. *Development*. 130, 1069-78.
- Yanagisawa, H., Hammer, R. E., Richardson, J. A., Williams, S. C., Clouthier, D. E., Yanagisawa, M., 1998a. Role of Endothelin-1/Endothelin-A receptor-mediated signaling pathway in the aortic arch patterning in mice. *J Clin Invest*. 102, 22-33.
- Yanagisawa, H., Yanagisawa, M., Kapur, R. P., Richardson, J. A., Williams, S. C., Clouthier, D. E., de Wit, D., Emoto, N., Hammer, R. E., 1998b. Dual genetic pathways of endothelin-mediated intercellular signaling revealed by targeted disruption of endothelin converting enzyme-1 gene. *Development*. 125, 825-36.
- Yanagisawa, M., Masaki, T., 1989. Molecular biology and biochemistry of the endothelins. *Trends Pharmacol Sci*. 10, 374-8.
- Yang, S. H., Galanis, A., Sharrocks, A. D., 1999. Targeting of p38 mitogen-activated protein kinases to MEF2 transcription factors. *Mol Cell Biol*. 19, 4028-38.
- Zang, M. X., Li, Y., Xue, L. X., Jia, H. T., Jing, H., 2004. Cooperative activation of atrial natriuretic peptide promoter by dHAND and MEF2C. *J Cell Biochem*. 93, 1255-66.
- Zhu, B., Gulick, T., 2004. Phosphorylation and alternative pre-mRNA splicing converge to regulate myocyte enhancer factor 2C activity. *Mol Cell Biol*. 24, 8264-75.

Publishing Agreement

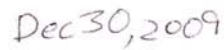
It is the policy of the University to encourage the distribution of all theses, dissertations, and manuscripts. Copies of all UCSF theses, dissertations, and manuscripts will be routed to the library via the Graduate Division. The library will make all theses, dissertations, and manuscripts accessible to the public and will preserve these to the best of their abilities, in perpetuity.

Please sign the following statement:

I hereby grant permission to the Graduate Division of the University of California, San Francisco to release copies of my thesis, dissertation, or manuscript to the Campus Library to provide access and preservation, in whole or in part, in perpetuity.



Author Signature



Date